

**Assessment of Greenhouse Gas Reduction Options for the Iron, Gold, and
Potash Mining Sectors**

by

Anil Kumar Katta

A thesis submitted in partial fulfillment of the requirements for the degree of

Master of Science

in

ENGINEERING MANAGEMENT

Department of Mechanical Engineering
University of Alberta

© Anil Kumar Katta, 2019

Abstract

Canada has one of the world's highest greenhouse gas (GHG) emissions per capita among developed countries and was the 10th largest global GHG emitter in 2017. Consistent with the Paris Agreement's goal of controlling the temperature increase by 2°C to 1.5°C, Canada aims to reduce GHG emissions by 30% in 2030 and 80% in 2050 from 2005 levels. The Canadian government is focusing on several GHG abatement pathways in various energy demand and supply sectors to reduce GHG emissions.

In 2016, the Canadian industrial sector was responsible for 36% of the total energy demand sector's GHG emissions. The industrial sector comprises of mainly upstream mining (including oil and gas), mineral mining, and manufacturing activities. It is important to identify the energy use and GHG emissions at the process and technology levels in different sub-sectors to develop effective GHG reduction strategies. In this work, disaggregated energy use and GHG emissions data were developed for the iron, gold, and potash mining sectors. The end-use processes were identified for each mining operation, and energy demand trees were developed. The energy intensities for each end-user were calculated and used in a bottom-up, energy-environmental model to determine the associated end-use process GHG emissions. A bottom-up approach uses end-use device data; this approach is well suited for analyzing technical energy-saving opportunities. The results were used to develop Sankey diagrams that allow us to visualize the energy and GHG emissions flows from resource to end use by sector, fuel type, and province. The energy demand shares by province in 2015 were 38% (32.4 PJ) in Saskatchewan, 23% (19.4 PJ) in Quebec, 19% (16.3 PJ) in Newfoundland and Labrador, and 15% (12.8 PJ) in Ontario. 56% of the iron mining energy demand was from Newfoundland and Labrador; 54% of the gold mining energy demand was from

Ontario; and 98% of the potash mining energy demand was from Saskatchewan. More than half (56%) of the GHG emissions were from Saskatchewan, followed by Quebec (17%) and Newfoundland (15%). The overall energy and GHG emission intensities for iron, gold, and potash mining are 0.6, 164.8, 1.8 GJ/t and 31, 5278, and 157 kg CO₂ eq./t, respectively. The results provide baselines of Canadian average energy and GHG emission intensities and can help industry determine whether mine-specific operations are underperforming. Also, the disaggregated data can be used to identify equipment or processes that will benefit the most from new technological or operational improvements.

Following this disaggregation, we assessed the potential and associated costs of various GHG mitigation pathways for the iron, gold, and potash mining sectors in Canada. These sectors have not widely accepted the available energy management options and so there is a potential to improve energy efficiency and reduce GHG emissions. We investigated the potential for improvements in energy efficiency and GHG mitigation and also the incremental costs associated with GHG abatement. Twenty-four GHG emission reduction options not yet implemented in Canada were identified following a review of current processes and operations. The data from 102 mine sites were studied to identify the existing technologies and potential for implementing new GHG mitigation options. The market share of technology options was modelled through development of correlation models where applicable, and a cost-benefit analysis was conducted for each pathway using a bottom-up approach. The results suggest that cumulative energy savings and GHG mitigation potentials are 98 PJ and 8 Mt CO₂ eq. for iron mining, 323 PJ and 10 Mt CO₂ eq. for gold mining, and 45 PJ and 3 Mt CO₂ eq. for the potash mining sector, respectively, by 2050 over a planning horizon of 30 years. These GHG mitigation potentials represent 10%, 20%, and 2% of sub-sectoral emissions with total marginal GHG abatement costs of -525, -1176, and -258 \$/tonne

CO₂ eq. for the iron, gold, and potash mining sectors, respectively. More than 80% of the emission reductions are from cost-effective measures, as indicated by the negative marginal GHG abatement costs. Decision-makers in Canada and other jurisdictions can use the developed cost curves to identify low-cost options to meet specific GHG reduction targets. The results could be used for policy formulation and investment decision-making.

Preface

This thesis is an original work by Anil Kumar Katta under the supervision of Dr. Amit Kumar. Some parts of this work have been submitted for publication in peer-reviewed journals. The details are given as follows:

Chapter 2 of this thesis, “Development of disaggregated energy use and greenhouse gas emission footprints in Canada’s iron, gold, and potash mining sectors,” coauthored by Anil Kumar Katta, Matthew Davis, and Amit Kumar, is submitted to *Resources, Conservation and Recycling*.

Chapter 3 of this thesis, “Assessment of GHG mitigation options for the iron, gold, and potash mining sectors,” coauthored by Anil Kumar Katta, Matthew Davis, and Amit Kumar, is submitted to the *Journal of Cleaner Production*.

I was responsible for defining the problem, data collection, data analysis, model development, and manuscript composition. Matthew Davis reviewed the research, provided feedback, and corrected the journal papers. Amit Kumar was the supervisory author and provided supervision on problem formulation, results, and manuscript edits.

Acknowledgements

I would like to express my sincere gratitude to my supervisor, Dr. Amit Kumar, for his guidance, mentorship, and support throughout my research work. His supervision, insight, and continuous feedback were invaluable in conducting the research. I would also like to extend sincere thanks to Matthew Davis for his timely feedback, knowledge sharing, and continuous support, which encouraged me towards the completion of my research. I would also like to thank Astrid Blodgett for editing my papers.

I am thankful to the NSERC/Cenovus/Alberta Innovates Associate Industrial Research Chair in Energy and Environmental Systems Engineering and the Cenovus Energy Endowed Chair in Environmental Engineering for financial support. I am also grateful to representatives from Alberta Innovates (AI), Suncor Energy Inc., Cenovus Energy Inc., Natural Resources Canada, and Environment and Climate Change Canada for their valuable input and comments in various forms. Many thanks to the University of Alberta's Future Energy Systems research initiative, which made this research possible, in part through the Canada First Research Excellence Fund (CFREF).

I highly appreciate the assistance of Drs. Eskinder Gemechu and Abayomi Olufemi Oni for their feedback on my journal papers. I am thankful to the members of the Sustainable Energy Research Group for their useful discussions throughout my research. Special thanks to my friends for sharing this journey. I am grateful to the University of Alberta Sustainability Scholar program, Mechanical Engineering Graduate Students Association, and Faculty of Engineering Graduate Research Symposium committee, which provided me with the opportunity for professional development.

Finally, I would like to acknowledge my parents and brother for their overwhelming support and for believing in me. I would not be the same person without their love and encouragement.

Table of Contents

Abstract.....	ii
Preface.....	v
Acknowledgements.....	vi
1 Chapter I: Introduction	1
1.1 Background	1
1.2 Canada’s energy and GHG emissions profile	2
1.2.1 Electricity generation sector	3
1.2.2 Energy demand sectors	5
1.3 Energy and GHG emissions profile of the industrial sector.....	8
1.4 Energy and emissions profile of the mineral mining sector and the scope of the study	10
1.5 Literature review and knowledge gaps.....	12
1.5.1 Disaggregation of energy and GHG footprints.....	12
1.5.2 Energy and environmental model	13
1.5.3 GHG mitigation options.....	15
1.6 Research objectives	16
1.7 Thesis outline	17
2 Chapter II: Development of disaggregated energy use and greenhouse gas emission footprints in Canada’s iron, gold, and potash mining sectors	18
2.1 Introduction	18

2.2	Method	22
2.2.1	Production data	23
2.2.2	Energy demand tree development.....	25
2.2.2.1	Iron ore mining	26
2.2.2.2	Gold mining.....	34
2.2.2.3	Potash mining	41
2.2.3	Energy and GHG emission analysis	44
2.2.4	Development of Sankey diagrams	45
2.3	Results and Discussion.....	46
2.3.1	Energy and GHG Sankey for iron mining	46
2.3.2	Energy and GHG Sankey for gold mining.....	47
2.3.3	Energy and GHG Sankey for potash mining	49
2.3.4	Integrated energy Sankey and GHG Sankey for all provinces with iron, gold, and potash mining operations.....	52
2.4	Implications and recommendations.....	57
2.5	Conclusion.....	58
3	Chapter III: Assessment of greenhouse gas mitigation options for the iron, gold, and potash mining sectors	60
3.1	Introduction	60
3.2	Method	64

3.2.1	Overview.....	64
3.2.2	Bottom-up model development for the iron, gold, and potash mining sectors.....	65
3.2.3	Business-as-usual (BAU) scenario	67
3.2.4	GHG mitigation scenario analysis	68
3.2.4.1	Cost of saved energy and total activity cost model	68
3.2.4.2	Market share model	70
3.2.4.3	Marginal GHG abatement cost	71
3.2.4.4	Scenario description and development	71
3.3	Results and discussion.....	84
3.3.1	Model validation and BAU scenario.....	84
3.3.2	Cost of saved energy (CSE) and total activity cost (TAC).....	86
3.3.3	Market share model results	90
3.3.4	Scenario analysis.....	91
3.3.5	Limitations	96
3.3.6	Sensitivity analysis.....	96
3.4	Conclusion.....	98
4	Chapter IV: Conclusion and future work	100
4.1	Conclusion.....	100
4.2	Recommendations for future work.....	108
	References.....	109

List of Tables

Table 2-1: Complied activity data for the study	24
Table 2-2: End-use process energy intensities of iron mining	31
Table 2-3: End-use process energy intensities of gold mining	38
Table 2-4: End-use process energy intensities of potash mining.....	42
Table 3-1: Electricity grid emission intensity factors (grams CO ₂ eq. /kilowatt-hour)	67
Table 3-2: End-use prices of electricity, natural gas, and diesel, from the NEB	69
Table 3-3: Description and energy savings of the scenarios.....	72
Table 3-4: CSE, TAC for scenarios in the iron mining sector	87
Table 3-5: CSE, TAC for scenarios in the potash mining sector	87
Table 3-6: CSE, TAC for scenarios in the gold mining sector	88

List of Figures

Figure 1-1: Greenhouse gas emissions - Canada	3
Figure 1-2: Energy use and GHG emissions in the Canadian electricity generation sector in 1990, 2005, and 2016.....	4
Figure 1-3: Energy use and GHG emissions share of different fuels in the Canadian electricity generation sector in 1990, 2005, and 2016	4
Figure 1-4: Energy demand and GHG emissions in Canadian end-use sectors in 1990, 2005, and 2016.....	6
Figure 1-5: Energy use and GHG emissions fuel shares in the Canadian demand sectors in 2005 (inner circle) and 2016 (outer circle)	7
Figure 1-6: Energy use (left) and GHG emissions (right) shares in the industrial sectors in 2016	9
Figure 1-7: Energy use and GHG emissions shares of different fuels in Canada’s industrial sector in 1990, 2005, and 2016.....	10
Figure 1-8: Energy use (left) and GHG emissions (right) share among the mineral extraction sub-sectors in 2016	11
Figure 2-1: Method used in the study for disaggregating energy and GHG emissions	23
Figure 2-2: Iron, gold, and potash producing mines of Canada.....	25
Figure 2-3: Energy demand tree for iron mining	33
Figure 2-4: Energy demand tree for gold mining	40
Figure 2-5: Energy demand tree for potash mining	43
Figure 2-6: Basic Sankey structure for sectoral energy and GHG emissions.....	46
Figure 2-7: Basic Sankey structure for Canada’s provincial energy and GHG emission.....	46

Figure 2-8: Sankey diagram for iron mining energy demand (left) and GHG emissions (right) in Canada in 2015	48
Figure 2-9: Sankey diagram for gold mining energy demand (left) and GHG emissions (right) in Canada in 2015	51
Figure 2-10: Sankey diagrams for potash mining energy demand and GHG emissions in Canada in 2015	54
Figure 2-11: Iron, gold, and potash mining energy (PJ) Sankey by province and fuel type in 2015	55
Figure 2-12: Iron, gold, and potash mining GHG (1000 tonnes CO ₂ eq.) Sankey by province and fuel type in 2015	56
Figure 3-1: Method for model development and scenario analysis	65
Figure 3-2: Modelling framework	66
Figure 3-3: Energy demand and GHG emission (excluding electricity-related emissions) validation for the iron, gold, and potash mining sectors	85
Figure 3-4: Market shares of electric haul trucks, diesel hybrid haul trucks, electric LHDs, and diesel hybrid LHDs in each province.....	91
Figure 3-5: Wedge curve of achievable GHG emissions reduction for the iron mining sector....	92
Figure 3-6: Wedge curve of achievable GHG emissions reduction for the gold mining sector ...	93
Figure 3-7: Canadian iron, gold, and potash mining sector combined marginal GHG emission abatement cost curve.....	95
Figure 3-8: IR-AHTs scenario sensitivity of abatement cost to capital cost, discount rate, diesel price, electricity price, and reference scenario growth	97

Figure 3-9: GO-AHTs_P scenario sensitivity of abatement cost to capital cost, discount rate, diesel price, electricity price, and reference scenario growth	98
Figure 3-10: PO-SG&PD scenario sensitivity of abatement cost to capital cost, discount rate, natural gas price, electricity price, and reference scenario growth.....	98
Figure 4-1: Sankey diagram for Canada’s iron mining energy demand (left) and GHG emissions (right) in 2015	104
Figure 4-2: Sankey diagram for Canada’s gold mining energy demand (left) and GHG emissions (right) in 2015	105
Figure 4-3: Sankey diagrams for Canada’s potash mining energy demand and GHG emissions in 2015.....	106
Figure 4-4: Canada’s iron, gold, and potash mining sectors combined marginal GHG emission abatement cost curve.....	107

Abbreviations

AG – Autogenous

BAU – Business-as-usual

CAD – Canadian dollar

CSE – Cost of saved energy

CIC – Carbon-in-column

CIL – Carbon-in-leach

CIP – Carbon-in-pulp

DSO – Direct shipping ore

EF – Emission intensity factor

GDP – Gross Domestic Product

GHG – Greenhouse gas

HPGR – High pressure grinding rolls

IPCC – Intergovernmental Panel on Climate Change

LEAP – Long range Energy Alternative Planning

MJ – Megajoule

Mt – Million tonnes

NRCan – Natural Resources Canada

PJ – Petajoule

SAG – Semi-autogenous

SEDAR – System for Electronic Document Analysis and Retrieval

TAC – Total activity cost

1 Chapter I: Introduction

1.1 Background

Human activities have caused changes in the earth's climate system. The increase in greenhouse gas (GHG) emissions due to human activity is likely the dominant cause of increased global warming since the mid-20th century (Edenhofer, 2015). Anthropogenic emissions have caused changes to the earth's near-surface temperature (Stott, 2003), precipitation levels (Zhang et al., 2007), sea-level pressure (Gillett et al., 2003), and ocean heat content (Barnett et al., 2005). Global GHG emissions increased at a rate of 1.3%/year between 1970 and 2000 and have further increased at a rate of 2.2%/year between 2000 and 2010. This increase is driven by population and economic growth (Edenhofer, 2015). The carbon dioxide (CO₂) emissions after 1970 account for nearly 50% of the total GHG emissions after 1750 (Edenhofer, 2015).

According to the Intergovernmental Panel on Climate Change (2018), the global mean surface temperature has increased by 1° C from pre-industrial levels and is projected to increase 1.5° C in the near future if GHG emissions continue to increase at the current rate. In order to combat climate change, several countries came together at the Conference of the Parties (COP) 21 in Paris on December 12, 2015 and agreed to accelerate and intensify actions for a sustainable low-carbon future (United Nations Framework Convention on Climate Change, 2015). The Paris Agreement aims to limit the global temperature rise to 2° C above pre-industrial levels and to further efforts to limit the increase to a more ambitious target of 1.5° C by end of this century. In December 2018, at COP 24 in Katowice, Poland, the countries agreed on what is known as the Katowice climate package, which sets out procedures, rules, and mechanisms to implement the Paris Agreement (United Nations Framework Convention on Climate Change, 2018). This aim of the climate

package is to lower CO₂ emissions by 25% from 2010 levels by 2030 and to reach net zero around 2070 in order to limit global warming to 2° C (Intergovernmental Panel on Climate Change, 2018).

Globally, GHG emissions have increased by 20%, from 38 gigatonnes (Gt) in 2005 to 46 Gt in 2014 (Environment and Climate Change Canada, 2019a). GHG emissions from developed countries have peaked already, while GHG emissions from developing nations are expected to peak after 2030 (Boothe and Boudreault, 2016). China generates 1/4 of the world's GHG emissions (more than any other country), and these GHG emissions are expected to increase substantially until 2030. The United States is the 2nd largest emitter and its GHG emissions peaked in 2000. India is the third largest emitter and its GHG emissions are expected to peak by 2043. Canada emits only about 1.6% of global GHGs but is among the top 10 global emitters and has been consistently in the top 3 when the top global emitters are compared in terms of per capita emissions over the years (Boothe and Boudreault, 2016).

Efforts are in place in all countries and economic sectors to reduce the GHG emissions. But the aggregate GHG emissions estimated for 2030 based on all the Intended Nationally Determined Contributions (INDCs) of 189 nations submitted to the United Nations Framework Convention on Climate Change (UNFCCC) will not fall within the 2° scenario, let alone for 1.5° scenario (United Nations Framework Convention on Climate Change, 2016). This calls for a drastic change in the global GHG emissions profile while simultaneously meeting the world's growing energy needs.

1.2 Canada's energy and GHG emissions profile

The 2016 Pan-Canadian Framework on Clean Growth and Climate Change shows Canada's commitment to climate change and supports efforts to reduce GHG emissions by 30% below 2005 levels by 2030 (Government of Canada, 2016). In 2016, the GHG emissions in Canada were 704

Mt CO₂ eq. and have fallen by 4% from 2005 levels (Environment and Climate Change Canada, 2018), as shown in Figure 1-1. GHG emissions are generated both from energy use in the electricity generation and energy demand sectors (residential, commercial/institutional, industrial, transportation, agriculture) and from non-energy use (land use, land-use change and forestry, waste, fugitive sources, etc.)

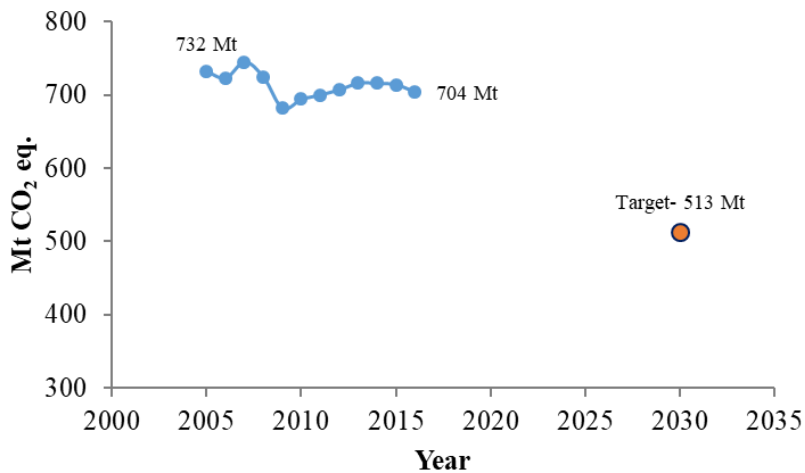


Figure 1-1: Greenhouse gas emissions - Canada [Data sources: (Environment and Climate Change Canada, 2018, 2019b)]

1.2.1 Electricity generation sector

The energy use and GHG emissions trend in the electricity generation sector are shown in Figure 1-2. Energy use was 4,102 PJ in 2016 and has increased by 37% and 3% from 1990 and 2005, respectively. GHG emissions in 2016 were 4% higher and 23% lower than 1990 and 2005 levels. The fuel mix over the years has changed, as shown in Figure 1-3. Notably, the share of coal use decreased (from 29% in 1990 to 26% in 2005 and to 16% in 2016), which reduced GHG emissions overall.

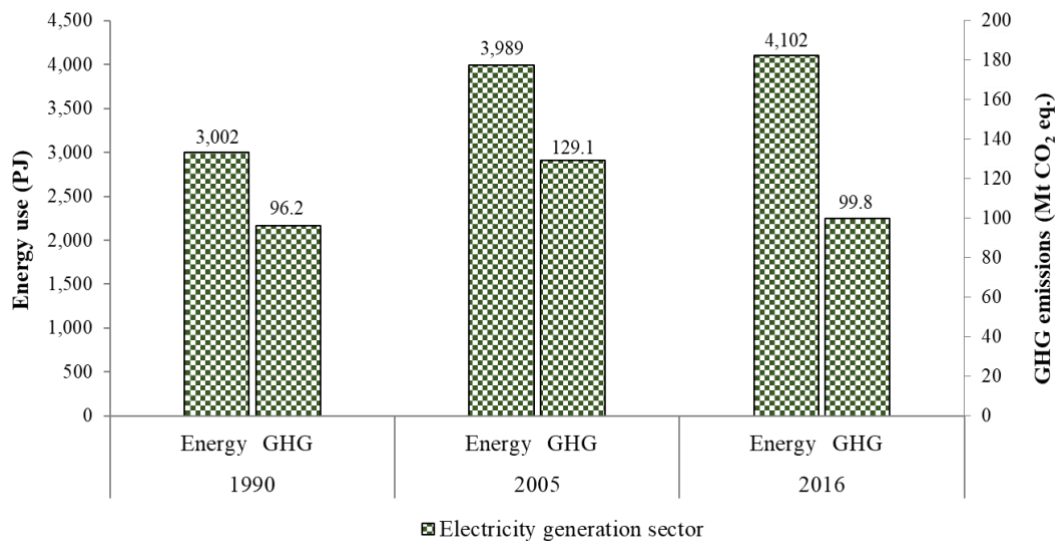


Figure 1-2: Energy use and GHG emissions in the Canadian electricity generation sector in 1990, 2005, and 2016 [Data source: (Natural Resources Canada, 2018b)]

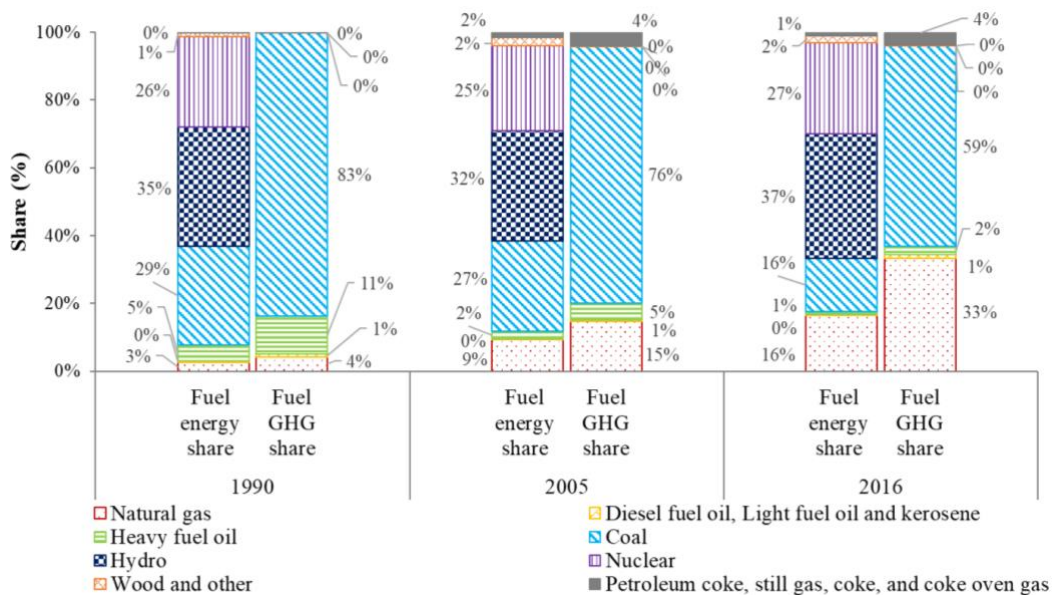


Figure 1-3: Energy use and GHG emissions share of different fuels in the Canadian electricity generation sector in 1990, 2005, and 2016 [Data source: (Natural Resources Canada, 2018b)]

1.2.2 Energy demand sectors

The residential, commercial and institutional, industrial, transportation, and agriculture sectors are the energy demand sectors and together consumed 8,786 PJ of energy in 2016 (Natural Resources Canada, 2018b). They shared 17, 11, 39, 30, and 3% of energy demand, respectively. Figure 1-4 illustrates their energy demand and GHG emissions in 1990, 2005, and 2016. The total energy demand increased by 4% in 2016 from 2005 due to the effects of activity, structure, weather, service level, capacity use rate, and energy efficiency (Natural Resources Canada, 2016b, 2018c). The activity effect, which refers to the changes in industrial gross domestic product, gross output, physical industrial output, floor space, and number of households, increased the energy demand by 1,557 PJ. This increase was offset by 1303 PJ because of structural and energy efficiency effects. Structure effects refer to sectorial shifts (relative increase in one industry over another) and energy efficiency effects result from improvements in technologies and processes. The share of the other effects is relatively lower. Sectorally, energy demand decreased by 3% in the residential sector and increased by 4% in the commercial and institutional, 4% in industrial, 6% in transportation, and 31% in agriculture sectors in 2016 from 2005.

Although energy demand increased, GHG emissions (474.7 Mt CO₂ eq.) fell by 2% in 2016 from 2005, as in Figure 1-4. The residential, commercial and institutional, industrial, transportation, and agriculture sectors had GHG emissions shares of 13, 9, 36, 38, and 4%. GHG emissions decreased by 21% and 15%, respectively, in the residential and commercial/institutional sectors, and increased by 2%, 3%, and 21%, respectively, in the industrial, transportation, and agriculture sectors between 2005 and 2016.

The decrease in GHG emissions in the residential and commercial/institutional sectors is due to the energy efficiency gains in space heating, water heating, lighting, and end-use appliances, as well as changes in the energy mix (natural gas and electricity use became more dominant while wood and oil use fell) (Natural Resources Canada, 2016b). Although there are efficiency gains in the other sectors, they could not fully compensate for the increase in GHG emissions because of the activity effect in the sectors (Natural Resources Canada, 2016b).

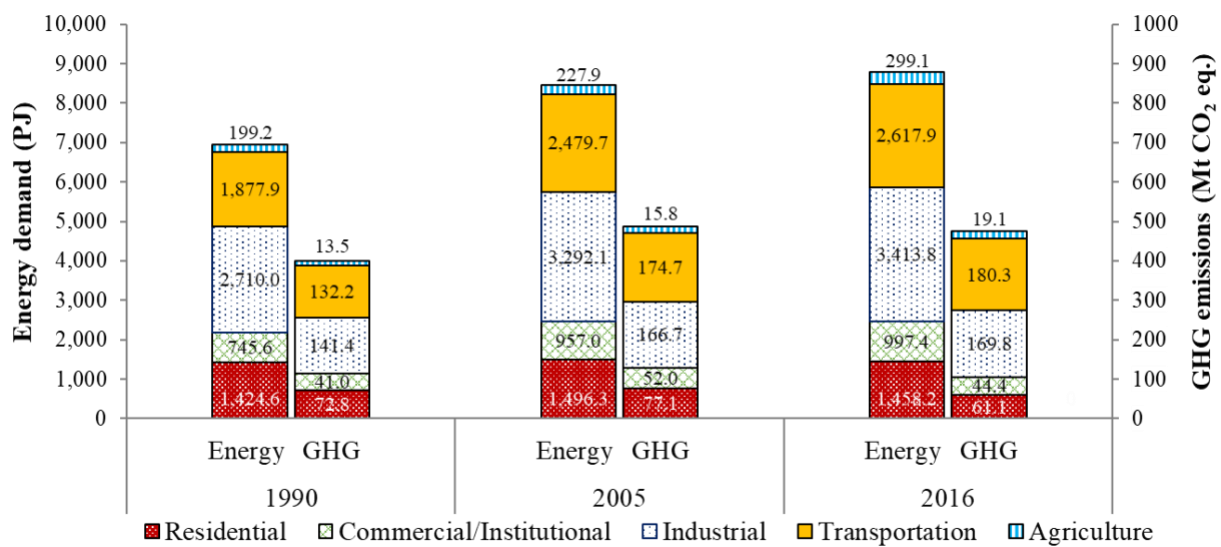


Figure 1-4: Energy demand and GHG emissions in Canadian end-use sectors in 1990, 2005, and 2016 [Data source: (Natural Resources Canada, 2018b)]

The energy use and GHG emissions' fuel shares are shown in Figure 1-5. The inner and outer circles represent the years 2005 and 2016, respectively. The main fuels used were electricity, natural gas, gasoline, and oil; they constituted around 80% of the energy use share. Of these fuels, the energy demand and GHG emissions shares of natural gas and gasoline increased and those of oil, still gas, and petroleum coke fell in 2016, which shows a shift towards less emissions-intensive fuels over the period. Changes in energy use and GHG emissions are not always proportional. The

energy use share of electricity decreased by 1%, but the GHG emissions share decreased by 7% (Natural Resources Canada, 2018b).

Overall, the industrial sector used the most energy and had the second highest GHG emissions share (36%) among all the end-use demand sectors in 2016. It is one of the sectors in which both energy demand and GHG emissions increased from 2005 levels. It comprises of several sub-sectors: upstream mining (including oil and gas extraction), mineral mining, and manufacturing activities. Hence it is imperative to break down the energy and GHG emissions profile of these subsectors and understand their contributions to Canadian totals.

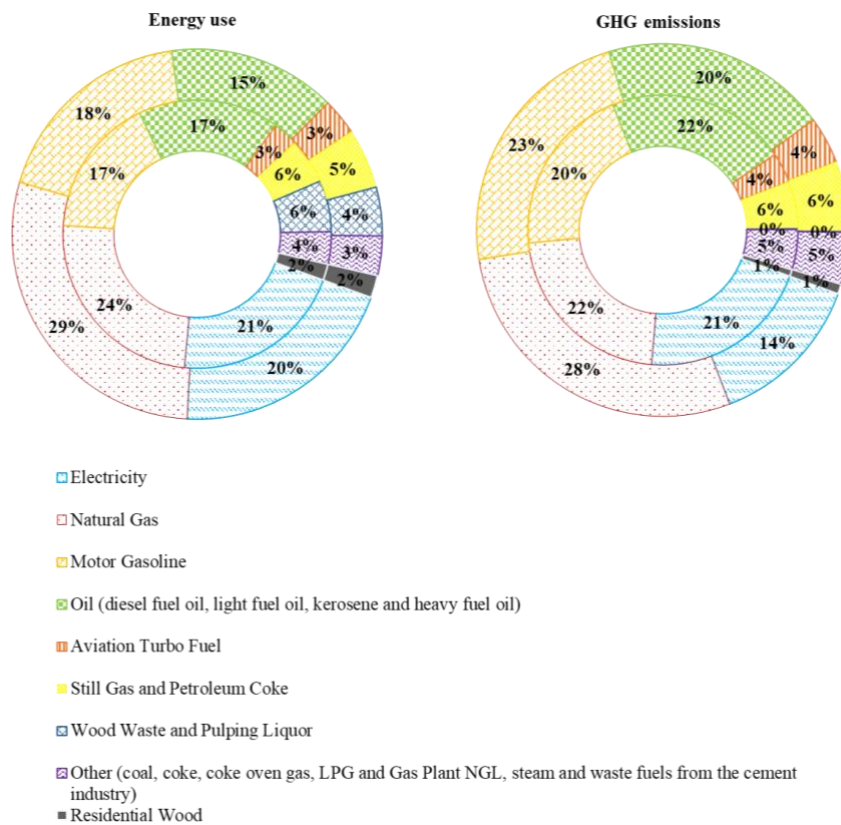


Figure 1-5: Energy use and GHG emissions fuel shares in the Canadian demand sectors in 2005 (inner circle) and 2016 (outer circle) [Data source: (Natural Resources Canada, 2018b)]

1.3 Energy and GHG emissions profile of the industrial sector

The industrial sector consumed 3441 PJ of energy and was responsible for 169.8 Mt CO₂ eq. of GHG emissions in 2016. The upstream mining and pulp and paper industries were responsible for 31% and 17% of the energy use, and the other sectors had shares of less than 10% each, as shown in Figure 1-6. Since 1990, energy demand in upstream mining and mineral mining has increased but demand in the other manufacturing sub-sectors has declined. This change can be attributed to increased industrial activity, structural changes in the industrial sector (i.e., decreased activity shares of energy-intensive industries such as pulp and paper), and an improvement in energy efficiency (11% between 1990 and 2015) (Natural Resources Canada, 2019b). During the same period, GHG emissions increased by 400% in upstream mining and decreased by 11% in mineral mining and 20% in the manufacturing sector.

Energy is mainly used to produce heat, generate steam, and for motive power. In 2016, natural gas and electricity were the main fuels used and had shares of 39% and 22% of industrial energy use, respectively, as shown in Figure 1-7. The energy demand shares of heavy fuel oil; coal, coke, and coke oven gas; and still gas and petroleum coke decreased from 7% to 1%, 2% to 1%, and 5% to 3%, respectively, from 1990 levels. The natural gas share increased from 31% to 39%. Although the share of electricity as an energy source decreased only by 3%, the share of GHG emissions fell appreciably from 29% to 16% as the coal share for electricity generation decreased.

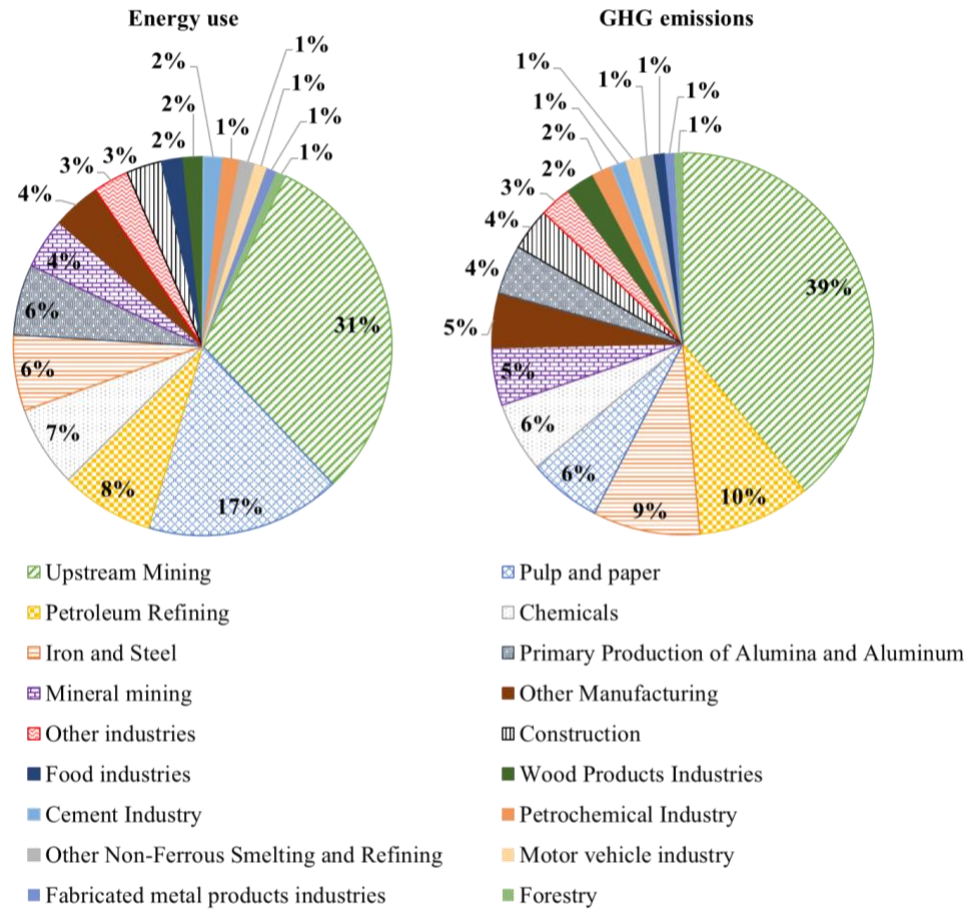


Figure 1-6: Energy use (left) and GHG emissions (right) shares in the industrial sectors in 2016 [Data source: (Natural Resources Canada, 2018b)]

It is important to disaggregate the energy use and GHG emissions to the process and technology level for the GHG emission-intensive subsectors (shown in Figure 1-6). To do so, it is necessary to identify energy- and GHG emission-intensive processes, provide baselines, and develop a long-term energy model. This has been done for the top GHG emitters – the oil sands mining (Katta et al., 2019), petroleum refining (Talaei, 2019), iron and steel (Talaei, 2019), pulp and paper (Shafique, 2017), and chemical (Talaei et al., 2018) subsectors. But for the Canadian mineral mining industry, which has the next highest GHG emissions share, only nationally aggregated data

is available. So, the main focus of this study is on the mineral mining industry, whose energy and emissions profile is discussed in the next section.

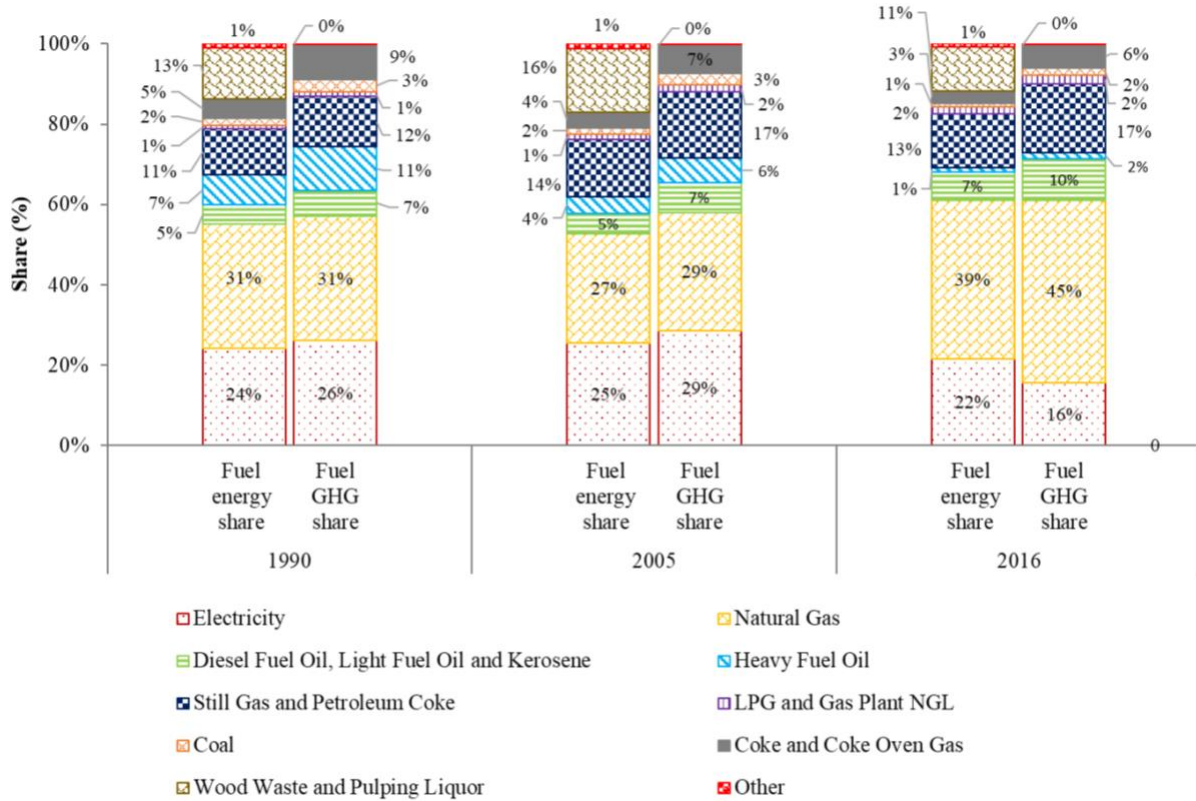


Figure 1-7: Energy use and GHG emissions shares of different fuels in Canada’s industrial sector in 1990, 2005, and 2016 [Data source: (Natural Resources Canada, 2018b)]

1.4 Energy and emissions profile of the mineral mining sector and the scope of the study

The mineral industry was responsible for 3.4% of the gross domestic product (GDP) and made up 18.2% of the exports’ value in 2016 (Mining Association of Canada, 2016). The industry consumed 4% of the country’s energy and contributed 5% of the GHG emissions that year (Natural Resources Canada, 2018b). The energy use and GHG emissions were 147.5 PJ and 8.3 Mt CO₂ eq. in 2016, an increase of 27% and 7%, respectively, from 2005. Electricity, natural gas, and diesel are the primary fuels used and shared 41%, 19%, and 28% of the energy use in 2015 (This

data is not available for the year 2016). The energy use shares of heavy fuel oil; natural gas; and coke and coke oven gas decreased from 14% to 9%, 23% to 19%, and 3% to 0%, respectively, between 2005 and 2015. During the same period, the energy shares of electricity increased from 28% to 41% and of diesel from 18% to 28%.

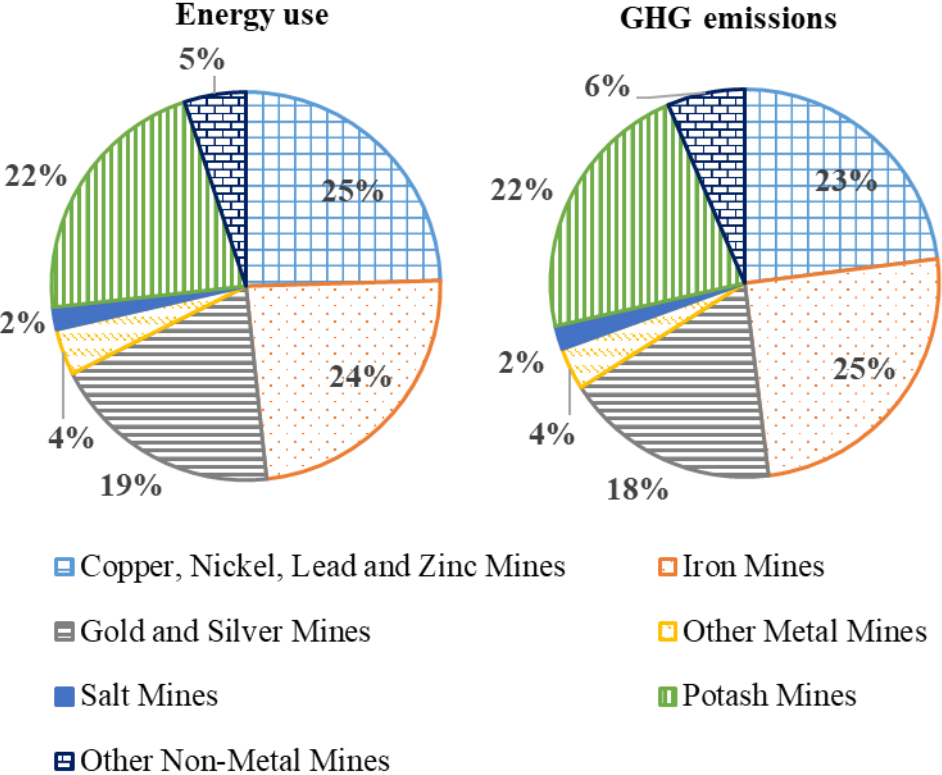


Figure 1-8: Energy use (left) and GHG emissions (right) share among the mineral extraction sub- sectors in 2016 [Data source: (Natural Resources Canada, 2018b)]

This industry can be disaggregated into metal (copper, nickel, lead, zinc, iron, gold and silver, and other metal mines) and other mineral mining sub-sectors (salt, potash, and other non-metal mines). The energy use and GHG emissions shares among the sub-sectors are shown in Figure 1-8. The iron, gold, and potash mines were responsible for more than half (about 65%) of the mineral extraction industry’s energy use and GHG emissions. The total energy use increased by 19%,

105%, and 8% between 2005 and 2014 for the iron, gold, and potash mining sectors, respectively. Moreover, Canada is the largest producer of potash, 5th largest producer of gold, and 9th largest producer of iron ore in the world (US Geological Survey, 2016). So, the scope of this study is on the iron, gold, and potash mining sub-sectors of Canada's mineral industry.

1.5 Literature review and knowledge gaps

This section briefly outlines the literature review and knowledge gaps that are described in more detail in subsequent chapters.

1.5.1 Disaggregation of energy and GHG footprints

The global industrial sector lacks a comprehensive and quality data on sub-sectoral process and technology energy use (Fischedick et al., 2014). The Canadian mineral mining sector is one such sector for which only the aggregated energy demand and GHG emissions at the national level are available. There are limitations associated with various past studies which quantified the energy intensities of iron, gold, and potash mining operations. Canadian benchmark studies have aggregated the mining operations into large subgroups and the scope is limited to studying the energy intensities of only a few iron and gold mines (Natural Resources Canada, 2005a, 2005b). The US Department of Energy modelled the energy requirements of some of the end-use processes for surface iron, gold, and underground potash mines (US Department of Energy, 2002a, 2002b, 2002c). Such modelling was not done for underground gold mining and potash solution mining operations. Griffing and Overcash (2010) estimated the aggregated energy intensity for extraction processes of taconite iron ore mining operations but not the end-use level intensities. Bleiwas (2011) estimated the energy requirements of only the electricity powered equipment used in ore extraction. For high-grade iron ores, Haque and Norgate (2015) gave a breakdown of energy and

GHG emission intensities for various mining and mineral processing steps. The study did not provide the energy requirements for low-grade ores, which require additional processing, or for pelletizing processes. For gold mining operations, Norgate and Haque (2012) estimated the GHG footprint but did not disaggregate the emissions into different end-use processes. Another Canadian benchmarking study on potash production facilities presents aggregated energy consumption by fuel type, energy intensity and GHG emissions for extraction and milling operations (Government of Canada, 2003). Like the other studies, there is no process-level disaggregated energy-use information.

The existing literature on iron, gold, and potash mining does not include a comprehensive study on energy usage of all end-use processes for different operations by fuel type. Furthermore, energy use and GHG emissions data in the Canadian iron, gold, and potash mining sectors are not disaggregated to the end-use level or the provincial level. This research fills these gaps. The breakdown of energy consumption and GHG emissions by energy type and end use provides a benchmark to quantify the environmental and economic benefits of GHG mitigation options (Brueske et al., 2012). Such an analysis is also required to understand what is required by the provinces and its industries to meet climate targets.

1.5.2 Energy and environmental model

The interactions between demand and supply in any economic sector can be studied using energy and environmental models. Such models can be used for long-term forecasting and to evaluate the GHG mitigation potentials of various technology options. The modeling approaches are classified into top-down and bottom-up. In a top-down model, the energy consumption is estimated using historical time-series data such as GDP and capital investment which limits the model's ability to

analyze new technologies as future projections based on historical data may fail to react to new improvements (Nyboer, 1997). On the contrary, in a bottom-up approach, the model is developed using the end-use device fuel intensities, and the production data. It is technologically explicit and will help determine the achievable reduction in energy use, GHG mitigation potential, and abatement cost over the life time of the technology (Nyboer, 1997). Krause (1996) reviewed the studies involving bottom-up models in Western Europe and found that they gave a closer approximation to the costs of mitigating carbon emissions compared to top-down approaches.

Several modelling tools such as MARKAL (Fishbone and Abilock, 1981), Integrated MARKAL-EFOM System (TIMES) (Loulou and Labriet, 2008), Energy 2020 (Systematic Solutions Inc, 2017b), Massachusetts Institute of Technology Emissions Prediction Policy Analysis (EPPA) (Babiker et al., 2001), and Long-range Energy Alternatives Planning (LEAP) system (Heaps, 2016) have been used in the past for integrated analyses of energy systems. Both the MARKAL and TIMES are dynamic linear optimization bottom-up models which search for least-cost combination of technologies over the planning period to meet the energy demand (Fishbone and Abilock, 1981; Loulou and Labriet, 2008). Yang et al. (2015) modelled California's energy system using the TIMES model and developed various GHG emission reduction scenarios identifying low-to-moderate cost pathways to deep de-carbonization. Jia et al. (2011) also applied the TIMES model to quantify China's future energy demand with scenario analysis and recommended specific sustainable development pathways. Energy 2020 is a system dynamics model which simulates the feedback between energy consumers, energy suppliers, and the economy using historical data. Various governments used Energy 2020 for analyzing and forecasting the GHG and economic impacts of a variety of policy considerations (Systematic Solutions Inc, 2017a). Gurgel and Paltsev (2014) estimated the economic impact of alternative policies and the costs of reducing GHG

emissions in Brazil using MIT EPPA model, which is a dynamic recursive general equilibrium model of the world economy. LEAP is an accounting-based tool that can be used to model different energy systems and make future projections based only on user defined data structures and is different from the other modeling tools. Huang et al. (2011) used the LEAP system to forecast the energy supply and demand in Taiwan. Davis et al. (2018a) analyzed Canada's past and future regional and sectoral GHG emission through a LEAP model. Other works have been done to develop energy models and identify the long-term GHG emission mitigation potentials for the commercial and institutional (Subramanyam et al., 2017a), residential (Subramanyam et al., 2017b), and chemical (Talaie, 2019) sectors using LEAP.

Various studies have been completed using different models for various sectors. But, to the best of the author's knowledge, an energy and environmental model for the mineral mining sector has not been developed. This work aims to address this gap by developing a comprehensive bottom-up energy and environmental model for the iron, gold, and potash mining sectors using LEAP.

1.5.3 GHG mitigation options

Previous studies on GHG mitigation options in these sectors have mainly compared alternative technologies of specific sub-processes. Lajunen (2015) compared the energy efficiency of different powertrains of mining machinery. McNab et al. (2009), Wang (2013), and Norgate and Haque (2010) compared the energy saving potential and costs associated with various alternative grinding operations. Bouchard et al. (2017) and Numbi et al. (2014) used optimization modelling to study control strategies and determined the energy saving potential for grinding and jaw crushing, respectively, but did not assess the GHG emission saving potential.

The studies discussed above reveals gaps in the literature. They compared relatively small sub-sets of equipment and lack long-term sectoral analysis. The technology penetration rates, and the associated life cycle cost were not studied. This study aims to address these gaps by developing a bottom-up, system-wide energy assessment framework that can compare various GHG mitigation options in terms of their energy savings, cost of saved energy, GHG emission reduction potential, and their abatement costs.

1.6 Research objectives

The overall aim of this thesis study is to identify and analyze the end-use processes energy demand and GHG emissions in Canada's iron, gold, and potash mining sectors, and to evaluate various options in terms of their GHG mitigation potential and associated implementation costs. The research has following specific objectives.

- Provide a disaggregated end-use energy analysis of Canada's iron, gold, and potash mining sectors for the year 2015 at the regional and national levels using Sankey diagrams;
- Develop end-use energy consumption demand trees for the iron, gold, and potash mining sectors;
- Calculate the disaggregated end-use energy intensities, energy demand, and GHG emissions, by fuel source for 2015;
- Develop and validate a long-term, multi-regional energy model the iron, gold, and potash mining sectors to 2050;
- Identify GHG emission mitigation options through energy-use reduction scenarios;
- Develop a market share model for applicable scenarios with competing alternative technologies to determine the penetration of various technologies; and

- Calculate the cost of saved energy, energy saving potential, GHG emission mitigation potential, and cost of mitigation for each scenario.

1.7 Thesis outline

This thesis has 4 chapters, a table of contents, list of tables, list of figures, list of abbreviations, list of references, and an appendix. Chapters 2 and 3 have been submitted as separate papers for publication.

Chapter 1 provides a background on Canada's energy use and GHG emissions profile and its mineral mining sector. It outlines the objectives and scope of this research.

Chapter 2 discusses the development of energy and GHG Sankey diagrams for the iron, gold, and potash mining sectors in Canada. The extraction and processing techniques of these minerals and the energy consumption demand trees are presented.

Chapter 3 presents the LEAP-CANMIN model development method and analysis of GHG mitigation scenarios. The GHG mitigation potential of 24 scenarios is discussed and abatement cost curves are presented.

Chapter 4 concludes the research work and provides recommendations for future work.

2 Chapter II: Development of disaggregated energy use and greenhouse gas emission footprints in Canada’s iron, gold, and potash mining sectors¹

2.1 Introduction

The industrial sector is a major contributor to global greenhouse gas (GHG) emissions. It accounted for 28% and 30% of global energy use and GHG emissions, respectively, in 2010 (Fischedick et al., 2014). Industrial GHG emissions grew at an average annual rate of 3.5% worldwide between 2005 and 2010, despite a growing number of climate change mitigation policies (Fischedick et al., 2014). Industrial sector energy demand and GHG emissions need to be disaggregated and analyzed both to understand how energy is used and to design cost-effective GHG reduction strategies.

According to the Intergovernmental Panel on Climate Change (IPCC), a key challenge in assessing energy use reduction and GHG mitigation potential for the global industrial sector is the lack of complete and quality data on sub-sectoral processes and technology energy use (Fischedick et al., 2014). The available data is mainly aggregated at the sectoral and regional and/or national level. A breakdown of energy consumption and GHG emissions by process and fuel type is required to identify the production steps that consume the most energy and are the highest GHG emitters (Eckelman, 2010). The disaggregation also provides a benchmark to quantify the environmental and economic benefits of improving energy efficiency, fuel switching, process substitutions, and

¹ A version of this chapter is submitted for publication, titled: A. K. Katta, M. Davis, A. Kumar, “Development of disaggregated energy use and greenhouse gas emission footprints in Canada’s iron, gold, and potash mining sectors,” Resources, Conservation and Recycling (Submitted), 2019.

carbon capture and storage (Brueske et al., 2012; Natural Resources Canada, 2005a). These quantifications help us compare and prioritize GHG mitigation opportunities.

The Canadian mineral mining industry lacks disaggregated energy and GHG emissions data. Globally, Canada is one of the leading mineral extraction countries and one of the largest producers of metals and non-metals (Mining Association of Canada, 2016). This industry accounted for 18.2% of the goods exports in value and contributed 3.5% of the country's gross domestic product (GDP) in 2014. Canada extracts a diverse range of minerals, but the primary energy demands for the industry are mainly driven by three sectors, iron, gold, and potash mining. These together consumed 65% (93.8 PJ) of the energy and emitted 66% (3 million tonnes (MT) CO₂ eq.) of the mineral extraction industry energy demand and GHG emissions, respectively, in 2014 (Natural Resources Canada, 2018b). Energy use increased by 19%, 105%, and 8% between 2005 and 2014 for the iron, gold, and potash mining sectors, respectively. Moreover, Canada is the largest producer of potash, fifth largest producer of gold, and ninth largest producer of iron ore in the world (US Geological Survey, 2016).

Past studies have quantified, to differing degrees, the energy intensities of iron, gold, and potash mining operations. Canadian benchmark studies have examined the energy intensities in iron and gold mining operations by comparing energy consumption in various facilities (Natural Resources Canada, 2005a, 2005b). The studies aggregate the mining operations into large subgroups and the scope is limited to three iron ore mines producing concentrates and fifteen gold mines producing gold bars. Moreover, the studies do not provide the energy use by fuel type, ore type, and for all the processes in mining operations. The US Department of Energy modelled the energy requirements of various equipment types for surface iron, gold, and underground potash mines (US Department of Energy, 2002a, 2002b, 2002c). However, the study estimated energy intensities

for only some of the end-use processes. Also, energy intensities were not estimated for underground gold mining and potash solution mining operations. Griffing and Overcash (2010) estimated the energy intensities of taconite iron ore mining operations. Their study was limited to the estimation of device-level energy intensities for concentration processes and aggregated energy intensities for extraction processes. Bleiwas (2011) estimated only the electricity energy requirements of ore extraction equipment. Haque and Norgate (2015) conducted a life cycle analysis (LCA) and gave a breakdown of energy and GHG emission intensities for various mining and mineral processing steps in Australian high-grade (typically 60%) iron mines. The study did not provide the energy requirements for low-grade ores, which require additional processing, or for pelletizing processes. Norgate and Haque (2012) also used LCA to estimate the GHG footprint in gold mining but did not disaggregate the emissions into different end-use processes. Another Canadian study on potash production facilities presents aggregated energy consumption, energy intensity, energy use by type, and GHG emissions for extraction and milling operations (Government of Canada, 2003). Like the studies cited above, there is no process-level disaggregated energy-use information.

The existing literature on iron, gold, and potash mining does not include a comprehensive study on end-use energy intensities by fuel type for all operations. Past studies have been limited to aggregated energy intensities for some operations. Furthermore, energy use and GHG emissions data in the Canadian iron, gold, and potash mining sectors are not disaggregated to the end-use level. This research fills these gaps.

Another novelty of this study is the application of Sankey diagrams to illustrate the disaggregation of energy use and GHG emissions in iron, gold, and potash mining sectors. A Sankey diagram is a process visualization tool that shows the flow of energy from source to end use with arrows; the

width of the arrows represents the magnitude of the flow (Davis et al., 2018b). Its efficacy for showing energy and GHG emissions has been shown in the literature. Schmidt (2008) presented historical uses of these diagrams in energy and material management flow. Leal-Ayala et al. (2015) used a Sankey diagram to illustrate the energy consumption and mass flow from tungsten ore extraction to different end products. Brueske et al. (2012) mapped the flow of energy to various end uses in the US manufacturing sector in the form of a Sankey diagram that serves as a baseline for calculating the benefits of improved energy efficiency. Zhao et al. (2016) illustrated industrial residual energy flows via Sankey diagrams for 12 high energy consuming industry sectors in China. Their analysis found energy recovery potential in different sectors. Griffin et al. (2013) modelled Sankey energy flow diagrams of the UK's pulp and paper, chemical, iron and steel, food and drink, and cement manufacturing sectors. Perez-Lombard et al. (2011) used Sankey diagrams to map the energy flows of heating, ventilation, and air-conditioning systems used in office buildings in Spain and identified HVAC systems loads and losses. Cullen and Allwood (2010) mapped the global flow of energy from fuels through conversion devices and passive systems to final services in the form of Sankey diagram. Davis et al. (2018b) mapped the energy flow from primary fuel to end use in all the provinces and territories in Canada and used the mapped Sankeys to calculate the energy losses and useful energy consumption. Subramanyam et al. (2015) developed the Sankey diagrams for Alberta's energy demand and electricity generation supply sectors.

Sankey diagrams have also been used for GHG emission analysis. Davis et al. (2018a) used Sankey diagrams to illustrate GHG emissions in different Canadian economic sectors and the resources responsible for the emissions. Griffin et al. (2018) evaluated a GHG mitigation potential of 80% (between 1990 and 2050) for UK's pulp and paper sector through a Sankey diagram. The World

Resources Institute used a Sankey diagram to map global GHG emissions for the year 2000 (Baumert et al., 2005). Other examples include using Sankey diagrams to map global energy balances (International Energy Agency, 2019), US energy consumption (Lawrence Livermore National Laboratory, 2018), global exergy and carbon flow (Global climate and energy program (GCEP), 2009), and the substance flow of recycled materials from waste batteries and raw ore (Song et al., 2017). As these studies show, Sankey diagrams are an effective means of analyzing the energy use, energy type, and emissions, and they help focus efficiency improvement efforts in areas of high energy savings and GHG mitigation potential. However, an analysis does not exist for any mineral mining sector.

Hence, the objective of this study is to provide a disaggregated end-use energy and emissions analysis of three mining sectors in Canada for the year 2015 at the regional and national levels using Sankey diagrams. The specific objectives are to:

- Develop end-use energy consumption demand trees for the iron, gold, and potash mining sectors;
- Calculate the disaggregated end-use energy intensities, energy demand, and GHG emissions by fuel source for 2015 for Canada's iron, gold, and potash mining sectors; and
- Create Sankey diagrams that illustrate energy use and GHG emissions at the national, provincial, sectoral, and end-use levels for Canada's iron, gold, and potash mining sectors for the year 2015.

2.2 Method

The study had four main steps as illustrated in Figure 2-1. First, the production activity data related to 102 iron, gold, and potash mines in Canada for the years 2010 to 2015 was compiled (and is

discussed further in Section 2.2.1). Second, the end-use devices, fuels used, and their energy intensities were calculated to develop energy consumption demand trees (Section 2.2.2). Third, Long range Energy Alternatives Planning (LEAP) model (Davis et al., 2019; Heaps, 2016) was used to calculate the energy use and GHG emissions for the years 2010 to 2015 (Section 2.2.3). The aggregated results were validated by comparing them with Natural Resources Canada (2018b) data. Finally, Sankey diagrams were developed for the year 2015 (Section 2.2.4). 2015 was considered the study year since it was the latest year for which data is available.

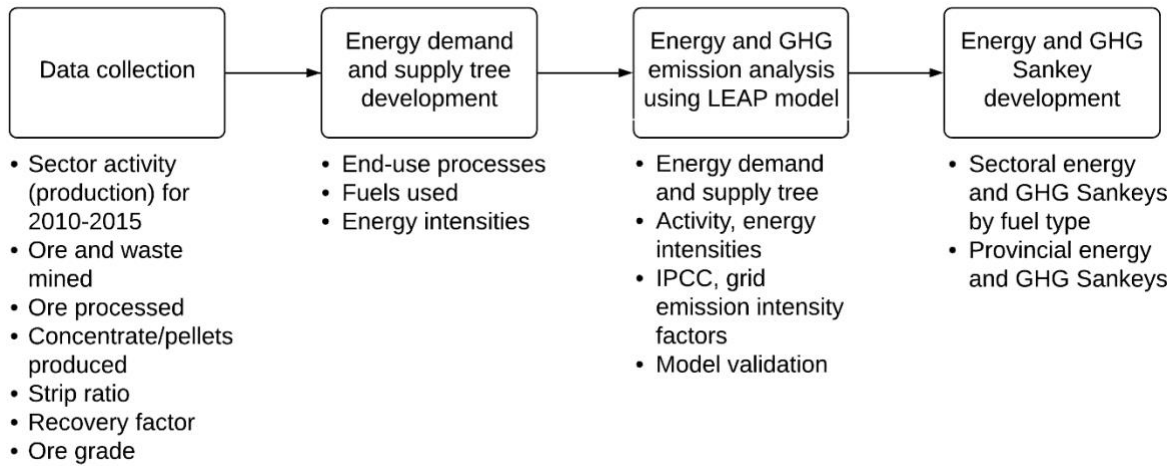


Figure 2-1: Method used in the study for disaggregating energy and GHG emissions

2.2.1 Production data

A dataset of annual iron, gold, and potash mining production activity for the years 2010 to 2015 in each Canadian province was compiled. A list of individual operating mines for both underground and open-pit mining operations in each province was obtained from the mining industry report (Mining Association of Canada, 2016) and are shown in Figure 2-2. Then, company reports from the System for Electronic Document Analysis and Retrieval (SEDAR) database (SEDAR, 2017) and annual statistics of mineral production by NRCan (Natural Resources Canada,

2018a) were used to obtain activity data. Activity data includes the ore and waste extracted, ore processed, ore produced, and the processing routes for each mine. We compiled calendar-year data of the ore type, ore grade, strip ratio and recovery factor, reported by companies. When data was not reported, we assumed that these values remained the same as they were the previous year, as the annual change for a given mine was not significant. Also, the total extracted ore in a given year is assumed to be sent for processing if the companies did not report them separately.

The study is limited to energy and GHG emissions from mines where iron, gold, and potash are the primary products. For example, gold is produced as a co-product or by-product in many other metal mines; those mines were excluded. This is in accordance with the North American Industry Classification System (NAICS) for mining industries (Statistics Canada, 2018), in which the mines with iron, gold, and potash as primary products are classified under NAICS codes 21221, 21222, 212396, respectively. The activity data compiled for the iron, gold, and potash sectors is shown in Table 2-1.

Table 2-1: Compiled activity data for the study

Iron ore mining	Gold ore mining (Both open-pit and underground mining)	Potash mining (Both conventional and solution mining)
Ore mined	Ore mined	
Waste mined	Waste mined	
Ore processed or milled	Ore processed or milled	Ore mined
Concentrate produced	Ore processed in gold extraction	Ore processed or milled
Pellets produced	Gold produced	Potash produced
Strip ratio	Strip ratio	Concentration ratio
Recovery factor	Ore grade (g/tonne)	

2.2.2 Energy demand tree development

The data related to end-use processes, fuel types used, energy intensities, and associated production from the different stages of iron, gold, and potash mining were obtained as described below. With this data, we developed end-use process energy consumption demand trees and calculated fuel-use intensities. These demand trees are a structured way of showing end-use processes and fuel types used in each sector.



Figure 2-2: Iron, gold, and potash producing mines of Canada (contains information licensed under the Open Government License – Canada (Natural Resources Canada, 2019a))

2.2.2.1 Iron ore mining

Iron is the second most abundant metal in the earth's crust. A typical iron-bearing ore consists of a variety of minerals in which the iron is primarily bonded with oxygen, water, carbon dioxide, or sulphur (US Department of Energy, 2002b). Among the minerals that constitute an iron ore deposit, the most important are magnetite (Fe_3O_4), hematite (Fe_2O_3), goethite ($\text{Fe}_2\text{O}_3 \cdot \text{H}_2\text{O}$), and limonite ($\text{Fe}_2\text{O}_3 \cdot \text{H}_2\text{O}$). They contain different amounts of iron, reaching up to 70% in hematite and 63% in goethite (Yellishetty et al., 2010). Canada has three types of iron ores deposits: high-grade ores (>50% Fe) of hematite/goethite known as direct shipping ores (DSOs), medium-grade (up to 41% Fe) specularite magnetite iron ore formations known as metataconites, and low-grade (15 to 30% Fe) magnetite ore formations known as taconites (Conliffe et al., 2012; Government of Newfoundland and Labrador, 2017). Over the past five decades, Canadian iron ore production has been concentrated in a geological region known as the Labrador Trough in Western Labrador and Northeastern Quebec, where metataconite and DSO deposits are mined continuously (Conliffe et al., 2012). The extracted iron ore is concentrated and made into pellets or sintered for feeding into a blast furnace to produce iron; this represents almost 95% of all the metals used by the industrial sector (Griffing and Overcash, 2010). In 2015, Canada produced 47 million tonnes of iron with production shares of 55%, 42%, and 3% in Quebec (QC), Newfoundland and Labrador (NFL), and Nunavut (NU), respectively (Arcelor Mittal, 2017; Cleveland Cliffs Inc., 2017; SEDAR, 2017). The stages of the mining process from ore extraction to a processed mineral can be divided into extraction, haulage, and ore processing (Härkisaari, 2015) and are described further below.

Energy use in ore extraction and haulage

The extraction stage involves the removal of overburden to reveal the underlying ore body. The ore body is subjected to drilling and blasting operations and is then loaded by electrical shovels, rope shovels, and hydraulic excavators onto haul trucks (Härkisaari, 2015). Drilling is done with ammonium nitrate fuel oil (ANFO) loader trucks, diamond drills, rotary drills, percussion drills, and drill boom jumbos, which run on electricity, diesel or compressed air (US Department of Energy, 2007). Soft ores are dug rather than drilled. Digging is a process of excavating or making a passage in the ore body for blasting (US Department of Energy, 2007). A benchmark study on the energy consumption of Canadian open-pit mines found the weighted average energy intensity of the drilling operation to be 1.05 Megajoule/tonne (MJ/t) of material removed, where the material removed is the sum of ore (O) mined and the waste (W) (top soil, overburden) excavated (Natural Resources Canada, 2005a). For the digging process, the energy intensity is estimated to be 1.33 MJ/t of W+O (US Department of Energy, 2007). The current study is limited to the use of fuels for energy consumption alone and hence the blasting operation, which uses emulsions, is excluded from the analysis. For the loading operation, the energy intensity of the electric power shovels and diesel wheel loaders is 3.24 MJ/t of W+O (Bleiwass, 2011) and 2.55 MJ/t of W+O (Natural Resources Canada, 2005a), respectively. Haulage is required to transport the ore to the processing facility. The haulage units include off-road dump trucks, conveyors, and trains. The haulage equipment is powered by diesel with an energy intensity of 11.73 MJ/t of W+O (Natural Resources Canada, 2005a).

Processing energy use

Processing involves upgrading and recovering the metal through beneficiation, which involves comminution and concentration to remove impurities and improve ore quality (Härkisaari, 2015). Comminution is the crushing and grinding of the ore to liberate minerals from the ore matrix and increase the surface area for higher reactivity. The comminution circuit can have a few to several stages of crushing, grinding, and screening (Jankovic, 2015). Gyratory, jaw, and cone crushers compress and break large rocks into coarse particles. After crushing, autogenous/semi-autogenous (AG/SAG) mills, ball mills, or pebble mills are used to grind the ore into even smaller uniform-sized particles. The energy intensity of the crushing, AG/SAG mill, and ball mill operations, which consume electricity, are 4.6, 20, and 91 MJ/t of ore crushed or milled, respectively (Griffing and Overcash, 2010; Natural Resources Canada, 2005a). Ball mills have a higher energy intensity than either crushing or the AG/SAG mill as they produce high grade concentrates suitable for pelletizing.

The concentration processes are gravity separation (to separate gangue and waste), magnetic separation (to separate magnetite), and flotation (to separate hematite) (US Department of Energy, 2002b). Electricity is the primary source of fuel in these processes. Gravity separation techniques include dense medium separation (DMS), jigging, and spiraling (Maré et al., 2015). The DMS process is the best choice for a non-porous feed. The separation medium is a dense liquid made up of very fine ferrosilicon particles in water. In the jigging process, a bed of ore is formed on a screen deck inside a water-filled chamber. A pulsing cycle, created with upward and downward movements of the water column, allows heavier particles to settle faster than lighter particles. Spiraling involves a combination of centrifugal and fluid-related responses to separate fines and

coarse particles, especially for wet fines processing. Hydroclone classifiers are used to separate particles by shape, size, and specific gravity in grinding circuits. Magnetic separation is used to remove non-magnetic materials from the ore. The flotation process, unlike the others, is energy intensive and expensive. In general, it is used after the ore has been enriched by other separation techniques. In the flotation process, the ore surface is treated with chemicals and suspended in a mechanically agitated and aerated water chamber. The valuable hydrophobic portion of the ore attaches to the air bubbles and rises to the surface for collection. The production flow diagram of iron ore processing is shown in Figure A1 in Appendix A. Jankovic (2015) discusses the processing methods in detail. The separation and concentration process energy intensities were obtained from NRCan (Natural Resources Canada, 2005a) and literature (Griffing and Overcash, 2010).

The high-grade DSOs are subjected to simple dry or wet processing of beneficiation to meet size requirements (Jankovic, 2015). The main processes are crushing and screening to separate lumps and fines. The ore is also subjected to density separation and then magnetic separation to remove magnetite content in the ore if necessary. Compared to DSOs, metataconite ores are much finer grained, and therefore processing involves significant crushing and grinding of run-of-mine ore to liberate magnetite from its silicate matrix, followed by gravity separation, flotation, and magnetic separation to produce concentrate (C) (Jankovic, 2015). The flotation process sometimes requires clusters of cyclones to remove ultrafine material. Some portion of the produced concentrate is filtered and passed to the pelletizing plant.

Pelletization energy use

Pelletizing involves pretreatment, agglomeration (balling), sieving, and firing to form pellets (P) of a consistent size (Griffing and Overcash, 2010). In the pretreatment process, the ore is ground into fines, dried, and pre-wetted for balling (Yamaguchi et al., 2010). The balling equipment consumes electricity and uses centrifugal force to form spheroids that are dried, fired, and then cooled in an indurating furnace. Hot and cold gases are moved in the furnace by fans or blowers. The energy intensities of the pelletizing operations were estimated from literature (Griffing and Overcash, 2010; Singh et al., 2015). The shares of coke and heavy fuel oil in the firing process were estimated by taking the ratio of energy demand for these fuels from NRCan's Energy Use Database (Natural Resources Canada, 2018b).

The other processes include drying and dewatering to separate water from the minerals using thickeners and filters (New Millennium Capital Corp., 2010). In addition, pumps for tailings disposal, conveyors, and material handling are used, as well as other equipment for support activities, service, and road maintenance (Natural Resources Canada, 2005a).

Some companies report annual strip ratio instead of the total material removed and annual recovery factor instead of the total material milled. The strip ratio is defined as the ratio of waste mined to ore mined and the recovery factor is defined as the ratio of iron concentrate (ore) produced to ore milled or processed. In such cases, the energy intensities available in terms of MJ/t of W+O for extraction processes were converted into MJ/t of O using the strip ratio, as shown in Equation 2-1. The energy intensity of comminution processes was converted from MJ/t of ore crushed or milled into MJ/t of C using the recovery factor and Equation 2-2.

$$\frac{\text{MJ}}{\text{t of O}} = \frac{\text{MJ}}{\text{t of W+O}} \times \left(1 + \frac{\text{W}}{\text{O}}\right) \quad (\text{Equation 2-1})$$

$$\frac{\text{MJ}}{\text{t of C}} = \frac{\text{MJ}}{\text{t of ore processed}} \div \text{Recovery factor} \quad (\text{Equation 2-2})$$

Extracted ore and concentrate and pellet production data were obtained from SEDAR (SEDAR, 2017), ArcelorMittal (Arcelor Mittal, 2017), and Cleveland-Cliffs (Cleveland Cliffs Inc., 2017) and are shown in Table A1 in Appendix A. DSO ores are mined only in Newfoundland. The concentrate production in the table includes the concentrate used for pellet production. The end-use processes and fuels used are shown in the form of energy consumption demand tree in Figure 2-3, and their energy intensities are in Table 2-2.

Table 2-2: End-use process energy intensities of iron mining

Process	Sub-process	Fuel	Energy intensity	Units	Source
Ore extraction	Drilling	Diesel	1.0	MJ/t material removed	(Natural Resources Canada, 2005a)
	Digging	Diesel	1.3	MJ/t material removed	(US Department of Energy, 2007)
	Loading (wheel loaders)	Diesel	2.6	MJ/t material removed	
	Loading (electric shovels)	Electricity	3.2	MJ/t material removed	(Bleiwas, 2011)
	Haulage (trucks)	Diesel	11.7	MJ/t material removed	(Natural Resources Canada, 2005a)
	Haulage (conveyors)	Electricity	4.1	MJ/t ore	(Ferreira and Leite, 2015)
	Support activities	Diesel	2.5	MJ/t material removed	(Natural Resources Canada, 2005a)
	Dewatering	Electricity	1	MJ/t material removed	
Comminution (DSO)	Crushing	Electricity	20	MJ/t ore processed	(Griffing and Overcash, 2010)
Comminution (Metataconite ore)	Primary crushing	Electricity	4.6	MJ/t ore processed	(Natural Resources Canada, 2005a)
	Grinding	Electricity	14.3	MJ/t ore processed	
	Ball mill grinding	Electricity	91	MJ/t ore processed	(Griffing and Overcash, 2010)
	Screening	Electricity	0.2	MJ/t ore produced	(US Department of Energy, 2002b)

Process	Sub-process	Fuel	Energy intensity	Units	Source
	Conveyors	Electricity	0.0003	MJ/t ore produced	(Griffing and Overcash, 2010)
	De-sliming	Electricity	5.0	MJ/t ore produced	(US Department of Energy, 2007)
Processing	Density separator/flotation	Electricity	31.6	MJ/t ore produced	(Griffing and Overcash, 2010)
	Magnetic separation	Electricity	8	MJ/t ore produced	(Griffing and Overcash, 2010)
	Spiral plant	Electricity	5.0	MJ/t ore produced	(US Department of Energy, 2007)
	Pumps for slurry transport	Electricity	1	MJ/t of ore produced	(US Department of Energy, 2007)
	Hematite plant	Electricity	1.1	MJ/t ore produced	(Griffing and Overcash, 2010)
Pelletization	Filtering	Electricity	65.6	MJ/t pellets produced	(Griffing and Overcash, 2010)
	Balling	Electricity	51.8	MJ/t pellets produced	
	Firing	Heavy fuel oil/Coke	946	MJ/t pellets produced	
	Firing	Electricity	3.6	MJ/t pellets produced	
Other activities	Tailings pumps	Electricity	6.7	MJ/t ore processed	(Natural Resources Canada, 2005a)
	Process water	Electricity	6.1	MJ/t ore processed	
	Other plant energy	Electricity	9.8	MJ/t ore processed	(New Millennium Capital Corp., 2010)
	Drying	Diesel	54.7	MJ/t ore produced	
	Stacking and reclamation	Diesel	1.8	MJ/t ore produced	(Haque and Norgate, 2015)
	General and administrative	Electricity	4.7	MJ/ore processed	(Natural Resources Canada, 2005a)
	Port operations	Electricity	3.2	MJ/t ore produced	(Haque and Norgate, 2015)

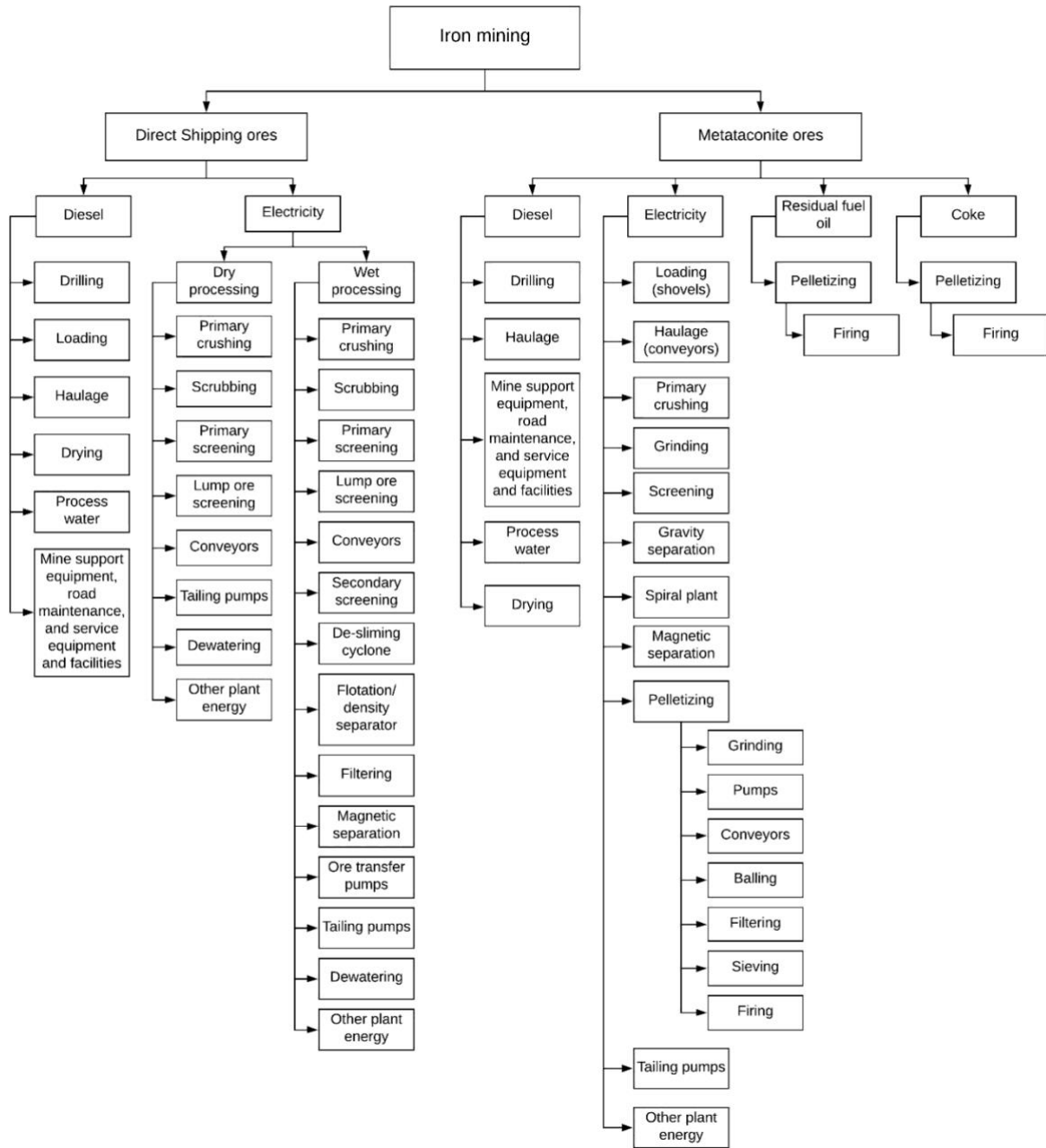


Figure 2-3: Energy demand tree for iron mining

2.2.2.2 Gold mining

Gold production in Canada is mainly concentrated in Ontario and Quebec, where, in 2015, 50% and 28% of the country's 148,953 kilograms of gold was produced (SEDAR, 2017). 3% of this total production was a by-product of other metal mining operations. 9%, 8%, 2%, 2%, and 1% of the gold production in 2015 was from British Columbia (BC), Nunavut (NU), Saskatchewan (SK), Manitoba (MB), and Yukon (YU), respectively. The mining process can be divided into ore extraction, comminution, gold extraction, gold recovery, and post-recovery processes (Marsden, 2006; US Department of Energy, 2002a).

Ore extraction and comminution energy use

Ore is extracted through open-pit and underground mining (Mining Association of Canada, 2016). In 2015, 64% of production was from underground mines, and 94% of underground mine production is from Ontario and Quebec (SEDAR, 2017). Apart from drilling and blasting operations, underground mining requires underground crushing, ore hoisting, ventilation, and backfilling (Natural Resources Canada, 2005b). The energy intensities for ore extraction processes were obtained from previously developed benchmarks (Natural Resources Canada, 2005b). After extraction, the ore is crushed and ground into uniformly sized particles. Sulphide ores have a higher energy demand than other ore types as they are subjected to roasting, chlorination, bio-oxidation, or autoclaving to oxidize the sulphide-bearing minerals (US Department of Energy, 2002a). The energy intensity is defined as MJ/t of O+W removed for open-pit ore extraction processes, MJ/t of O for underground ore extraction, and MJ/t of ore processed for comminution processes, and is shown in Table 2-3. Ore haulage using diesel equipment has the highest energy intensity in open

pit mines. For underground mines, ventilation is responsible for about 50% of the total ore extraction energy demand.

Gold extraction energy use

Flotation, gravity concentration, and leaching (heap leaching or tank leaching) are used to extract gold from ore (Marsden, 2006). Leaching is done by applying lime, sodium, or potassium cyanide solution to open heaps or to ore slurry in tanks; the former is used to extract gold from low-grade ores and the latter for high-grade ores (Marsden, 2006; US Department of Energy, 2002a). Gravity concentration is used to separate free elemental gold in the ore before the leaching process. Flotation is used prior to leaching if the ore contains sulphides (Norgate and Haque, 2012). The slurry, flotation, and gravity concentrate undergo processes to recover gold. The energy intensity is defined as MJ/t of ore processed. Electricity and natural gas are the fuels used in these processes; their energy intensities are shown in Table 2-3.

Gold recovery energy use

The different recovery methods include the Merrill-Crowe process and the activated carbon adsorption process. In the Merrill-Crowe process, zinc is added to precipitate the gold and form a zinc-cyanide complex, which undergoes solid-liquid separation (US Department of Energy, 2002a). The energy use details data for this process is not available in the literature. The carbon adsorption process can be done through the carbon-in-pulp (CIP), carbon-in-column (CIC), or carbon-in-leach (CIL) method (Norgate and Haque, 2012). In the CIP process, the activated carbon granules are added to a series of agitated slurry tanks to adsorb the gold. As the slurry flows from tank to tank, the gold in the slurry gets loaded onto the carbon. The CIL process is used to treat

carbonaceous ores when leaching and adsorption occur in a single process. The CIC operation is primarily used for heap leach solutions in which the solution flows upward through a series of fluidized bed columns (Kubach, 1994). The energy demand in these processes is from the use of electricity to agitate and pump the slurry. The energy intensities for the end-use processes in the recovery stage are shown in Table 2-3.

Post-recovery energy use

The gold is stripped from the activated carbon and plated through electrowinning and then smelted (Marsden, 2006). Electrowinning is the process of plating the gold from the solution onto a cathode (US Department of Energy, 2002a). In some cases, the gravity or flotation concentrate is directly smelted. The energy intensity in terms of MJ/t of product (Au) is shown in Table 2-3.

The total material extracted, ore extracted in open-pit and underground mines, ore milled, and ore processed through gold extraction and recovery techniques for the years 2010 to 2015 are shown in Table A2 in Appendix A. Depending on the ore, mining companies use a mix of extraction and recovery techniques. Therefore, for each operating mine, we used the process flow sheets to consolidate the production of gold through different extraction, recovery, and post-recovery processing routes in each province. The data is shown in Table A3 in Appendix A. Around 50% of the gold is extracted through agitated cyanide leaching, 83% is recovered through CIP and CIL, and 79% is electrowinned. This approach is used for each province to calculate the total energy consumption and emissions.

The process flow diagram for gold mining is shown Figure A2 in Appendix A. The intensities for ore extraction and comminution processes were obtained from NRCan (Natural Resources Canada,

2005a, 2005b) and SEDAR (SEDAR, 2017). For the gold extraction and recovery processes, Norgate and Haque (2012) estimated the energy intensities and fuels used for an ore grade of 3.5g/t Au. These values were adjusted to the Canadian ore grades to calculate energy consumption. The total energy used for mine air heating was calculated using Equation 2-3, obtained from literature (Mine Wiki, 2018), as device-level energy intensity is not available in the literature. The energy is met by propane fuel.

$$\text{Propane energy consumption} = \frac{\frac{m_{\text{air}}}{m_{\text{ore}}} \times C_{p,\text{air}} \times (T_{\text{req,air}} - T_{\text{amb,air}}) \times m_{\text{ore}}}{\eta_{\text{propane heater}} \times \left(\frac{12}{N}\right)} \quad (\text{Equation 2-3})$$

In the equation, $\frac{m_{\text{air}}}{m_{\text{ore}}}$ is the ratio of mass air flow required per mass ore produced, $C_{p,\text{air}}$ is the specific heat capacity of air, $T_{\text{req,air}}$ is the recommended temperature to which air is heated, $T_{\text{amb,air}}$ is the ambient temperature of the outside air, $\eta_{\text{propane heater}}$ is the efficiency of the propane heater, and N is the number of months of air heating required.

The ratio of mass air flow required per mass ore produced is 2.4 for the block caving mining method and 11.8 for non-block cave mining methods (Wallace, 2001). The methods used by mining companies in Canada were obtained from SEDAR (SEDAR, 2017). The recommended air temperature is 50° C, the efficiency of the propane heater is 90%, the number of months mine air heating is required was considered to be 3, and the specific heat of air is 1.005 kJ/kg.K (Mine Wiki, 2018). The average ambient air temperatures were obtained from Environment Canada's Temperature Climatology Map (Government of Canada, 2018a). Using these values and Equation 2-3, we calculated the total propane energy consumption to be in the range of 0.01 to 1.02 GJ, as shown in Table A4 in Appendix A. The energy demand tree is shown in Figure 2-4.

Table 2-3: End-use process energy intensities of gold mining

Process	Sub-process	Fuel	Energy intensity	Units	Source	
Ore extraction	Open pit mining					
		Drilling	Diesel	1.0	MJ/t material removed	
		Transport/haulage	Diesel	11.7	MJ/t material removed	
		Support equipment	Diesel	2.5	MJ/t material removed	(Natural Resources Canada, 2005a)
		Dewatering	Electricity	1.0	MJ/t material removed	
		Loading	Diesel	2.5	MJ/t material removed	
			Electricity	3.2	MJ/t material removed	(Bleiwas, 2011)
		Underground mining				
		Drilling	Diesel	29.6	MJ/t of ore mined	
		Mucking	Diesel	23.3	MJ/t of ore mined	
		Transport	Diesel	11.7	MJ/t of ore mined	
		Underground crushing	Electricity	3.3	MJ/t of ore mined	(Natural Resources Canada, 2005b)
		Hoisting	Electricity	33.0	MJ/t of ore mined	
		Ore transport to mill	Diesel	11.7	MJ/t of ore mined	
		Ventilation	Electricity	159.6	MJ/t of ore mined	
		Backfill	Electricity	14.9	MJ/t of ore mined	
		Dewatering	Electricity	13.6	MJ/t of ore mined	
	Other underground support	Diesel	21.2	MJ/t of ore mined		
	Mine air heating	Propane	Table A4 in Appendix A			
Comminution	Crushing	Electricity	5.6	MJ/t of ore processed	(Natural Resources Canada, 2005a)	
	Grinding	Electricity	46.8/23.3/83.4/61.2/28.8	MJ/t of ore processed	(Natural Resources Canada, 2005a; 2015)	
Gold extraction	Flotation concentrate autoclave	Natural gas	6.8	MJ/t of ore processed		
		Electricity	43.6	MJ/t of ore processed		
	Flotation and agitated cyanide leaching	Electricity	43.6	MJ/t of ore processed		
	Gravity concentration	Electricity	11.1	MJ/t of ore processed		
	Agitated cyanide leaching	Electricity	5.0	MJ/t of ore processed	(Norgate and Haque, 2012)	
	Flotation only	Electricity	10.8	MJ/t of ore processed		
	Flotation and gravity concentration	Electricity	21.9	MJ/t of ore processed		
	DMS and gravity concentration	Electricity	21.9	MJ/t of ore processed		
	Cyanidation in grinding	Electricity	5.0	MJ/t of ore processed		
Gold Recovery	Merrill-Crowe	Electricity	NA			
	Intensive cyanidation	Electricity	20.9	MJ/t of ore processed	(Norgate and Haque, 2012)	
	CIP,CIL,CIC	Electricity	20.9	MJ/t of ore processed		
Post recovery	Electrowinning	Electricity	11160	MJ/t of Au	(Norgate and Haque, 2012)	
	Smelting	Natural gas	0.4	MJ/t of Au		

Process	Sub-process	Fuel	Energy intensity	Units	Source
Other activities	Mill heating	Natural gas	19.8	MJ/t of ore mined	(Natural Resources Canada, 2005a)
	Tailings	Electricity	4.1	MJ/t of ore mined	
	General and administrative	Electricity	4.7	MJ/t of ore mined	

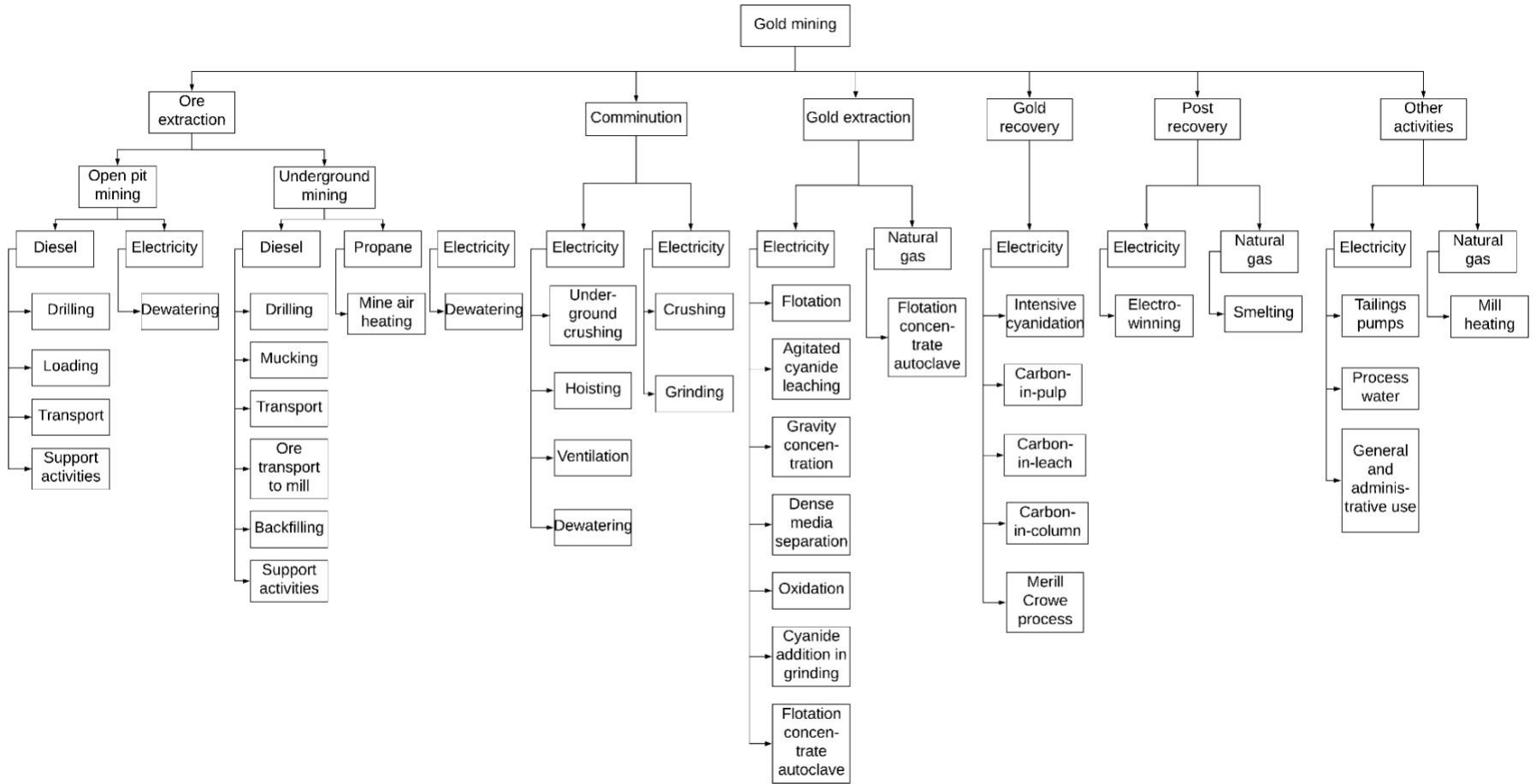


Figure 2-4: Energy demand tree for gold mining

2.2.2.3 Potash mining

Potash refers to potassium compounds and potassium-bearing materials that exist predominantly in mineral form as sylvinite containing sylvite or potassium chloride (KCl) and halite (NaCl) (Garrett, 1996). Potassium is mined through conventional mining and solution mining (Garrett, 1996; Government of Canada, 2018b). Canada has 10 mines in SK and 1 in NB (SEDAR, 2017). 2 mines in SK use solution mining and the rest (87%, as of 2015) use conventional mining. Conventional mining involves drilling, blasting, and using continuous mining machines to mine the mine seam. Then conveyors transfer the ore to underground bins that are hoisted to the surface. In solution mining, brine is injected into the mine and circulated underground to dissolve the potash and salt. The brine is then pumped to an evaporation pond on the surface where the potash and salt crystals settle to the bottom of the pond. The potash is removed from the pond and pumped to the mill for recovery. Solution mining is highly energy intensive compared to conventional mining due to the high thermal and electricity requirement for steam generation and pumping operations. The obtained ore is crushed to free the KCl, which is ground into fine particles, and then the clay is scrubbed off. Then, potash is separated using flotation and dried in natural gas kilns. Later, it is screened to classify the particles, and the fine particles are compacted to make a larger size. The energy demand tree is shown in Figure 2-5 and the process flow diagram is shown in Figure A3 in Appendix A. The share of the energy use of ore extraction, crushing, flotation, screening, and compaction end-use devices were obtained from a study by the US Department of Energy (US Department of Energy, 2002c). Using these shares, the total energy intensities from a benchmark study on Canadian potash facilities (Government of Canada, 2003) were disaggregated to obtain the energy intensities of the sub-processes shown in Table 2-4. Potash production data was taken from companies' annual reports, technical reports, and filings by SEDAR and the US Securities

and Exchange Commission (SEDAR, 2017; US Securities and Exchange Commission) and is as shown in Table A5 in Appendix A.

Table 2-4: End-use process energy intensities of potash mining

Process	Sub-process	Fuel	Energy intensity	Units	
Ore Extraction	Conventional mining				
		Mining machines	Electricity	43.2	MJ/t product
		Hoisting	Electricity	37.8	MJ/t product
		Conveyors	Electricity	9.5	MJ/t product
		Ventilation	Electricity	17.3	MJ/t product
		Dewatering	Electricity	38.6	MJ/t product
		Air heating	Natural gas	64.8	MJ/t product
		Backfill pumps	Electricity	0.2	MJ/t product
		Trucks	Diesel	18.6	MJ/t product
		Solution mining			
		Steam and crystallization pumps	Electricity	791.9	MJ/t product
		Steam generation	Natural gas	817.2	MJ/t product
		Trucks	Diesel	18.6	MJ/t product
Recovery		Crushing	Electricity	1.4	MJ/t product
		Grinding	Electricity	268.7	MJ/t product
		Flotation	Electricity	17.9	MJ/t product
		Screening	Electricity	0.04	MJ/t product
		Compactor	Electricity	0.04	MJ/t product
		Building heating, steam generation and product drying	Natural gas	2782.8	MJ/t product

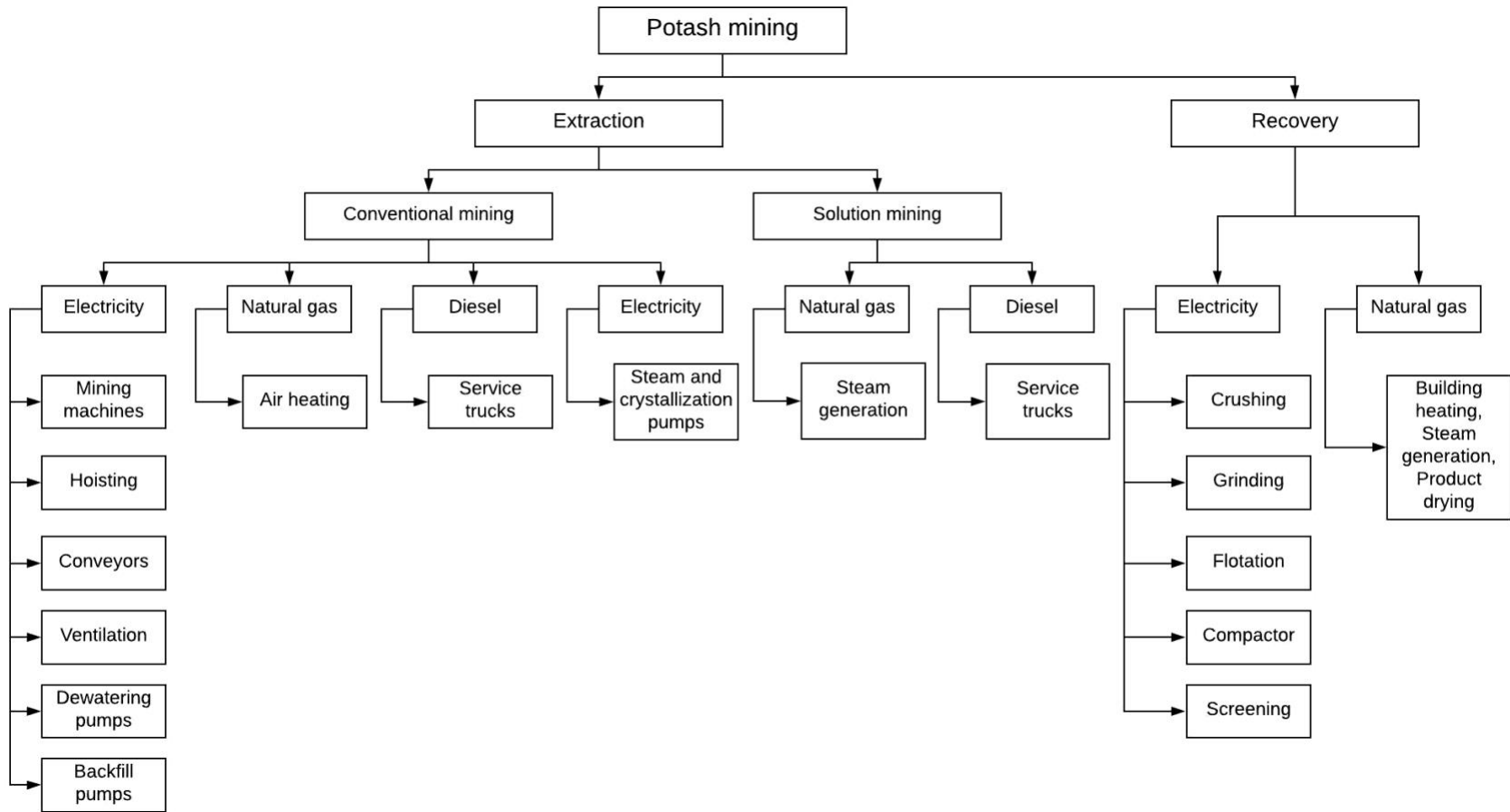


Figure 2-5: Energy demand tree for potash mining

2.2.3 Energy and GHG emission analysis

The energy demand trees and process energy intensities defined above were used to develop a bottom-up energy-environmental model of Canada's iron, gold, and potash mineral mining sectors (LEAP-CANMIN). The LEAP modeling system was chosen to model these sectors because it is a bottom-up energy and environmental modeling tool with extensive scenario analysis capabilities. LEAP is a widely used model for energy and GHG emission analysis. Its efficacy has been demonstrated through its use in many countries, including in submissions to the United Nations Framework on Climate Change (UNFCCC), developing the energy demand outlook by the Association of Southeast Asian Countries (ASEAN) (Stockholm Environment Institute, 2018), for national and provincial energy and GHG analysis (Davis et al., 2018a, 2018b; Subramanyam et al., 2015), and for GHG mitigation scenario analysis in the cement industry (Talaie et al., 2019) and the residential sector (Subramanyam et al., 2017b).

The energy intensities and corresponding mining activity were used to calculate annual sectoral and end-use process-level energy consumption for the years 2010 to 2015. The corresponding GHG emissions (CO₂ eq.) were calculated by applying IPCC emission factors through LEAP's Technology Environmental Database (TED). For electricity-related emissions, the provincial grid emissions factors estimated by Davis et al. (2019) were used in the LEAP-CANMIN model (shown in Table A6 of Appendix A).

The LEAP-CANMIN model calculates the end-use energy demand and GHG emissions from each fuel type for all the mining operations in each Canadian province using Equation 2-4 and Equation 2-5. The activity data variable (A) varies depending on the end-use, as explained in section 2.2. The LEAP-CANSIM model was validated by comparing the output of total energy demand and

GHG emissions in iron, gold, and potash mining for the years 2010 to 2015 with NRCan data (Natural Resources Canada, 2018b) .

$$\mathbf{E}_{ij_x} = (\mathbf{e}_i)_j \times \mathbf{A} \quad (\text{Equation 2-4})$$

$$\mathbf{GHG}_{ij_x} = (\mathbf{E})_{ij_x} \times \mathbf{EF} \quad (\text{Equation 2-5})$$

In these equations, E_{ij} is the energy consumption in end-use device i by fuel type j , e is the energy intensity, i is the end-use device, j is the fuel type (electricity, diesel, heavy fuel oil, coke, natural gas), A is the activity (material removed [ore+waste] or ore mined or ore processed or ore produced), x is the sector (iron, gold, or potash mining), $GHG_{ij,x}$ is the CO₂ eq. emissions in process i by fuel type j , and EF is the emission intensity factor.

2.2.4 Development of Sankey diagrams

Sankey diagrams for energy and GHGs were developed using the software “e!Sankey pro” for the year 2015 (Hamburg, 2019). In a Sankey diagram, the width of the bands or arrows is proportional to the amount of energy the process consumes or the GHGs it emits. The energy and GHG Sankeys are used to illustrate the flow of energy through each energy carrier to end use and the associated GHG emissions. The Sankeys for each sector are structured as shown in Figure 2-6 with the arrows representing energy or GHG emissions. In addition, in order to understand provincial energy demand and GHG emissions from each sector, we developed the Sankeys shown in Figure 2-7.

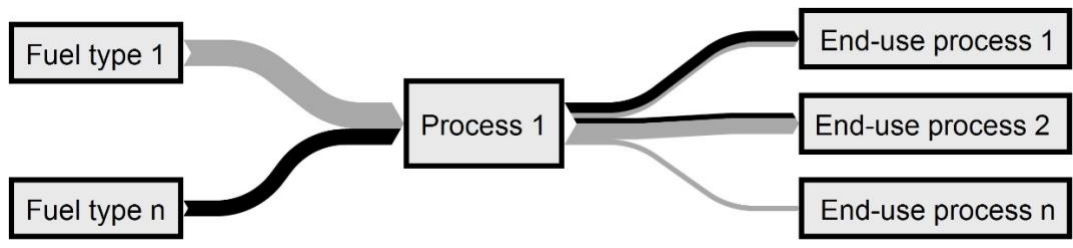


Figure 2-6: Basic Sankey structure for sectoral energy and GHG emissions

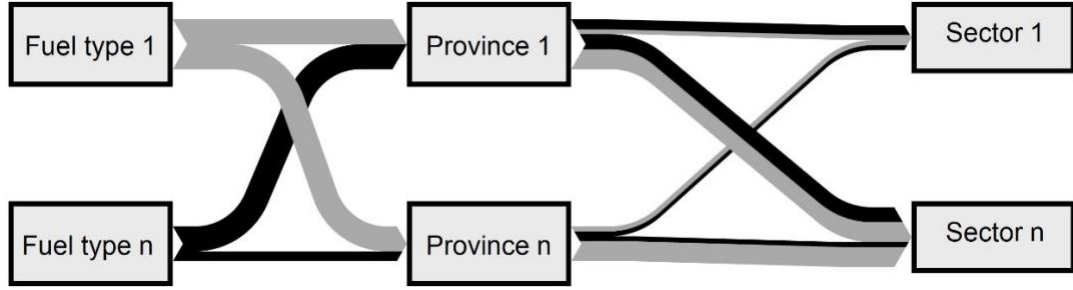


Figure 2-7: Basic Sankey structure for Canada's provincial energy and GHG emission

2.3 Results and Discussion

2.3.1 Energy and GHG Sankey for iron mining

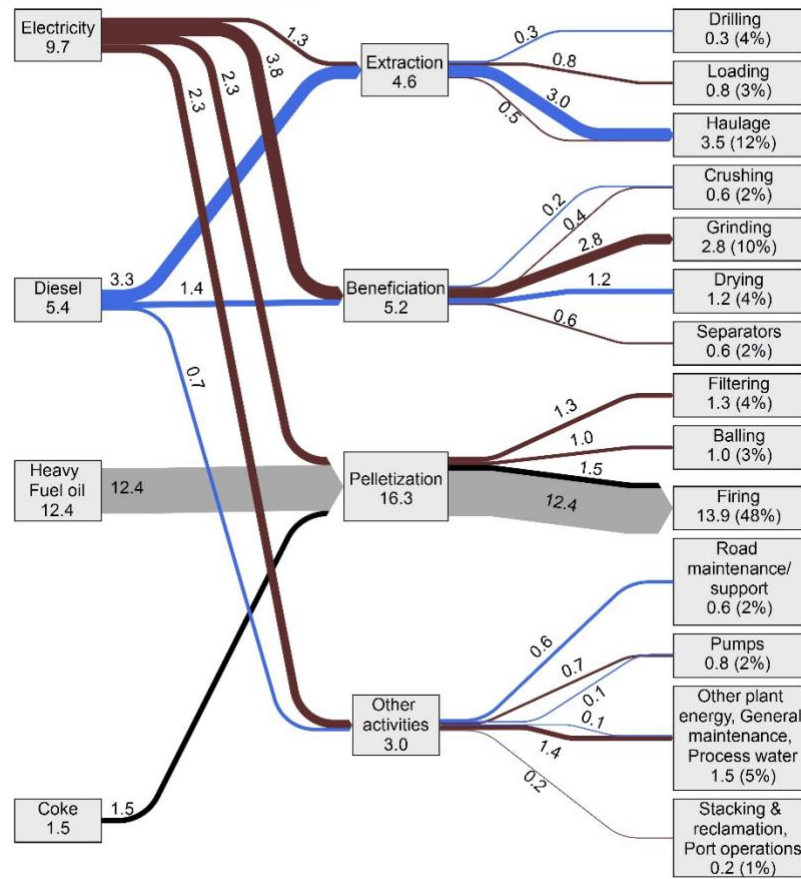
The energy and GHG Sankeys for Canada's iron ore mining sector are illustrated in Figure 2-8. In 2015, 43%, 33%, 19%, and 5% of the 29 PJ energy demand was met by heavy fuel oil, electricity, diesel, and coke, respectively. 33% of the electricity used was for comminution, 55% of the diesel used was for haulage activities, and 100% of the heavy fuel oil and coke was used in the firing operations. The pelletization process consumed 56% of the energy, while extraction, beneficiation, and other activities consumed 16%, 17%, and 11%. At the end-use level, the firing process consumed 48% of the energy intake followed by 12% each in haulage and comminution operations. In 2015, DSOs represented 5% of the production and consumed only 2% of the total energy demand.

In 2015, 1506 thousand tonnes of GHGs were emitted by the sector. Most of the emissions (85%) were from heavy fuel oil and diesel. 30% of the electricity-related emissions were from the comminution process, and emissions shares from the other operations ranged from 6% to 17%. 69% of the diesel emissions were from haulage and road maintenance fleet. At the end-use level, firing and haulage were responsible for 68% and 15% of the total emissions, respectively. It can be noted that although 19% of the sectorial energy demand was met by electricity, it contributed only 6% of the emissions due to its lower emissions intensity factor.

2.3.2 Energy and GHG Sankey for gold mining

The gold mining sector's energy demand and GHG emissions are shown in Figure 2-9. In 2015, the 24 PJ energy demand was met by electricity (57%), diesel (32%), natural gas (6%), and propane (6%). The post-recovery operations, electrowinning and smelting, consumed 2,340 GJ and had a negligible share (0.01%) of energy demand. The electricity-intensive ventilation and grinding operations consumed 35% and 29% of the electricity used. 33% of diesel use was for ore haulage and 100% of propane use was for mine air heating. Ore extraction energy consumption was 13.2 PJ, which accounted for 62% of the energy demand. Of this total, open-pit mining operations were responsible for 26% of energy use and 74% was consumed by underground mines. The high energy demand of underground mines was due to ventilation requirements to meet the air quality. Ventilation consumed 49% of underground extraction operations' energy demand. Among the end uses, ventilation, comminution, and haulage operations were responsible for 50% of the energy use with shares of 21%, 21%, and 10%, respectively.

Energy demand (Units in PJ)



GHG emissions (Units in 1000 tonnes)

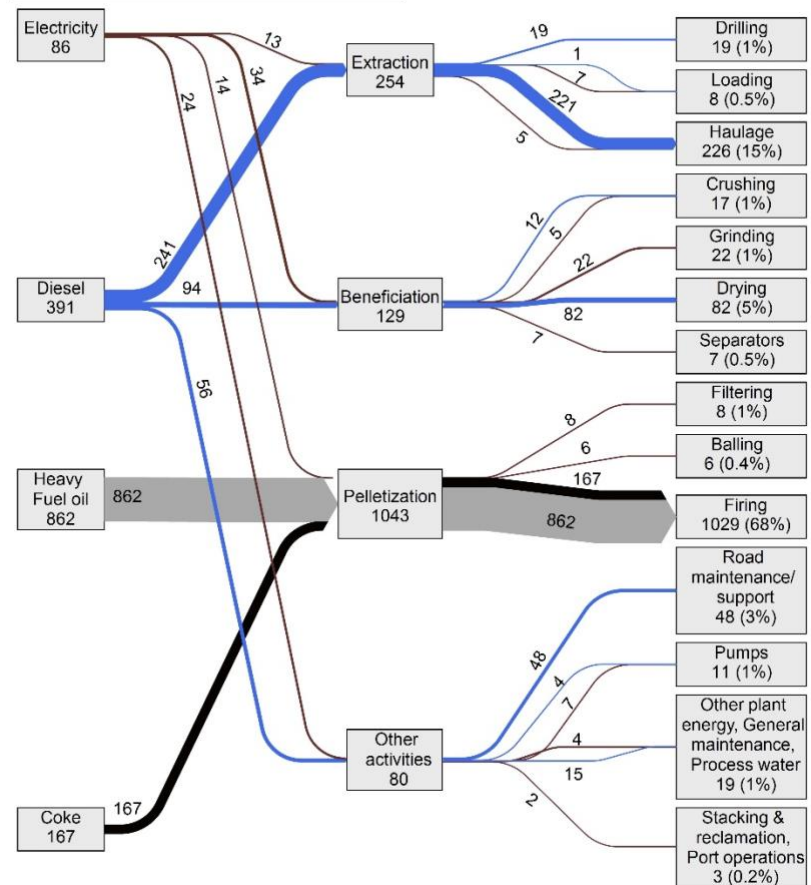


Figure 2-8: Sankey diagram for iron mining energy demand (left) and GHG emissions (right) in Canada in 2015

In 2015, Canada's gold mining sector emitted 762 thousand tonnes of GHGs. A significant share (69%) of these emissions were from diesel consumption. Among the processes, ore extraction emissions were 76% of the total. 29% of the electricity-related emissions were due to ventilation, followed by 17% from comminution operations. At the end-use level, 31% of the emissions were from ore transportation in both open-pit and underground mines. The emissions from gold extraction, recovery, and post-recovery processes were insignificant, ~0-3%, primarily because a major share (75%) of gold production was from Quebec and Ontario, where electricity generation is through renewable energy sources. In addition, 57% of the energy demand was met by electricity, but the emissions were only 10% of the total.

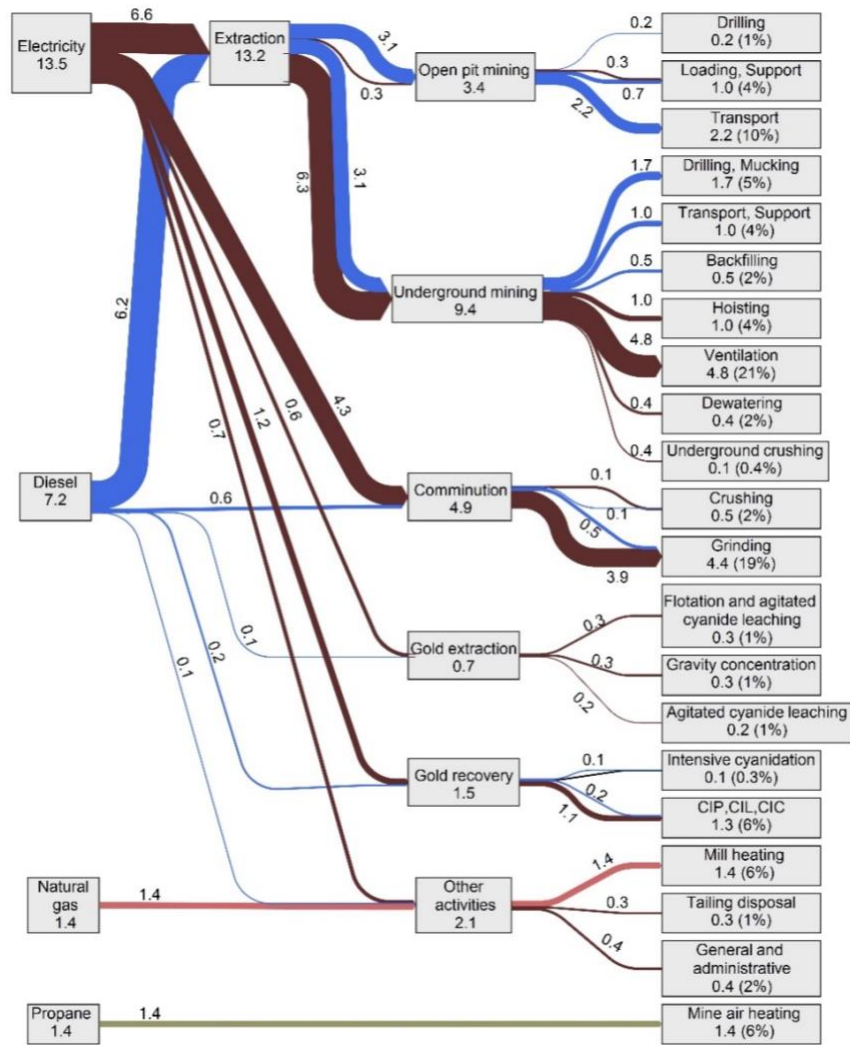
2.3.3 Energy and GHG Sankey for potash mining

Potash mining energy demand was 33.1 PJ in 2015. The different fuels used, the end uses, and their energy consumption and GHG emissions are illustrated in Figure 2-10. 69%, 29% and 1% of the energy demand was met by natural gas, electricity, and diesel, respectively. Crushing and grinding operations consumed 53% of the total electricity. Diesel is used primarily in conventional mining for haulage operations, and its use in solution mining is limited to service trucks. Solution mining consumed 29% of the natural gas used to generate steam, which is pumped into underground mines. The heat and steam generation units used for product drying and steam generation in recovery operations made up 67% of the sectorial natural gas demand. Although only 13% of the extracted potash was through solution mining, it consumed 69% of the extraction energy demand of 12.3 PJ. Compared to extraction operations, recovery processes had a high energy consumption (20.1 PJ, or 63% of the potash mining energy demand). Among the end uses, the heat and steam generation units in the recovery process were responsible for 47% of the energy

demand followed by the solution mining steam generation units and crushing/grinding operations, with shares of 20% and 15%, respectively.

In 2015, Canada's potash mining sector emitted 2974 thousand tonnes of GHGs. 50%, 49%, and 1% of these emissions were from natural gas, electricity, and diesel use, respectively. Conventional extraction mining emits 37% fewer emissions than solution mining as the latter uses natural gas to generate steam. Overall, the extraction operations emitted 1165 thousand tonnes (39%) and the recovery processes emitted 1809 thousand tonnes (61%). More than half (52%) the electricity related emissions were in comminution, followed by 20% share for steam and crystallization pumps. Natural gas usage for steam generation in extraction and recovery processes represented 29% and 67% of the total sectorial natural gas related emissions. Among the end-uses, significant amount of emissions were from the heat and steam generation units in potash recovery operations (34%) and crushing/grinding (25%).

Energy demand (Units in PJ)



GHG emissions (Units in 1000 tonnes)

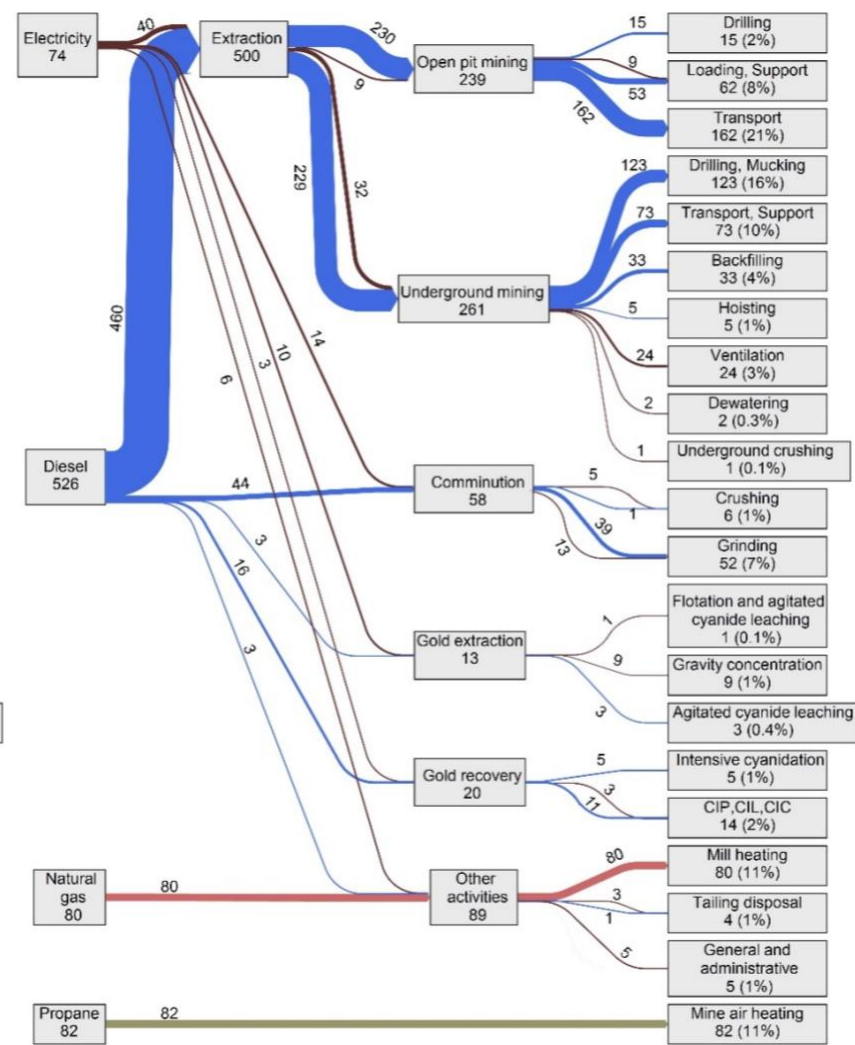


Figure 2-9: Sankey diagram for gold mining energy demand (left) and GHG emissions (right) in Canada in 2015

2.3.4 Integrated energy Sankey and GHG Sankey for all provinces with iron, gold, and potash mining operations

The total energy demand for the iron, gold, and potash mining sectors in Canada was estimated to be 84.6 PJ in 2015 and is shown in Figure 2-11. Of this total, the potash mining sector consumed the most energy, 33.1 PJ (39%), followed by the iron mining sector 29 PJ (34%) and the gold mining sector 23.8 PJ (28%). The energy demand was highest in SK (32.4 PJ, 38%), followed by QC (19.4 PJ, 23%), NFL (16.3 PJ, 19%), and ON (12.8 PJ, 15%). Only 4% of the total was from BC, NB, YK, and NU. SK's high energy demand was due to its potash production (the world's largest). ON's high energy demand was a result of its gold mining operations; it has more than any other province. QC's energy demand was due to both iron and gold mining operations and NFL's was mainly due to iron mining operations. SK's electricity (30%) and natural gas demand (92%) were highest due to the comminution and recovery operations in potash mining. ON and QC consumed 69% and 28% of the propane. Almost all of Canada's underground gold mines are in those provinces. Coke and heavy fuel oil were used in iron ore pelletizing processes, which are concentrated in QC and NFL. YK's energy demand was driven by placer gold mining activities. In NU, iron mining commenced in 2014 and consumed only 0.3 PJ (0.3%) in 2015. NB's share of potash production was only 4% of the country's production and consumed only 0.9 PJ, or 3% of total potash mining sector energy demand. The overall energy intensities for iron, gold, and potash mining is 0.6, 164.8, and 1.8 GJ/tonne of product, respectively. The overall energy intensity for iron mining is lower in NFL than in QC. This is because around 12% of the ore extracted in NFL was from DSO ores that contain higher concentrations of iron. ON and QC have higher overall energy intensities for gold mining than other provinces as almost 73% and 67% of the ore extracted

in ON and QC is from underground mines. In the case of potash mining, the high overall energy intensity is due to solution mining in SK.

The iron, gold, and potash mining sectors' GHG emissions in the year 2015 were estimated to be 5242 thousand tonnes CO₂ eq. The overall GHG emissions intensity for iron, gold, and potash mining is 31, 5278, and 157 kg CO₂ eq./tonne of product, respectively. The emissions were disaggregated for each province by sector and fuel type, as shown in Figure 2-12. The emissions were highest for electricity (31%), followed by natural gas (30%), diesel (18%), heavy fuel oil (16%), coke (3%), and propane (2%). A significant amount of GHG emissions was from SK (2935 thousand tonnes or 56% of total emissions from the three sectors). Electricity-related emissions were highest in SK; there, only 21% of the generation was from renewables compared to 99% in QC, 93% in ON, and 92% in NFL. The only propane emissions were in ON and QC, which share 94% of Canada's underground gold production. Diesel emissions were high in ON (243 thousand tonnes) due to gold mining operations; the province produces 50% of the country's gold.

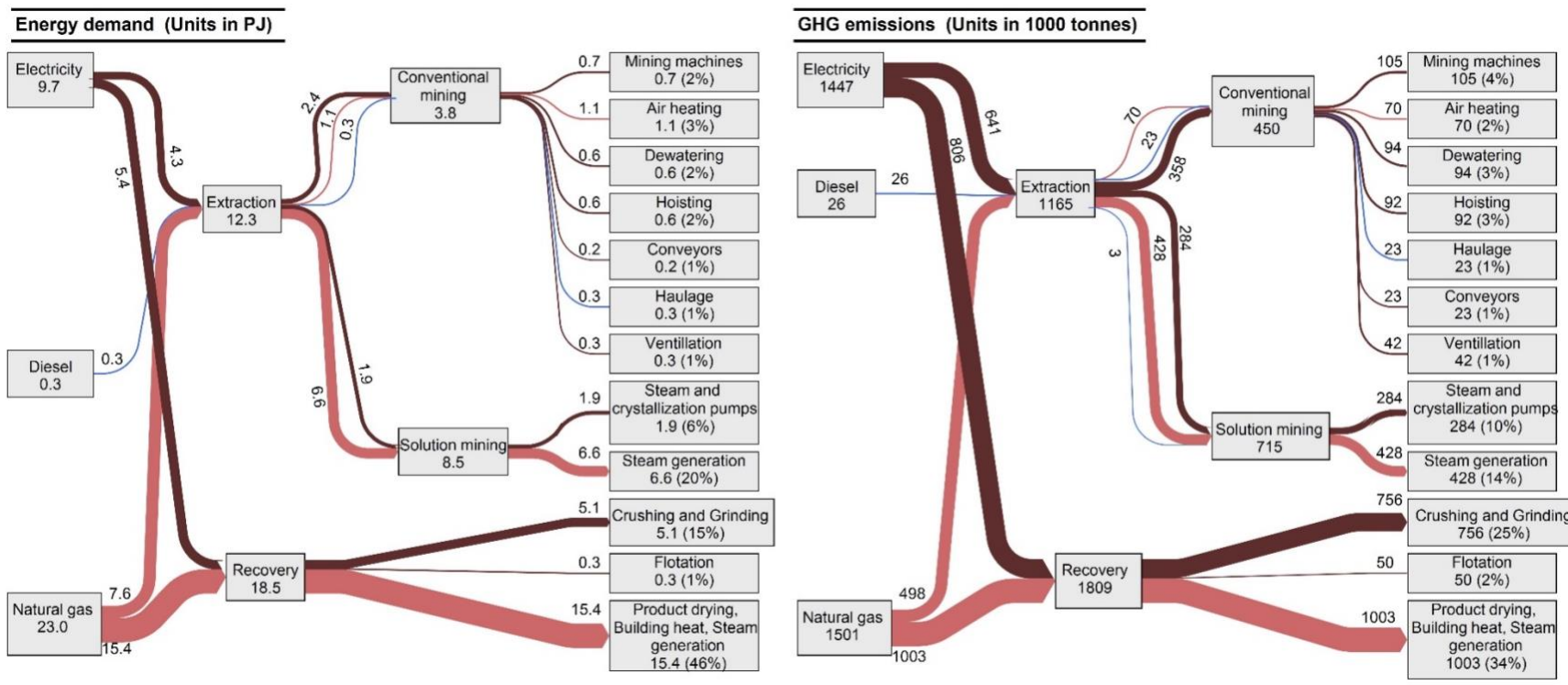


Figure 2-10: Sankey diagrams for potash mining energy demand and GHG emissions in Canada in 2015

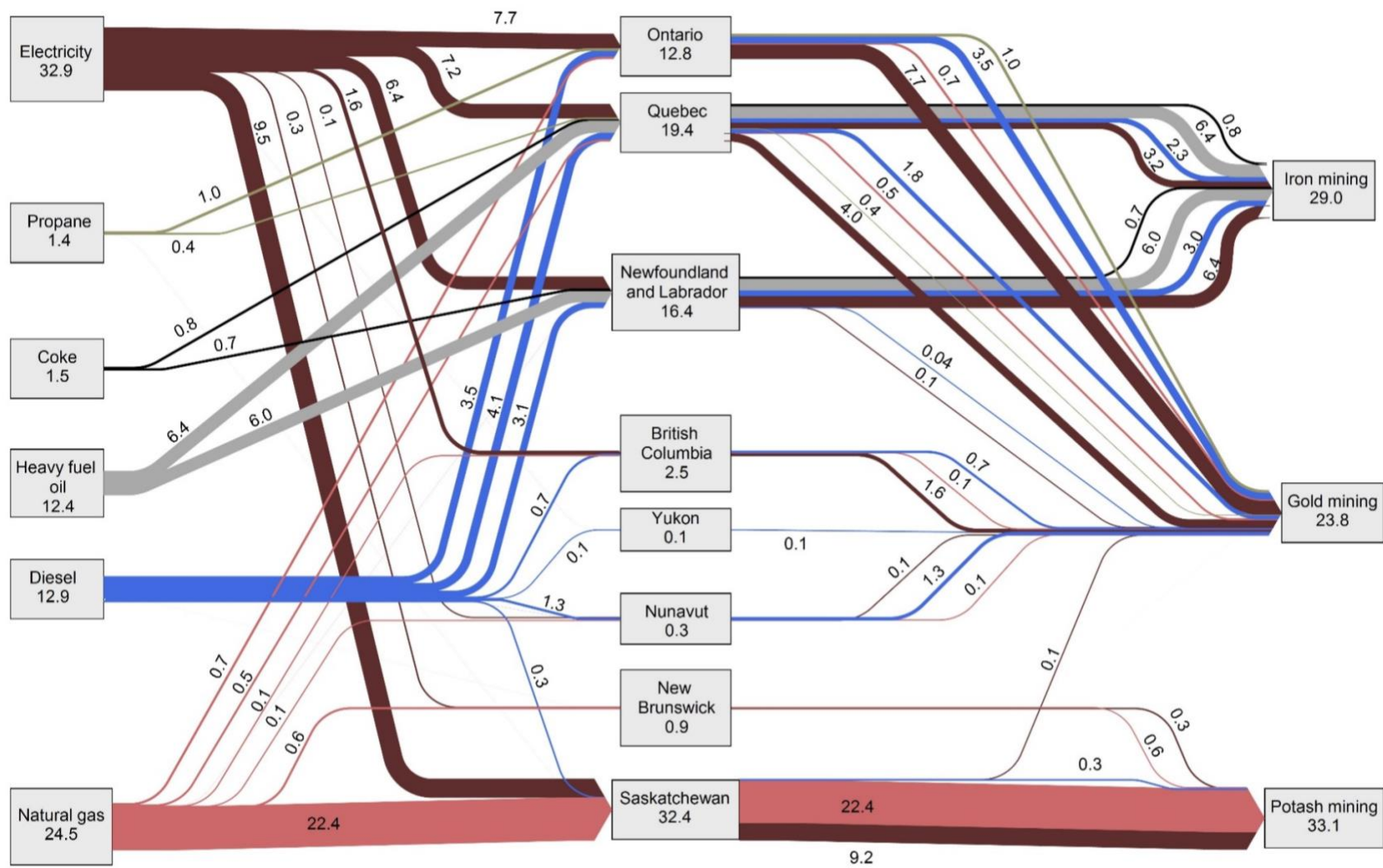


Figure 2-11: Iron, gold, and potash mining energy (PJ) Sankey by province and fuel type in 2015

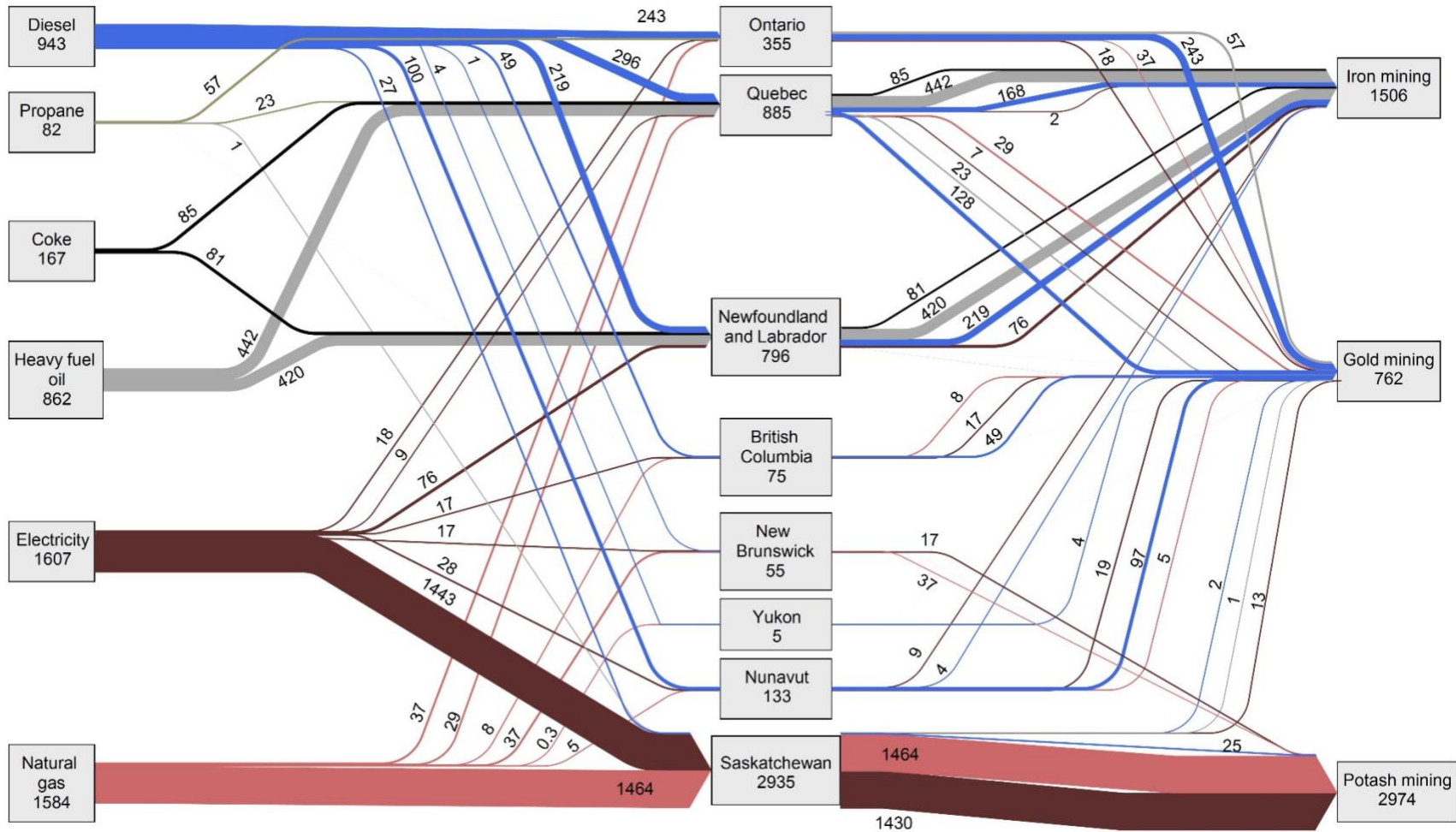


Figure 2-12: Iron, gold, and potash mining GHG (1000 tonnes CO₂ eq.) Sankey by province and fuel type in 2015

2.4 Implications and recommendations

Previous studies have shown that there is significant potential in the mineral mining industry for energy efficiency improvement and GHG mitigation (Kaarsberg et al., 2007; US Department of Energy, 2007). The first step in understanding this potential is to identify how energy is currently being used, in what form, and what the associated GHG emissions are. This study's disaggregation of existing process-level energy inputs and GHG emissions provides baselines. These baselines represent Canadian average energy and GHG emission intensities and can help industry determine whether mine-specific operations are underperforming. Doing so can also help develop realistic performance strategies and targets. Moreover, the specificity of the disaggregated data is at the process level, which allows us to identify equipment or processes that might benefit most from new technology investment, fuel switching, and/or operational improvements.

The disaggregated data provided in this research also make it possible to develop a sector-wide, bottom-up, long-term energy model. Such a model can be used to project future energy use and GHG emissions and assess the long-term GHG mitigation potential and associated costs of equipment changes, process and operations improvements, fuel switching, and low carbon strategies. These assessments can inform industry decision makers and government policy makers and help them choose energy-use reduction and GHG mitigation strategies best suited for specific mineral mines in Canada. Lastly, a long-term energy and GHG emission analysis of Canada's mineral mining sector could quantify its contribution potential to Canada's international climate commitments for GHG mitigation and provide more options for cost-effective GHG mitigation.

2.5 Conclusion

Canada's iron, gold, and potash mining and ore processing techniques were studied. Production shares of different processing methods were estimated, and energy consumption demand trees were developed. The end-use process energy intensities for each sector were calculated and used to develop an energy-environmental model that was used to determine end-use process-level energy use and GHG emissions. The process-level energy use and GHG emissions flow from source to end use were mapped for each sector and province using Sankey diagrams for the year 2015.

The major energy and GHG emission-intensive end-use processes were identified. Pelletization in iron mining and heat and steam generation in the product recovery process in potash mining were found to be responsible for about 50% of the energy demand in the respective sectors. These processes were also the highest contributors to GHG emissions. In gold mining, ventilation and comminution were the dominant energy-use processes and each shared 21% of the energy demand. Diesel-related emissions from ore transportation had the highest share of GHG emissions. The mix of fuel shares in the output processes were also estimated using the Sankey diagrams.

This study also identified the provincial distribution of energy use and GHG emissions in the iron, gold, and potash mining sectors. Newfoundland had 56% and Quebec, 44%, of the iron mining energy demand. Ontario and Quebec together made up 82% of the gold mining energy use as the two provinces accounted for 78% of Canada's gold production and 81% of the underground ore mined. Only 4% of the energy demand was from British Columbia, New Brunswick, Yukon, and Nunavut. A significant amount of emissions were from Saskatchewan (2935 thousand tonnes, or 56%), Quebec (885 thousand tonnes, 17%), and Newfoundland (803 thousand tonnes, 15%).

The results of this study can be used by industry to identify mine operations that performs below the Canadian average. It is recommended that the results be used to project future GHG emissions numbers and test GHG mitigation strategies. This is a needed step to quantify the potential for GHG mitigation in Canada's mineral mining sector and determine the potential to contribute to Canada's GHG reduction targets and international climate commitments.

3 Chapter III: Assessment of greenhouse gas mitigation options for the iron, gold, and potash mining sectors²

3.1 Introduction

The global mineral mining industry (metal and non-metal mineral resource extraction) has increased in value by about 110% in the past 2 decades (Ericsson, 2010). Projections suggest that the world's gross domestic product (GDP) will double by 2030 (Gros and Alcidi, 2014), which will undoubtedly accelerate resource extraction rates. The mining of minerals makes up about 2.7% of world-wide industrial energy use (Fischedick et al., 2014). The mineral mining industry is an energy-intensive sector that contributes to a significant share of national industrial energy use in some regions, reaching 80% in Botswana and Namibia, over 50% in Chile, and about 15% in South Africa (Fischedick et al., 2014). Moreover, ore grades have been declining over the years and newly discovered mineral deposits are deeper, more complex, and finer grained (Mudd, 2007a). This will increase the amount of energy required to extract the same amount of metal or non-metal in the future. Thus, the industry is experiencing increased pressure to reduce its energy use and greenhouse gas (GHG) emissions to help mitigate anthropogenic global warming.

The mining sector is at risk of falling behind societal expectations on climate change (Tost et al., 2018), as the available energy management practices have not been widely accepted in the industry (Levesque et al., 2014). Furthermore, as per the Intergovernmental Panel on Climate Change (IPCC) report, there is significant potential in this sector to improve energy, emissions, and

² A version of this chapter is submitted for publication, titled: A. K. Katta, M. Davis, A. Kumar, "Assessment of greenhouse gas mitigation options for the iron, gold, and potash mining sectors," *Journal of Cleaner Production* (Submitted), 2019.

material efficiencies (Fischedick et al., 2014). Kaarsberg et al. (2007) pointed out that average energy use in U.S. mineral mining is 115% higher than the practical minimum energy use (2007). The U.S. Department of Energy estimated that the U.S. mineral mining industry consumes approximately 1,315 PJ per year and there is potential to reduce energy consumption by 705 PJ and carbon dioxide (CO₂) emissions by 40.6 million tonnes (U.S. Department of Energy, 2007). In Canada, Natural Resources Canada's (NRCan) CanmetMINING's green mining initiative has also highlighted the need to reduce energy use in the country's mineral mining sector (Natural Resources Canada, 2016a).

Past energy conservation and GHG mitigation efforts have focused on waste heat recovery, managing electricity demand, mine ventilation, and implementing renewable energy sources (Levesque et al., 2014). However, comminution and material handling (loading and hauling) operations make up 44% and 17%, respectively, of the energy use across the industry. Thus, there are opportunities to mitigate GHG emissions through energy efficiency improvements, technology replacement, and fuel switching.

Energy use reduction and GHG mitigation measures have been studied mainly by comparing alternative mining technologies. Lajunen (2015) used Autonomie vehicle simulation modelling to compare the energy efficiency of conventional, diesel hybrid, and fuel cell hybrid powertrains of mining machinery (2015). The scope of this study is limited to mining machinery powertrains and does not include those technologies. McNab et al. (2009), Wang (2013), and Norgate and Haque (2010) compared the efficiency and costs associated with various alternative grinding operations using geometallurgical models, JK SimMet software, and life cycle assessment, respectively. Bouchard et al. (2017) and Numbi et al. (2014) studied control strategies to determine energy saving potential for grinding and jaw crushers using optimization modelling, respectively. Neither

strategy was assessed in terms of GHG emission savings. The studies discussed above reveal a gap in the literature. Existing studies on the mining sector are limited to specific sub-process in mining operations, compare relatively small sub-sets of equipment, and lack long-term sectoral analysis. In other words, a long-term, system-wide analysis that compares several GHG mitigation strategies across entire mining sectors involving all the equipment has not been done. In addition, the market penetration rates of alternative technologies in the mining sectors are not well covered in the literature. This study, therefore, aims to address the gaps by developing a bottom-up, system-wide energy assessment framework. The key novelties of this work are the analysis of a wide range of mining GHG mitigation options on a single platform, which gives a fair comparison of results for the different options, and the assessment of the penetration rate for relevant competing technologies in mining operations.

The present analysis uses the Canadian mineral mining industry as a case study; however, the methods used and scenarios developed can be applied to any mineral mining sector in any jurisdiction by modifying the regional production data, energy costs, and energy intensities to suit the mining processes, ore grades, and strip ratios.

Canada's mineral mining industry made up 3.4% of the Canada's GDP in 2016 (Marshall, 2017). Among the mineral extraction activities in Canada, iron, gold, and potash extraction and processing activities together were responsible for a significant 65% and 66% of the mineral mining industries' energy consumption and GHG emissions, respectively, in 2015 (Natural Resources Canada, 2018b). Therefore, this research is specifically focused on these top energy users (iron, gold, and potash mining). Moreover, these are the predominant minerals extracted globally. Iron has the highest global metal value share (27%) (Ericsson, 2010). It is used as a

primary raw material for steel production and its demand is forecasted to grow because of increasing steel demand (Wen et al., 2014). Gold makes up 16% of the global metal value (Ericsson, 2010). It is a precious metal used in jewelry, electronics, healthcare, and the clean technology sector, and its growth is driven by the expanding middle class and evolving use of gold across the technology space (World Gold Council). Although potash's share is low in terms of value, it is one of the main minerals extracted in Canada. Canada is the world's largest producer of potash (The Mining Association of Canada, 2017), an ore primarily used to produce fertilizers (Food and Agriculture Organization of the United Nations, 2017).

The overall objective of this study is to develop a bottom-up energy and environmental model for Canada's iron, gold, and potash mining sectors and to quantify the potential and associated costs of GHG emissions mitigation through various energy-use reduction pathways. The specific objectives of this study are to:

- Develop and validate a long-term, multi-regional energy model for Canada's iron, gold, and potash mining sectors to 2050
- Identify GHG emission mitigation options through energy-use reduction for the iron, gold, and potash mining sectors
- Develop a market share model for applicable scenarios with competing alternative technologies
- Calculate the cost of saved energy, energy saving potential, GHG emission mitigation potential, and incremental cost of mitigation for each scenario

3.2 Method

3.2.1 Overview

Figure 3-1 illustrates the method used in this study. In the first step, data related to the iron, gold, and potash mining sectors was collected. The information on 102 mine sites in Canada were obtained from the System for Electric Document Analysis and Retrieval (SEDAR) database (SEDAR, 2017). From these, process flow sheets, mine characteristics (open pit/underground type, strip ratio, etc.), and the activity data related to ore, waste extracted, and ore processed were compiled. The flow sheets were consolidated to examine the existing types of technologies and processes used. In Chapter 2, we calculated fuel intensities of devices and developed energy consumption demand trees. The present study is an extension of that work and uses the data developed to conduct marginal GHG abatement cost scenario analysis through bottom-up modelling. In a bottom-up approach, end-use technologies are identified, and their fuel-use energy intensities and associated activity are defined. Then the calculated end-use energy demand and GHG emissions are aggregated to obtain sectorial energy consumption and GHG emissions. The Canadian mineral mining model, the LEAP-CANMIN model, was developed in Long-range Energy Alternatives Planning (LEAP) software from the demand trees and device energy intensities (discussed further in Section 3.2.2). The model was validated for the years 2010 to 2015 using historical data. A business-as-usual (BAU) scenario was modelled for the study period (2016-2050) (Section 3.2.3). The method of predicting the penetration of alternative technologies and calculating the cost-benefits of each scenario was established (Section 3.2.4.2). GHG mitigation scenarios were then developed and modelled using unique parameters for equipment capital costs, O&M costs (labour cost, energy cost, overhaul cost, and non-fuel operating costs), lifetime, and fuel consumption (Section 3.2.4.4). Using the LEAP-CANMIN model, we found the

GHG mitigation potential and marginal costs for each scenario. The final results are presented in the form of marginal GHG abatement cost curves.

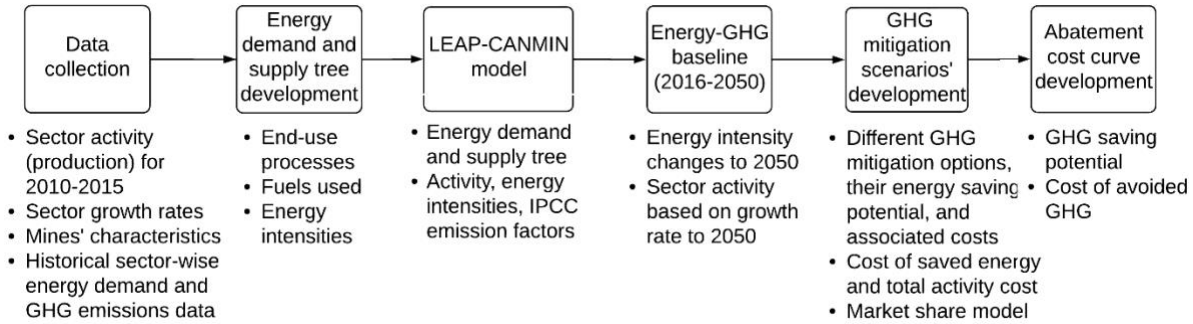


Figure 3-1: Method for model development and scenario analysis

3.2.2 Bottom-up model development for the iron, gold, and potash mining sectors

There are several ways of developing an integrated energy, environment, and economic model to assess GHG mitigation potential. These methods are mainly generalized as top-down, bottom-up, hybrid, optimization, simulation, and accounting models (Hall and Buckley, 2016). Among these, bottom-up models such as LEAP are technologically explicit and are well suited for analyzing technical energy-saving opportunities (Nyboer, 1997). LEAP has been established as a useful tool for energy policy analysis and climate change mitigation assessment in several studies. It has been used to assess Canada's GHG emissions (Davis et al., 2018a; 2019), energy-use improvement options for the chemical (Talaie et al., 2018), commercial and institutional (Subramanyam et al., 2017a), and residential (Xu et al., 2012) sectors, and for long-term forecasting of energy demand and supply (Huang et al., 2011; Tao et al., 2011). The results of the models can be used to develop marginal GHG abatement cost curves (relationships between CO₂ price and tonnes of emissions abated), which are an important tool for policy-makers to evaluate climate mitigation options and their economics (Brown, 2001).

The LEAP integrated framework, shown in Figure 3-2, consists of energy demand and supply modules. The demand module was developed using the energy consumption demand trees, end-use energy intensities, and production data from Chapter 2 as inputs. This module details the end-use energy demand in the iron, gold, and potash mining sectors in Canada. These sectors are divided into sub-processes and further divided into end-use processes that consume different types of fuel. For example, in the case of iron mining, ore extraction and processing are sub-processes with end-use processes such as drilling, crushing, etc. In some cases, such as gold extraction, the end-use is further divided into different energy-consuming devices because of widely different gold extraction techniques. The detailed description of the various end-use processes and the energy intensities can be found in Tables 2-2 through 2-4 in Chapter 2.

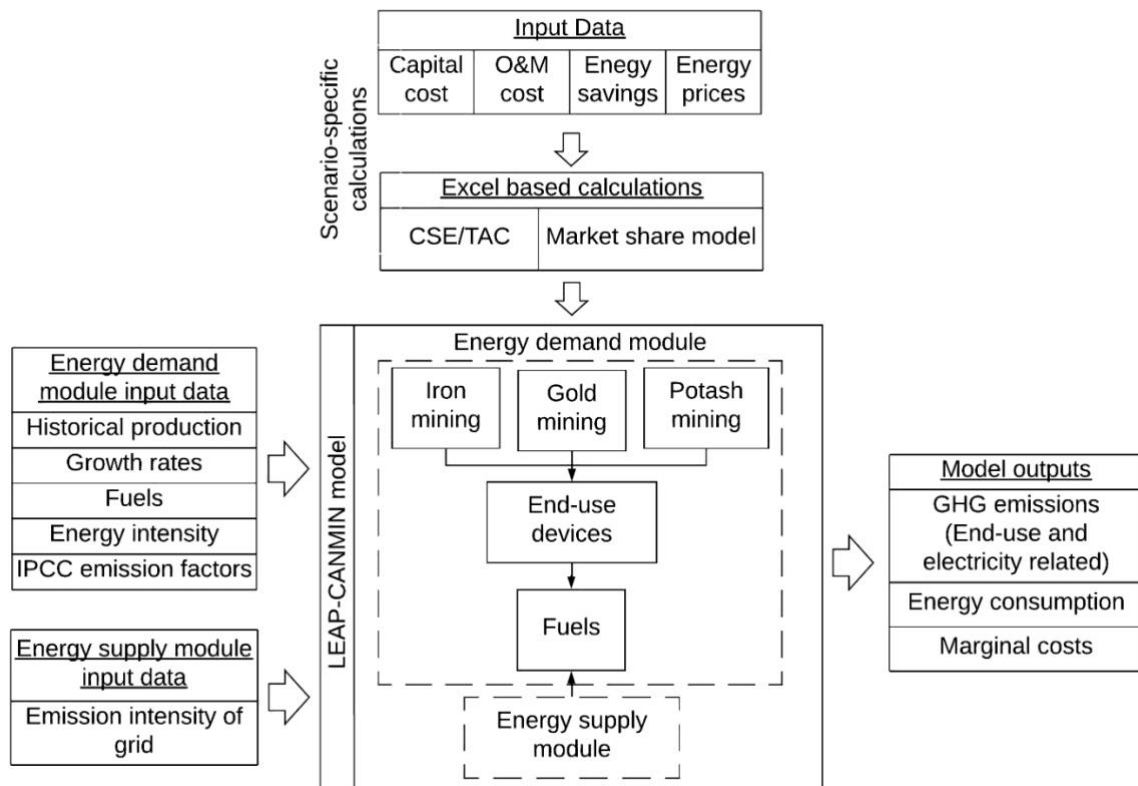


Figure 3-2: Modelling framework

LEAP’s Technology Environment Database’s built-in Tier 1 IPCC emission factors were allocated to the fuels used in the demand module. LEAP’s scenario management capabilities were used to develop the BAU and the different GHG mitigation scenarios. The inputs for scenario development in the LEAP model are the cost of saved energy (CSE)/total activity cost (TAC) and the technology penetration rates. The energy supply module has processes that convert resources/fuels to produce output fuels and supply fuels to the demand module. It was developed in work by Davis (2017) for all the Canadian provinces and includes grid emission factors, as shown in Table 3-1.

Table 3-1: Electricity grid emission intensity factors (grams CO₂ eq. /kilowatt-hour)

Province	2010	2015	2020	2025	2030	2035	2040	2045	2050
British Columbia (BC)	41.0	38.3	13.1	14.2	12.9	12.9	12.7	12.5	12.4
Saskatchewan (SK)	593.5	545.9	500.9	413.1	279.7	273.9	223.3	185.7	145.4
Manitoba (MB)	42.5	38.6	20.9	16.8	5.1	5.3	5.2	5.1	4.9
Ontario (ON)	121.3	8.3	32.2	70.4	49.6	37.6	41.1	44.0	46.6
Quebec (QC)	5.5	6.3	5.8	6.1	6.4	6.0	6.2	6.2	5.9
New Brunswick (NB)	344.5	214.9	213.0	211.4	205.7	205.3	199.4	198.9	198.3
Newfoundland and Labrador (NFL)	13.5	14.2	16.4	16.4	15.1	17.7	17.7	17.7	17.7
Yukon (YK)	36.7	1.4	122.3	8.6	1.3	1.3	1.3	1.3	1.3
Nunavut (NU)	639.2	638.8	441.0	450.3	449.8	457.9	457.1	458.5	460.0

3.2.3 Business-as-usual (BAU) scenario

The LEAP-CANMIN was validated against historical energy consumption and GHG emissions data from NRCAN for the years 2010 to 2015. The list of iron, gold, and potash mining companies with mining operations at 102 mine sites was obtained from Mining Association of Canada (The Mining Association of Canada). The historical records of ore mined, production processes used, strip ratios, ore milled, and production data by mine were obtained from SEDAR database reports (SEDAR, 2017). The mines’ process flow sheets were studied to identify existing technologies and to understand the applicability of the technology scenarios described in Section 3.2.4.4. This

data was used to calculate the energy intensities and production shares of various processing methods as explained in Chapter 2.

The BAU scenario (2016-2050) was developed using provincial growth rate projections for the sectors up to 2021 (Systematic Solutions Inc, 2017a) with the exception of Nunavut and Saskatchewan, where growth rate projections were available to 2030 (The Conference Board of Canada, 2017). For the years beyond 2021 and 2030 that have no projections available, the annual change in the mining sector growth rate is assumed to be the same as the change in the GDP projections in literature (Bonyad, 2014; Davis et al., 2018a; National Energy Board, 2018). The province-wise activity data for iron, gold, and potash in Canada and the growth rates used for future projections are provided in Appendix A (Tables A1-A3, A5, A7). The energy intensity for different hauling and loading diesel equipment is considered to decrease at the rate of 0.8% per year (Hill et al., 2011), and for all other processes is assumed to be constant.

3.2.4 GHG mitigation scenario analysis

3.2.4.1 Cost of saved energy and total activity cost model

The cost of saved energy (CSE) or the total activity cost (TAC) for the scenarios was calculated using Equations 3-1 and 3-2 and input to the LEAP-CANMIN model. Whether to use CSE or TAC depends on the available data. The CSE and TAC are expressed in dollars per gigajoule (\$/GJ) and dollars per tonne (\$/t), respectively. The associated costs of the energy efficiency options were obtained from several studies and will be explained in Section 2.5.

$$CSE = \frac{(CC_{\text{eff}} - CC_{\text{exist}}) \times \left(\frac{(1+i)^S}{((1+i)^S - 1)} \right) + (SV_{\text{eff}} - SV_{\text{exist}}) \times \left(\frac{1}{((1+i)^S - 1)} \right) + (O\&M_{\text{eff}} - O\&M_{\text{exist}}) - E \times P}{E} \quad (\text{Equation 3-1})$$

$$TAC = \frac{(CC_{\text{eff}} - CC_{\text{exist}}) \times \left(\frac{(1+i)^S}{((1+i)^S - 1)} \right) + (SV_{\text{eff}} - SV_{\text{exist}}) \times \left(\frac{1}{((1+i)^S - 1)} \right) + (O\&M_{\text{eff}} - O\&M_{\text{exist}}) - E \times P}{A} \quad (\text{Equation 3-2})$$

In these equations, CC_{eff} is the capital cost of energy efficient technology, CC_{exist} is the capital cost of existing technology, $O\&M_{\text{eff}}$ is the operating and maintenance cost of energy efficient technology, $O\&M_{\text{exist}}$ is the operating and maintenance cost of existing technology, SV_{eff} is the salvage value of energy efficient technology, SV_{exist} is the salvage value of existing technology, s is the life span of the equipment, i is the discount rate (10%), E is the energy saved annually, P is the per unit energy price, and A is the total activity (tonnes).

The end-use prices of electricity and natural gas are in 2016 Canadian dollars (CAD) for the industrial sector and were obtained from government projections to the year 2040 (National Energy Board, 2017) and extrapolated to 2050 using the linear forecast of the years 2018-2040. Table 3-2 shows the electricity, natural gas, and diesel prices. All costs were adjusted to 2016 CAD using the Bank of Canada’s Inflation Calculator (Bank of Canada, 2017), as the available fuel prices were in 2016 CAD at the time of study.

Table 3-2: End-use prices of electricity, natural gas, and diesel, from the NEB (National Energy Board, 2017)

Pro- vince	Electricity end-use price (2016 CAD/GJ)					Natural gas end-use price (2016 CAD/GJ)					Diesel end-use price (2016 CAD/GJ)				
	2019	2020	2030	2040	2050	2019	2020	2030	2040	2050	2019	2020	2030	2040	2050
NFL	28.3	28.3	25.6	23.2	20.6	4.2	4.3	4.6	4.9	4.6	39.0	39.9	45.7	48.8	54.1
NB	18.9	18.9	19.1	19.3	19.5	5.7	5.8	6.2	6.5	6.3	39.2	40.0	45.3	48.1	52.9
QC	13.6	13.7	13.8	13.9	14.1	8.8	9.2	9.6	9.9	9.7	43.8	45.1	50.5	53.3	58.5
ON	33.4	34.1	35.8	36.2	38.0	5.8	5.9	6.3	6.6	6.4	36.3	37.1	42.6	45.5	50.5
MB	12.4	12.5	12.6	12.8	13.0	3.6	3.6	4.0	4.3	4.1	37.6	38.4	44.2	47.3	52.6
SK	20.7	21.0	23.4	25.6	27.8	3.3	3.4	3.8	4.1	3.9	36.4	37.2	42.7	45.6	50.6
BC	19.2	19.2	19.6	20.0	20.4	7.1	7.2	7.2	7.3	7.3	40.0	40.6	45.2	47.4	51.5
YK	20.9	21.0	21.6	22.3	22.9	4.2	4.3	4.6	4.9	4.6	37.7	38.7	45.3	48.9	55.0
NU	53.6	53.9	55.5	57.2	58.9	3.5	3.6	4.0	4.3	4.1	38.3	39.2	45.8	49.3	55.4

3.2.4.2 Market share model

The market share of the various technologies considered in each scenario for every year was modelled using the inverse function as shown in Equation 3-3 (Mau et al., 2008; Nyboer, 1997). The annualized life cycle cost ($LCC_{k,t}$) for each technology was calculated based on the capital cost, operating & maintenance (O&M) cost, and the energy cost (Equation 3-4 (Mau et al., 2008; Nyboer, 1997)). This modelling was limited to scenarios with more than one competing technology having the potential to replace existing technology. Linear penetration rates were considered for the other scenarios, as described in Section 2.5.

$$MS_{k,t} = \frac{LCC_{k,t}^{-n}}{\sum_{k=1}^v LCC_{k,t}^{-n}} \quad (\text{Equation 3-3})$$

$$LCC_{k,t} = \left(CC \times \left(\frac{(1+i)^s}{((1+i)^s - 1)} \right) \right) + O\&M_t + \sum E_{tj} \quad (\text{Equation 3-4})$$

In these equations, $MS_{k,t}$ is the market share of technology k in year t , $LCC_{k,t}$ is the annualized life cost of technology k in year t , v is the number of technologies in a competition node, CC is the capital cost, $O\&M_t$ is the operating and maintenance cost in year t , E_{tj} is the cost of energy form j in year t , and n is the cost variance (power function) parameter. The yearly market share values calculated using Equation 3-3 can be fit into Fisher and Pry's substitution model (Fisher and Pry, 1971). This model gives an S-shaped curve for the penetration of the technology, whose equation, as shown in work by Cho et al. (2015), can be used directly for future studies. Further details of this model are in Appendix A.

3.2.4.3 Marginal GHG abatement cost

The marginal abatement cost of a GHG mitigation option is defined as the ratio of the net present value (NPV) and the mitigated CO₂ eq. emissions, as shown in Equation 3-5. The NPV was calculated using the CSE and TAC at a discount rate, *i*, of 5% using Equation 3-6:

$$AC_s = \frac{NPV_s}{\Delta ME_s} \quad (\text{Equation 3-5})$$

$$NPV_s = \sum_{t=2018}^{2050} \frac{\sum_{a=1}^k (CSE \times E)_{jt}}{(1+i)^{t-2018}} \quad \text{or} \quad \sum_{t=2018}^{2050} \frac{(TACXA)_t}{(1+i)^{t-2018}} \quad (\text{Equation 3-6})$$

where AC_s is the abatement cost of scenario *s*, NPV_s is the NPV of scenario *s*, ΔME_s is the difference in CO₂ eq. between scenario *s* and the BAU case, *E* is the amount of energy saved annually from each energy from *j*, *A* is the production activity, *t* is the specific year, *k* is the number of energy forms, and *i* is the discount rate.

3.2.4.4 Scenario description and development

The literature on current processes and operations of Canadian iron, gold, and potash mines (102 mine sites in total) was reviewed, and twenty-four GHG mitigation options that had not been investigated were identified. The options for each sub-sector are briefly explained in Table 3-3 and are further discussed in detail below.

Table 3-3: Description and energy savings of the scenarios

Scenario	Description	Energy savings
IR-AHTs, GO-AHTs_P, GO-AHTs_U, PO-AHTs_U - New alternative haul truck powertrain technologies for open-pit iron mining, gold mining, and underground gold mining and potash mining	These scenarios assess the energy savings, GHG mitigation achievable, and the costs associated with replacing diesel haul trucks used for extraction of ore with electric and diesel hybrid vehicles. It should be noted that in case of underground mining, additional energy savings can be achieved due to reduction in ventilation requirements	54% (electric haul trucks) 22% (diesel hybrid haul trucks) 60% (ventilation electricity savings for electric haul trucks) 20% (ventilation electricity savings for diesel hybrid haul trucks)
IR-HTO, GO-HTO, PO-HTO - Haul truck operating mode improvement for iron, gold, and potash mining	The fuel consumed is more for a haul truck stopping and then accelerating as compared to the truck continuing at a constant speed. These scenarios analyze the energy savings and GHG mitigations due to elimination of one stop per payload cycle	3.6% (diesel)
IR-TMS, GO-TMS, PO-TMS - Haul truck thermal management system for iron, gold, and potash mining	The engine cooling system rejects approximately 30% of the fuel supplied energy to the ambient. This scenario assumes that diesel trucks use an advanced thermal management control system and assesses the fuel savings translating to energy savings and GHG mitigation	8% (diesel)

Scenario	Description	Energy savings
GO-ALHDs_P, GO-ALHDs_U - New alternative LHD powertrain technologies for open-pit and underground gold mining	These scenarios assess the energy efficiency improvement potentials of electric, diesel hybrid, and fuel cell load-haul-dump (LHD) equipment	67% (electric LHD) 30% (diesel hybrid LHD) 50% (fuel cell LHD) 40% (ventilation electricity savings for electric LHD) 30% (ventilation electricity savings for diesel hybrid LHD) 38.5% (ventilation electricity savings for fuel cell LHD)
IR-SOE - Shovel operator efficiency improvements for iron mining	This scenario assess the energy and GHG savings due to operator skill improvement in ore loading operations	10.2% (electricity)
IR-HPGR1 - High pressure grinding rolls technology option 1 for iron mining	In these scenarios, a HPGR and ball mill is considered for grinding operation, resulting in electricity savings as HPGR requires less energy to achieve the same degree of size reduction as compared to AG or SAG mill. HPGR1 and HPGR2 represent two different product sizes	21% (electricity)
GO-HPGR1- High pressure grinding rolls technology option 1 for gold mining		27% (electricity)
GO-HPGR2 - High pressure grinding rolls technology option 2 for gold mining		14% (electricity)
GO-HPGR_S - High pressure grinding roll and stirred mill technology for gold mining		This scenario assesses energy use improvement by using a HPGR and stirred mill circuit in the gold mining comminution circuits

Scenario	Description	Energy savings
IR-HPGR2 - High pressure grinding rolls technology option 2 for iron mining	This scenario assesses energy use improvement by using a HPGR and pebble mill circuit in the iron mining sector	22% (electricity)
IR-PAG - Pebbles addition in grinding for iron mining	This scenario analyses the energy savings, GHG mitigation achievable, and the costs associated with addition of pebbles instead of metal balls in grinding operations	13% (electricity)
GO-PAG - Pebbles addition in grinding for gold mining		
IR-PSOT - Pellet size optimization technology for iron mining	This scenario analyses the benefits of producing a uniform distribution of pellets before induration	6% (heavy fuel oil), 6% (coke), electricity (2%)
GO-VOD, PO-VOD - Ventilation on demand for gold and potash mining	VOD systems use sensors to ventilate specific areas of the mine based on the demand. This scenario evaluates the GHG mitigation potential and cost savings due to reduction in electricity consumption	30% (electricity)
PO-SG&PD - Steam generation and product drying efficiency improvements for potash mining	This scenario assesses the energy and GHG savings due to energy efficiency improvement in industrial boilers	0.3%/year (natural gas)

New alternative haul truck powertrain technologies for open-pit mining (IR-AHTs and GO-AHTs_P scenarios)

Ore is generally extracted with diesel equipment. Diesel engines face regulatory scrutiny and have environmental concerns (they emit harmful emissions). Electrical and hybrid electric vehicles can potentially replace existing diesel vehicles. The scenarios IR-AHTs and GO-AHTs_P assess the energy savings, GHG mitigation achievable, and marginal costs associated with replacing diesel haul trucks with electric and diesel hybrid vehicles in iron and gold mining open-pit operations, respectively. There is no open-pit potash mining in Canada.

Electrical equipment has no tail pipe emissions, uses less heat, and has lower ventilation, power, and maintenance costs than diesel (Varaschin, 2016). Diesel engines are 40-45% efficient; electric motors are 90-95% efficient. Moreover, in terms of availability, electric equipment has a higher availability of 97% than 85% for diesel. Fuel savings were calculated using Equation 3-7 and assuming a 3000 tonnes per day hard rock operation requiring 3,000 kilowatt (kW) haul truck operations. Electric vehicles have an energy intensity of 54% less than that of a diesel vehicle. The average load factors (the ratio of actual fuel consumption to the maximum fuel consumption at full engine load) for diesel engines and electric motors are 0.55 and 0.80, respectively. The motor's power (kW) is approximately 70% of a diesel engine's power. The diesel fuel consumption is 0.3 litre/kWh (Varaschin, 2016; Varaschin and De Souza, 2015).

$$\text{Energy savings (E)} = (\text{kW required} * \frac{\text{litre}}{\text{kWh}} * \text{Operating hours} * \frac{\text{GJ}}{\text{litre}} * \text{Number of trucks} * \text{Avg. load factor})_{\text{diesel}} - (\text{Motor kW} * \text{Number of trucks} * \text{Avg. load factor} * \text{Operating hours} * \frac{\text{GJ}}{\text{kWh}})_{\text{electric}} \quad (\text{Equation 3-7})$$

Diesel hybrid vehicles have better fuel economy and operating efficiency than those with diesel engines. Diesel hybrid vehicles can provide fuel savings of 22% in an open-pit mine (Esfahanian and Meech, 2013). The energy savings were calculated using Equation 3-8.

$$\text{Energy savings}(E) = \text{Energy intensity} \left(\frac{\text{GJ}}{\text{A}}\right) * 22\% * A \quad (\text{Equation 3-8})$$

The parameters used in the equations are shown in Table A8 in Appendix A. The diesel haul truck energy intensity data is from Chapter 2. The energy savings and other parameters were used in Equation 3-2 to calculate the TAC for electric and diesel haul trucks.

The first all-electric mine in Canada is expected to be ready by 2021. Hence, for market share calculations (as per Section 3.2.4.2), it is assumed that 100% of the existing haul truck fleet is diesel in 2021, and after 2021, the retiring diesel fleet will be replaced by diesel, electric, and diesel hybrid vehicles until 2031. The existing diesel fleet stock in 2021 is assumed to be retiring linearly and become zero by 2031, considering that the lifetime of diesel haul trucks is approximately 10 years (Varaschin, 2016). After 2031, the market share of electric mining equipment is estimated to be more than 40% (International mining, 2018). So, it is assumed that the retiring stock from 2031 is only replaced by electric and diesel hybrid vehicles and from 2041 only by electric vehicles. The market share of each of these vehicle types is calculated by Equation 3-3 using the LCCs and a variance parameter of 10.

New alternative haul truck powertrain technologies for underground mining (GO-AHTs_U, and PO-AHTs_U scenarios)

Underground mining requires ventilation to provide fresh air to the workers and diesel engines and to drive away toxic equipment exhaust gases, diesel particulate matter, heat, dust, and blasting

fumes (Varaschin and De Souza, 2015). Ventilation is responsible for approximately 50% of the energy consumed (Natural Resources Canada, 2005b). The power consumed by the ventilation system is proportional to the volume of air supplied, which is related to the diesel power used in mines (Varaschin and De Souza, 2015). Therefore, using new alternative powertrain haul truck technologies will reduce both diesel consumption and ventilation power consumption. Apart from the 100% diesel savings and 54% less energy intensity for electric vehicles as calculated for scenarios IR-AHTs and GO-AHTs_P, energy savings of 60% in ventilation was calculated for electric haul truck operations compared to diesel haul truck operations. Varaschin and De Souza (2015) estimated a reduced mine air flow (cubic feet per minute) of 28% for a mine operating with electric haul trucks. The 28% reduction implies a 60% reduction in power, calculated using Equations 3-9 and 3-10.

$$P_{fan} = \frac{H_T \times Q}{\eta} \quad (\text{Equation 3-9})$$

$$H_T \propto Q^2 \quad (\text{Equation 3-10})$$

In these equations, P_{fan} is the power required, Q is the mine air flow requirement, H_T is the total system pressure, and η is the efficiency of the fan.

For a mine that uses diesel hybrid haul trucks, the air flow requirement is considered to be 1/5 that of diesel trucks, given that the diesel savings are ~20%. This translates into electricity savings of approximately 10%. The LCCs are calculated using Equation 3-4 considering the energy savings from both ventilation and fuel switching. The market share is calculated using the model described in Section 3.2.4.2.

Haul truck operating mode improvement (IR-HTO, GO-HTO, and PO-HTO scenarios)

A typical truck operation includes five modes: travelling while empty, loading, stopped while loaded, travelling while loaded, and stopped while empty. In a case study by the Australian government, it was found that the greatest amount of time is spent stopped while empty (Australian Government-Department of Resources, 2011). More fuel is consumed by the truck stopping and then accelerating than continuing at a constant speed. Eliminating one stop per payload cycle could result in a fuel savings of 3.6% (Australian Government-Department of Resources, 2011). IR-HTO, GO-HTO, and PO-HTO are the scenarios for iron, gold, and potash mining, respectively. It is assumed that all the mines will eliminate one stop per payload cycle linearly by 2030 and realize a 3.6% fuel savings in haul trucks.

Haul truck thermal management system (IR-TMS, GO-TMS, and PO-TMS scenarios)

The advanced thermal management system (TMS) can reduce the specific fuel consumption and improve overall engine performance (Nessim et al., 2013). The engine cooling system rejects approximately 30% of the fuel-supplied energy to the surroundings. The scenarios IR-TMS, GO-TMS, and PO-TMS assume that diesel trucks use an advanced TMS and show fuel savings of 8% for iron and gold mining. The penetration of TMS in haul trucks is assumed to increase linearly and reach 100% in 2030.

New alternative LHD powertrain technologies for open-pit gold mining (GO-ALHDs_P scenario)

This scenario assesses efficiency improvements in electric, diesel hybrid, and fuel cell load-haul-dump (LHD) equipment use in open-pit gold mining operations. For a base case of a 3000 tonnes

per day hard rock operation operating at 3000 hours per annum, 1350 LHD kW are used (Varaschin and De Souza, 2015). This operation requires 9 diesel LHDs, or 9 fuel cell LHDs, for a use efficiency of 0.61, or 8 electric LHDs at a use factor of 0.68. The energy savings from an electric LHD are 67% (100% diesel savings) (Equation 3-7), 30% from a diesel hybrid LHD (Lajunen, 2015), and 50% from a fuel cell vehicle LHD (McKinney et al., 2015). The fuel cell LHD has low heat production and zero emissions (Lajunen, 2015) and is twice as efficient as a diesel vehicle (McKinney et al., 2015); fuel cell LHDs require 20 kg of hydrogen for 12 hours of operation (McKinney et al., 2015). The hydrogen cost is currently \$17.51/kg and is expected to fall to \$12.52/kg by 2025 (Hydrogen energy systems, 2016). The parameters and costs assumed are shown in Table A9 in Appendix A. The market share of fuel cells was calculated using W.P. Nel's diffusion equation (Nel, 2004). The retiring diesel LHD stock from 2021 is assumed to be replaced by electric, diesel hybrid, and fuel cell LHDs. The market share was calculated using the model in Section 3.2.4.2.

New alternative LHD powertrain technologies for underground gold mining (GO-ALHDs_U scenario)

This scenario analyzes the energy savings and GHG mitigation potential of implementing electric, diesel hybrid, and fuel cell LHDs in underground mining operations. Underground mines have ventilation energy savings in addition to the energy savings in open-pit mining found in scenario GO-ALHDs_P (Varaschin and De Souza, 2015). Using Equations 3-9 and 3-10, we calculated ventilation energy savings of 40% for a mine operating with electric LHDs. Ventilation energy savings of 30% and 38.5% were calculated for diesel hybrid and fuel cell LHDs, respectively. The market share was obtained using the model developed in Section 3.2.4.2 and the parameters in Table A9 in Appendix A.

Shovel operator efficiency improvements for iron mining (IR-SOE scenario)

The operator's skills and practices significantly affect energy use in loading operations. The trajectory of the loading bucket and the speed of executing the trajectory are determined by the operator. These in turn determine production rate and energy consumption, specifically the bucket fill factor and the cycle time. Awuah-Offei (2016) observed that the average shovel energy use difference between the best operator and others is around 10.2%. The scenario IR-SOE assumes a 10.2% shovel energy intensity reduction for iron mining. Shovels are only used in open-pit iron mining and hence are not considered for gold and potash mining. Scenario IR-SOE does not include any technological advancement and so a linear penetration is assumed to reach 100% by 2020.

High pressure grinding roll technology option 1 for iron mining (IR-HPGR1 scenario)

High pressure grinding roll (HPGR) technology for crushing and milling processes can reduce energy consumption and operating costs (Ballantyne et al., 2018; McNab et al., 2009). In Canada, all iron processing plants use an autogenous (AG) or semi-autogenous (SAG) mill and a ball mill circuit. In the HPGR scenario, a milling circuit consisting of HPGRs and a ball mill is considered with a 21% electricity savings, as HPGRs require less energy to achieve the same degree of size reduction as an AG or SAG mill (Ballantyne et al., 2018; McNab et al., 2009). It is assumed that the adoption of HPGR circuits by all the mills will be linear and reach 100% by 2030. The various parameters used for the CSE calculation are shown in Table A10 in Appendix A.

High pressure grinding roll technology option 2 for iron mining (IR-HPGR2 scenario)

This scenario considers the use of HPGRs and a pebble mill circuit in the iron mining sector, which can reduce process electricity use by 22% (Ballantyne et al., 2018; McNab et al., 2009). The various parameters used for the CSE calculation are shown in Table A10 in Appendix A. Currently, there are no mills in Canada using this circuit. This scenario assumes that the mills adoption rate of this technology starts to linearly increase from 0% in 2020 and reach 100% by 2030.

Pebbles addition in grinding (IR-PAG, and GO-PAG scenarios)

The scenarios IR-PAG and GO-PAG assume 13% energy savings and 25% reduction in ball consumption (Nkwanyana and Loveday, 2017), achieved by the addition of pebbles to ball mills in iron and gold mining, respectively. This application is limited to pilot plant tests as pebble consumption is very high. Thus, a penetration of 100% by 2050 is considered with a linear rate of adoption. The parameters used for calculating the CSE are shown in Table A11 in Appendix A.

High pressure grinding roll technology option 1 for gold mining (GO-HPGR1 scenario)

Gold ore comminution processes are dominated by AG, SAG, and ball mills, which are energy intensive and account for 80% of the overall process plant energy consumption (Abouzeid and Fuerstenau, 2009). These mills have an efficiency as low as 25% (Fuerstenau and Abouzeid, 2002). Implementing energy efficient technologies such as HPGR will improve the efficiency of the process. For a product size target of 160 μm , the HPGR-ball mill circuit-specific energy consumption is 27% less than the traditional SAG ball mill (SABC) circuit (Wang et al., 2013). The GO_HPGR1 scenario assumes HPGR circuits are implemented in the gold mining sector,

penetrate linearly, and reach 100% by 2030. The costs considered for calculating the CSE are shown in Table A10 in Appendix A.

High pressure grinding roll technology option 2 for gold mining (GO-HPGR2 scenario)

This scenario assesses the energy reduction achievable by implementing an HPGR-ball mill circuit for a target ore particle size of 75 μm . The electricity savings of 14% calculated by Wang et al. (2013) in their study on Canada's Huckleberry Mines was used in this scenario. The penetration rate is considered to increase linearly to 100% by 2030. The cost data is shown in Table A12 in Appendix A.

High pressure grinding roll and stirred mill technology for gold mining (GO-HPGR_S scenario)

Stirred mill technology is an energy-efficient grinding process consisting of a series of rotating discs over a shaft driven by a motor, in effect like a set of grinding chambers working together (Jankovic, 2015). This makes it a reliable means of achieving fine grinding sizes. An HPGR-stirred mill circuit consumes 31% less energy than an SABC circuit (Wang et al., 2013). This scenario considers implementing HPGR-stirred mill circuits in the gold mining sector and the penetration rate is assumed to be linear and reach 100% by 2030. The CSE is calculated based on the parameters in Table A12 in Appendix A.

Pellet size optimization technology for iron mining (IR-PSOT scenario)

Iron ore pellets are formed by agglomerating iron ore fines using discs or drums and then firing them in induration furnaces (Yamaguchi et al., 2010). The induration process requires a large amount of thermal energy (Borim et al., 2018). A uniform distribution of pellet sizes reduces the

resistance to the flow of gas through the bed and increases furnace efficiency. This also reduces the power required by the fans used for blowing the gases (Borim et al., 2018). This scenario assumes improvements in iron ore pelletization through a control and optimization strategy for the uniform distribution of pellets. Savings of 6% heavy fuel oil, 6% coke, and 2% electricity were considered (Borim et al., 2018; Furedy, 2010). It was also considered that the adoption of this technology will start in 2020 and reach 100% by 2030 at a linear rate.

Ventilation on demand (GO-VOD, and PO-VOD scenarios)

Ventilation on demand (VOD) systems use sensors to monitor the real-time air quality, vehicle use, and personnel to ventilate only specific areas of the mine instead of ventilating the whole mine all the time. The system includes monitoring environmental conditions, a communication system to control rooms, and automated control devices such as regulators, vent doors and fan speed controllers (McCambridge and Kuruppu, 2009). Such a system can bring energy savings of 30% (McCambridge and Kuruppu, 2009; Rockwell Automation, 2017), which is assumed for the GO-VOD and PO-VOD scenarios in gold and potash mining. In 2013, Glencore implemented a VOD system in one of its nickel mines in Ontario. Apart from that, the adoption of VOD by other mines in Canada is not known, even though VOD is not new. Hence, the penetration rate in gold mining is considered to increase linearly and reach 100% by 2030.

Steam generators and product drying efficiency improvements (PO-SG & PD scenario)

Industrial boiler efficiencies are typically around 80% (Gupta et al., 2011). This efficiency can further be improved by reducing excess air, installing combustion controls, improving insulation, and repairing leaks. An earlier study estimated that gas- and coal-fired boilers can improve by 0.3%/year (Interlaboratory Working Group, 2000). This scenario assumes the boiler efficiency of

steam generators used in potash mining sector increases. Since these improvements are not major technological advancements, the 0.3% increase in efficiency is considered annually from 2020 onwards.

3.3 Results and discussion

3.3.1 Model validation and BAU scenario

The LEAP-CANMIN was validated using NRCan's Comprehensive Energy Use Database statistics for the iron, gold, and potash mining sectors for the years 2010-2015. Figure 3-3 shows the differences between model-calculated and historical energy demand and GHG emissions. The average difference in energy demand is 8%, 7%, and 4% in the iron, gold, and potash mining sectors, respectively. The average difference in GHG emissions is 11%, 6%, and 5% in the iron, gold, and potash mining sectors, respectively.

There are 2 reasons for these differences. First, data on the source of electricity for some mines was not available. For the mines without this data, we assumed that the source of electricity was the provincial grid, thus the provincial grid factor was used to calculate GHG emissions. In reality (assumed to be reflected by the NRCan historical data set), some of these mines may actually be using diesel to generate electricity on site. Thus, the assumption taken in this study to use grid-sourced electricity for these mines could lead to slightly less energy demand and GHG emission results than NRCan's, where diesel might actually be used. The energy demand would be higher when diesel is used since the inefficiency of electricity conversion would lead to a higher energy footprint than direct electricity demand. The GHG emissions would also be higher where diesel is used since grid emission factors are lower than the diesel emission factor. This is consistent with

the validation results where NRCan has, on average, slightly higher values for energy demand and GHG emissions.

Second, NRCan uses a top-down national-level modelling approach, instead of modelling by province and then aggregating to the national level (bottom-up), as was done in this study. In general, this can lead to discrepancies in energy use and GHG emissions between NRCan and the LEAP-CANMIN results. For instance, NRCan’s electricity-related emissions are calculated using the average Canadian grid emission intensity factor. Since the mineral mining industry in Canada has different levels of activity across provinces, and provinces have different grid emission intensities than the Canadian average, NRCan may over- or under-estimate electricity-related emissions.

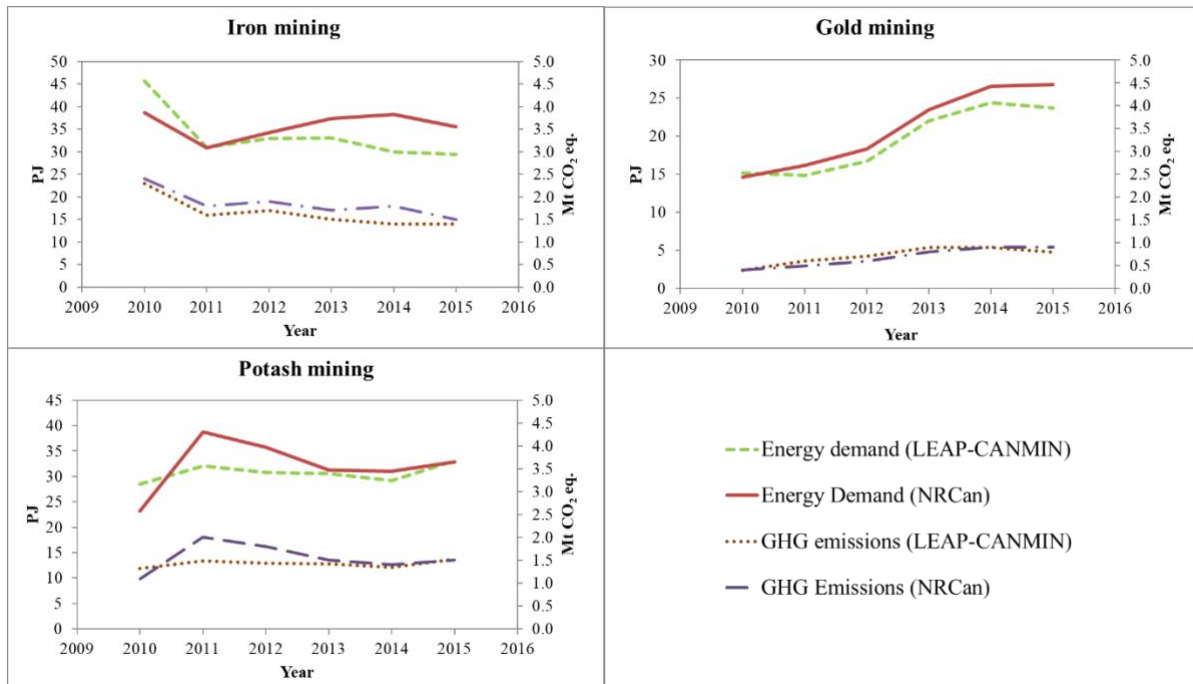


Figure 3-3: Energy demand and GHG emission (excluding electricity-related emissions) validation for the iron, gold, and potash mining sectors

BAU energy demand is expected to increase by 1.6, 2.0, and 2.1 in the iron, gold, and potash mining sectors, respectively, between 2015 and 2050. GHG emissions are expected to increase by 1.3, 1.4, and 1.5 in the iron, gold, and potash mining sectors. The increase is driven by growth in the sectors. Projected energy demand and GHG emission result tables for the iron, gold, and potash mining sub-sectors are in Table A13 and Table A14, respectively, in Appendix A.

3.3.2 Cost of saved energy (CSE) and total activity cost (TAC)

The CSE and TAC results for iron, potash, and gold mining for the years 2020-2050 are presented in Table 3-4, Table 3-5, and Table 3-6, respectively. For each scenario, a regression analysis of the CSE and TAC showed a linear upward trend with a coefficient of determination (R^2) > 0.98 between 2020 and 2050. This signifies that the CSE and TAC can be predicted accurately for any year using the range values.

The average TAC (for the years 2020-2050) for the scenarios IR-AHTs, GO-AHTs_P, GO-AHTs_U, PO-AHTs_U is from -1.3 to -3.0 \$/t and 0.04 to -6.7 \$/t for electric and diesel hybrid haul trucks, respectively, depending on the sector and province. It is better to use electric haul trucks than diesel hybrid haul trucks in all three sectors; there are higher energy savings and lower electricity prices with electric haul trucks, and diesel hybrid truck consume the higher-cost diesel fuel. In underground mines, using electric or diesel hybrid vehicles will lower the ventilation energy requirement and lower the CSE/TAC compared with those of open-pit mines. Diesel hybrid haul trucks show negative TAC only in the potash mining sector. The average TAC for electric, diesel hybrid, and fuel cell LHDs is from -3.9 to -0.3 \$/t, 0.9 to 3.6 \$/t, and 2.6 to 16.6 \$/t, respectively, among the provinces. For the scenarios in ore comminution, iron and gold mining have average CSEs of -46.7 to -31.5 \$/GJ and -25.1 to 35.8 \$/GJ, respectively. A scenario may not

show cost savings in every province due to differing energy prices, as in scenario GO-HPGR1, where Ontario and Nunavut have much higher positive CSEs than other provinces. All other scenarios have negative CSEs in each province of -0.3 to -56.4 \$/GJ.

Table 3-4: CSE, TAC for scenarios in the iron mining sector

Scenario		Range of CSE/TAC for the years 2020-2050		Units
		NFL	QC	
IR-AHTs	<i>Electric haul trucks</i>	-2.0 – -2.9	-2.6 – -3.3	\$/t
	<i>Diesel hybrid haul trucks</i>	0.03 – 0.05	0.04 – 0.04	\$/t
IR-HTO		-39.9 – -54.1	-45.1 – -58.5	\$/GJ
IR-TMS		-39.9 – -54.1	-45.1 – -58.5	\$/GJ
IR-SOE		-20.7 – 28.3	-13.7 – -14.1	\$/GJ
IR-HPGR1		-38.3 – -45.9	-31.3 – -31.7	\$/GJ
IR-HPGR2		-40.3 – -50.7	-36.0 – -36.4	\$/GJ
IR-PAG		-0.31 – -0.34	-0.27 – -0.28	\$/t
IR-PSOT		-20.7 – -28.3	-13.7 – -14.1	\$/GJ

Table 3-5: CSE, TAC for scenarios in the potash mining sector

Scenario		Range of CSE/TAC for the years 2020-2050		Units
		SK	NB	
PO-AHTs_U	<i>Electric haul trucks</i>	-0.9 – -1.9	-1.2 – -1.8	\$/t
	<i>Diesel hybrid haul trucks</i>	-0.00 – -0.02	0.01 – -0.02	\$/t
PO-VOD		-21.0 – -27.8	-18.9 – -19.5	\$/GJ
PO-SG&PD		-3.4 – -4.7	-5.8 – -7.1	\$/GJ
PO-HTO		-37.2 – -50.6	-40.8 – -52.9	\$/GJ
PO-TMS		-37.2 – -50.6	-40.8 – -52.9	\$/GJ

Table 3-6: CSE, TAC for scenarios in the gold mining sector

Scenario		Range of CSE/TAC for the years 2020-2050								Units
		NFL	QC	ON	MN	BC	SK	YK	NU	
GO-AHTs_P	<i>Electric haul trucks</i>	-1.6 – -2.5	-2.2 – -2.9	-1.3 – -1.9	-1.9 – -2.6	-1.8 – -2.4	-1.6 – -2.2	-1.7 – -2.5	-0.9 – -1.7	\$/t
	<i>Diesel hybrid haul trucks</i>	0.05 – 0.03	0.05 – 0.03	0.05 – 0.04	0.05 – 0.04	0.05 – 0.04	0.05 – 0.04	0.05 – 0.03	0.05 – 0.03	\$/t
	<i>Electric haul trucks</i>	-4.3 – -4.5	-3.5 – -4.2	-4.6 – -5.5	-3.1 – -3.9	-3.7 – -4.3	-3.6 – -4.8	-3.7 – -4.7	-6.1 – -7.3	\$/t
GO-AHTs_U	<i>Diesel hybrid haul trucks</i>	-0.2 – -0.1	-0.07 – -0.09	-0.23 – -0.28	-0.05 – -0.07	-0.11 – -0.13	-0.12 – -0.19	-0.12 – -0.16	-0.40 – -0.46	\$/t
	<i>eLHD</i>	-0.4 – -0.8	-0.6 – -0.9	-0.3 – -0.6	-0.5 – -0.8	-0.5 – -0.7	-0.4 – -0.6	-0.4 – -0.8	-0.2 – -0.5	\$/t
GO-ALHDs_P	<i>Diesel hybrid LHD</i>	3.7 – 3.6	3.6 – 3.5	3.7 – 3.6	3.7 – 3.6	3.7 – 3.6	3.7 – 3.6	3.7 – 3.6	3.7 – 3.6	\$/t
	<i>Fuel cell LHD</i>	17.1 – 16.3	17.0 – 16.2	17.1 – 16.4	17.1 – 16.4	17.1 – 16.4	17.1 – 16.4	17.1 – 16.3	17.1 – 16.3	\$/t
	<i>eLHD</i>	-2.2 – -2.1	-1.5 – -1.8	-2.4 – -3.0	-1.3 – -1.6	-1.7 – -2.0	-1.7 – -2.4	-1.7 – -2.2	-3.6 – -4.3	\$/t
GO-ALHDs_U	<i>Diesel hybrid LHD</i>	2.3 – 2.6	3.0 – 2.9	2.1 – 1.8	3.1 – 3.0	2.7 – 2.6	2.7 – 2.3	2.7 – 2.5	1.1 – 0.7	\$/t
	<i>Fuel cell LHD</i>	4.9 – 4.6	5.7 – 4.9	4.6 – 3.6	5.9 – 5.1	5.4 – 4.7	5.4 – 4.3	5.4 – 4.4	3.3 – 2.2	\$/t
	GO-HTO	-39.9 – -54.1	-45.1 – -58.5	37.1 – -50.5	-38.4 – -52.6	-40.6 – -51.5	-37.2 – -50.6	-38.7 – -55.0	-39.2 – -55.4	\$/GJ
GO-TMS	-39.9 – -54.1	-45.1 – -58.5	-37.1 – -50.5	-38.4 – -52.6	-40.6 – -51.5	-37.2 – -50.6	-38.7 – -55.0	-39.2 – -55.4	\$/GJ	
GO-PAG	-0.3 – -0.4	-0.3 – -0.4	-0.3 – -0.4	-0.2 – -0.3	-0.3 – -0.4	-0.3 – -0.4	-0.3 – -0.4	-0.3 – -0.4	-0.5 – -0.6	\$/t
GO-HPGR1	7.3 –	-7.4 –	13.0 –	-8.5 –	-1.9 –	-0.1 –	-0.0 –	32.9 –	\$/GJ	

Scenario	Range of CSE/TAC for the years 2020-2050								Units
	NFL	QC	ON	MN	BC	SK	YK	NU	
	-0.4	-7.0	16.9	-8.1	-0.7	6.7	1.9	37.9	
GO-HPGR2	7.7 –	-7.0 –	13.4 –	-8.1 –	-1.4 –	0.3 –	0.4 –	33.3 –	\$/GJ
	0.0	-6.6	17.3	-7.7	-0.3	7.1	2.3	38.7	
GO-HPGR_S	-9.6 –	-24.2 –	-3.8 –	-25.4 –	-18.7 –	-16.9 –	-16.9 –	-16.4 –	\$/GJ
	-17.2	-23.8	0.1	-24.9	-17.5	-10.1	-15.0	21.0	
GO-VOD	-28.3 –	-13.7 –	-34.1 –	-12.5 –	-19.2 –	-21.0 –	-21.0 –	-53.9 –	\$/GJ
	-20.6	-14.0	-38.0	-13.0	-20.4	-27.8	-22.9	-58.9	

3.3.3 Market share model results

The market share was modelled for electric and diesel hybrid haul trucks and LHDs and was used in modelling the scenarios IR-AHTs, GO-AHTs_P, GO-AHTs_U, GO-ALHDs_P, GO-ALHDs_U, and PO-AHTs_U. The market share in each province between 2020 and 2050 is shown in Figure 3-4. The penetration of electric haul trucks (top left in Figure 3-4) and LHDs (bottom left in Figure 3-4) is faster in Quebec than in other provinces. This is due to the cheaper electricity price, which lowers the LCC and increases the trucks' market share. The market shares of electric haul trucks and LHDs were estimated to be 60-80% and 20-30%, respectively, by 2030 among the provinces. By 2040, approximately 80% of the haul trucks and LHDs in mines operate on electricity. The difference in penetration rates between the provinces is not significant in the case of electric LHDs. The market shares of diesel hybrid haul trucks (top right in Figure 3-4) and LHDs (bottom right in Figure 3-4) are expected to increase until 2040 and then decrease due to the increased penetration of electric/fuel cell vehicles.

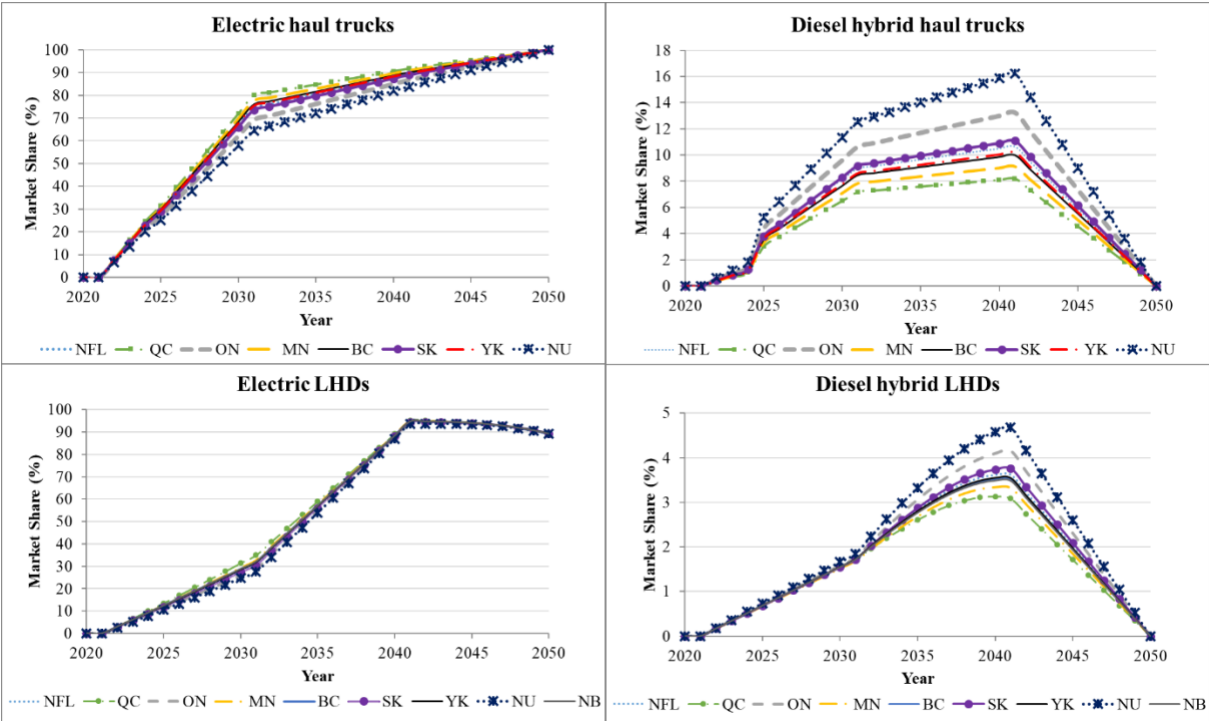


Figure 3-4: Market shares of electric haul trucks, diesel hybrid haul trucks, electric LHDs, and diesel hybrid LHDs in each province

3.3.4 Scenario analysis

The GHG emissions mitigation potential of multiple scenarios can be shown in the form of wedge curves, in which each wedge represents the trend and the avoidable GHG emissions for a particular scenario over the study period. Figure 3-5 and Figure 3-6 show the wedge curves developed for the IR-TMS, IR-AHTs, and IR-PSOT scenarios in iron mining, and GO-VOD, GO-HTO, GO-HPGR_S, GO-TMS, GO-ALHDs_U, GO-ALHDs_P, GO-AHTs_U, and GO-AHTs_P scenarios in gold mining that can be implemented concurrently. These figures also show the emissions profile in a BAU scenario and the resulting emissions profile following the penetration of GHG mitigation options by 2050. The maximum cumulative energy and GHG reduction achievable in the iron mining sector, considering the scenarios that can be implemented concurrently, are 98 PJ

(6% of the sector’s energy consumption) and 8 Mt CO₂ eq. (10% of the sector’s emissions), respectively, by 2050. For gold mining, the cumulative energy savings and GHG mitigation are 323 PJ (23% of the energy consumption) and 10 Mt (20% of GHG emissions) by 2050, respectively. For potash mining, energy savings and GHG mitigation achievable from PO-AHTs_U, PO-VOD, PO-SG&PD, and PO-HTO scenarios together are 45 PJ (2% of the sector’s energy use) and 3 Mt of CO₂ eq. (2% of the sector’s GHG emissions). Given the small mitigation achievable, a wedge curve was not developed for the potash mining sector.

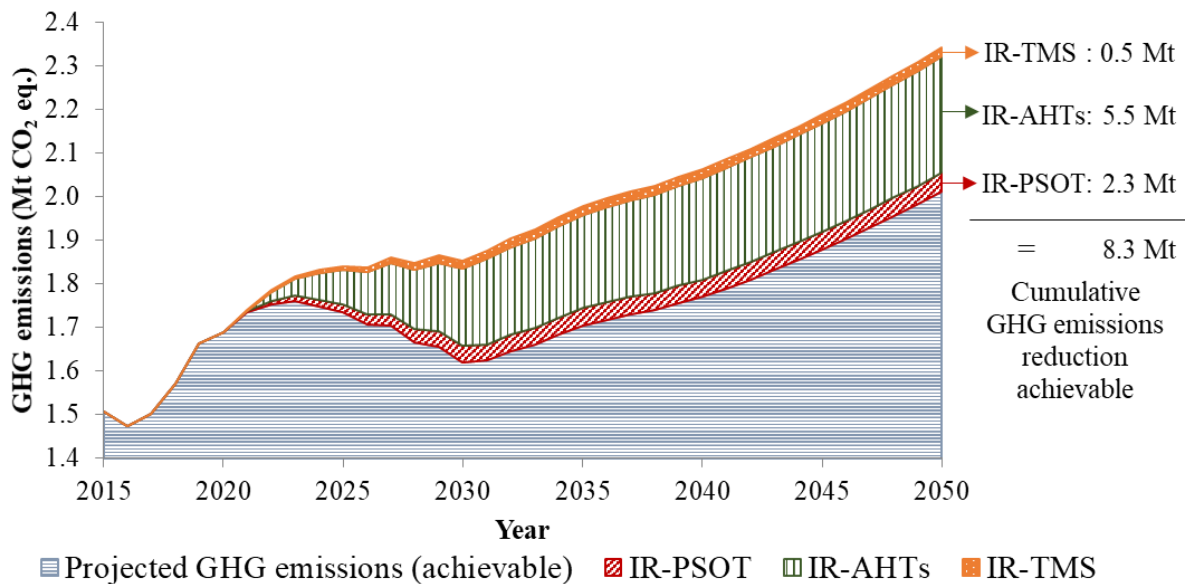


Figure 3-5: Wedge curve of achievable GHG emissions reduction for the iron mining sector

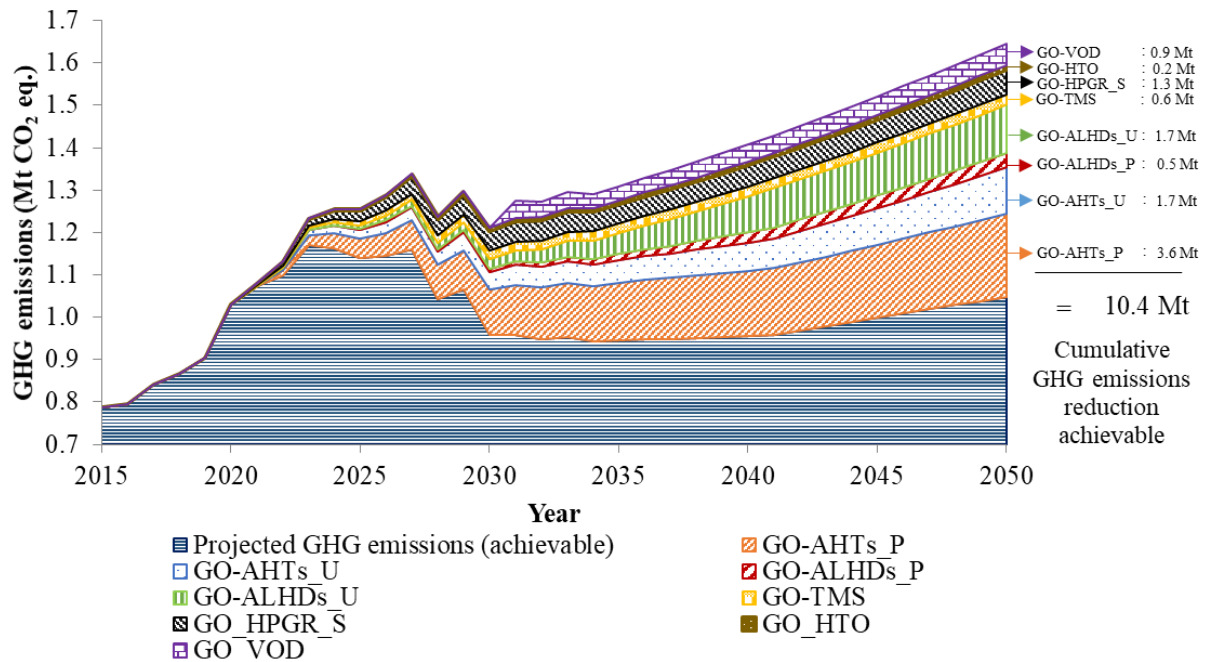
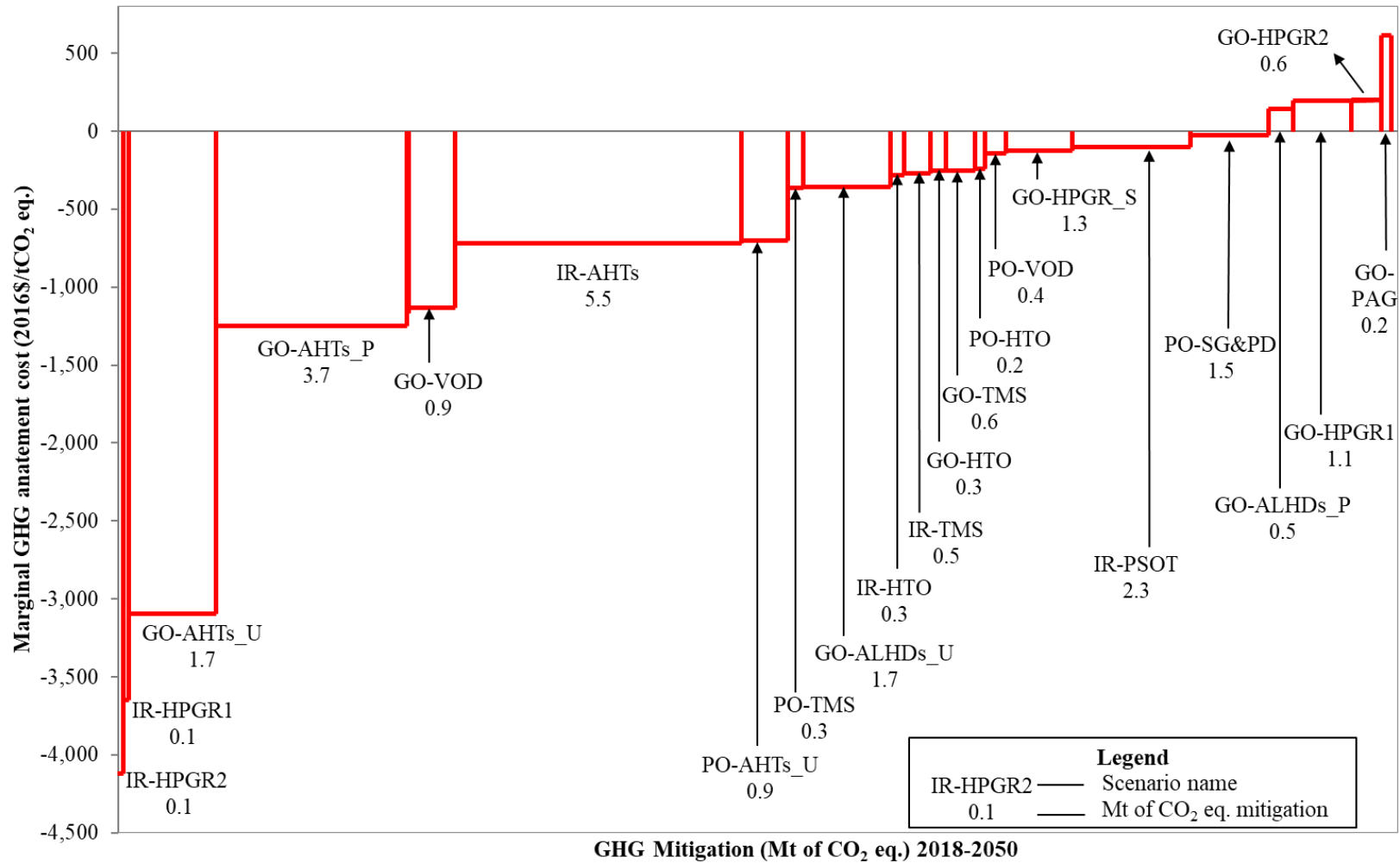


Figure 3-6: Wedge curve of achievable GHG emissions reduction for the gold mining sector

Figure 3-7 shows the cost curve for the scenarios in all the three sub-sectors. This figure illustrates comparative GHG mitigation potential and marginal GHG abatement costs for the scenarios. The horizontal axis shows the sum of the difference in GHG emissions between the efficient and BAU scenarios over the study period (in Mt of CO₂ eq.). The vertical axis shows the incremental cost of an energy use reduction option in 2016 Canadian dollars compared to existing technologies over the study period (in \$/tonne of CO₂ eq.) A negative cost indicates savings and a positive cost indicates that the capital cost to implement the scenario exceeds the cost saving because of energy consumption.

These cost curves are used to compare GHG mitigation potential and marginal GHG abatement costs in the scenarios across the three sub-sectors. The GHG mitigation costs ranged widely, from -4,120 to 614 \$/tonne of CO₂ eq. The cumulative energy demand reduction, GHG mitigation, marginal GHG abatement cost, and net present value (NPV) are presented in Table A16 in

Appendix A. The scenarios on alternative haul truck technology penetration (IR-AHTs, GO-AHTs_P, GO-AHTs_U, and PO-AHTs_U) for ore haulage show significant relative GHG reduction potential with marginal cost savings. Using these vehicles in underground mining has a lower marginal GHG abatement cost than in open-pit mining because of the additional energy savings in mine ventilation. The IR-AHTs scenario has a higher mitigation potential of 5.5 Mt, and the GO-AHTs_U scenario has a lower marginal GHG abatement cost of -3096 \$/tonne of CO₂ eq. than the other scenarios on ore haulage. For ore loading operations, the scenarios GO-LHDs_P and GO-LHDs_U for the gold mining sector showed 0.5 and 1.7 Mt of GHG emissions reductions by 2050 in open-pit and underground mines, respectively. However, the GO-LHDs_P scenario is not economical; it has a positive marginal GHG abatement cost. For ore comminution, introducing HPGR-ball mill circuits will save costs in the iron mining sector but not in the gold mining sector. This is mainly due to the higher energy intensity of the grinding operation in iron ore comminution, which leads to higher energy cost savings. Using HPGR-stirred mill technology for grinding gold ore will result in higher GHG mitigation and cost savings. Haul truck operating mode improvement scenarios reduce GHGs and costs more in iron mining than in the other two sectors. Some scenarios have only electricity-related energy savings and their mitigation potential depends on the electricity generation grid mix. Overall, 80% of the developed scenarios have cost savings because saved energy costs outweigh other costs. Although the magnitude of the GHG mitigation potential and the abatement costs will be different in other jurisdictions depending on energy intensity and grid emission factors, the relative comparison among the scenarios would be similar. Thus, the marginal GHG abatement cost curves of this study can provide useful information to other jurisdictions with similar mining operations.



* NPV of costs discounted to 2018

Figure 3-7: Canadian iron, gold, and potash mining sector combined marginal GHG emission abatement cost curve

3.3.5 Limitations

Mine-specific parameters such as ore grade and strip ratio were considered in our future projections to be the same as 2015 levels because no data is available on mining companies' future extraction activities. This assumption was made as ore grades are likely to remain almost constant (Mudd, 2007b), and although the strip ratio for a mine would decrease with the age of mine, the average strip ratio for all the mines together would be similar. The growth rates used in this study were for both metal and non-metal mining and the mining sector as a whole and not for the specific sub-sectors. The penetration rates for some of the scenarios were based on the economics of technologies, but unknown future macro-economic and policy changes might affect these rates.

3.3.6 Sensitivity analysis

Sensitivity analysis was performed to understand the impact of capital cost, fuel (electricity, natural gas, and diesel) price, and discount rate on the marginal GHG abatement cost. These variables were changed from -30% to +30% for each scenario. Figures 3-8, 3-9, and 3-10 show the sensitivity results for the IR-AHTs, GO-AHTs_P, and PO-SG&PD scenarios that have the highest GHG mitigation potential in their respective sectors. The results for the other scenarios are shown in Figures A4-A24 in Appendix A. For the scenarios in iron mining, the discount rate is the most influential variable and changes the marginal GHG abatement by 23-35% with a change of -30% in the discount rate. Capital cost changed the marginal GHG abatement cost by 15-16% in scenarios IR-HPGR1 and IR_HPGR2, but for the other scenarios, the change is less than 6%. A reduction in diesel price by 30% increased the marginal GHG abatement cost by 30% for the scenarios on haulage equipment. A -30% change in electricity price increased the marginal GHG abatement cost by 16%, 14%, and 9% in the IR-HPGR1, IR-HPGR2, and IR-PAG scenarios. The

reference scenario growth rate changed the marginal GHG abatement cost by only 0-1% for all the scenarios. For gold mining, the GO-ALHDs_P scenario changed by 330%, 90%, 557%, and 124% for a 30% increase in capital cost, discount rate, diesel price, and natural gas price, respectively. For the rest of the scenarios, the change in marginal GHG abatement cost ranged from -132-194% for capital cost, 29-38% for discount rate, -40-80% for diesel price, and -102- 65% for electricity price. The BAU scenario growth rate variable was found to be relatively less influential and changed the mitigation cost by 14% to -19%. For all the scenarios in potash mining, a change in the discount rate by +30% and -30% changed the marginal GHG abatement costs by approximately -25% and +35%, respectively. A 30% increase in diesel price reduced the mitigation cost by 55% and 30% in the PO-AHTs and PO-HTO scenarios, respectively. Overall, for all three sectors, an increase in diesel fuel price and a decrease in electricity price lowered the GHG mitigation cost because of the increased penetration of alternative powertrain technologies in the ore haulage scenarios. For scenarios on efficient comminution circuits, an increase in electricity price reduced the cost of saved energy and led to lower marginal GHG abatement costs.

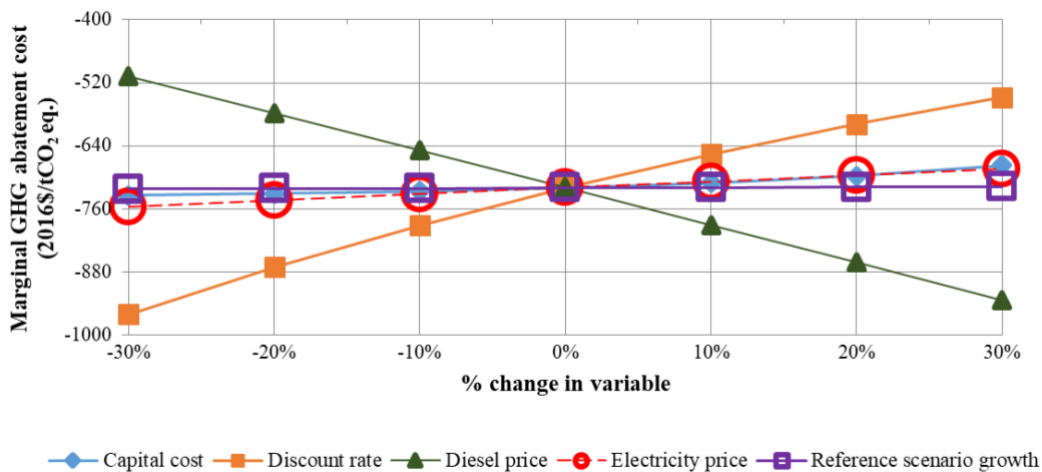


Figure 3-8: IR-AHTs scenario sensitivity of abatement cost to capital cost, discount rate, diesel price, electricity price, and reference scenario growth

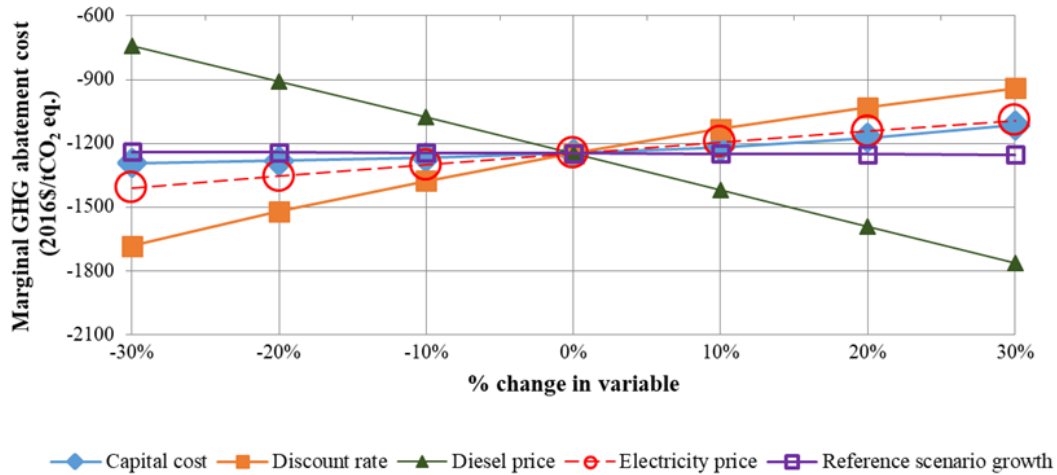


Figure 3-9: GO-AHTs_P scenario sensitivity of abatement cost to capital cost, discount rate, diesel price, electricity price, and reference scenario growth

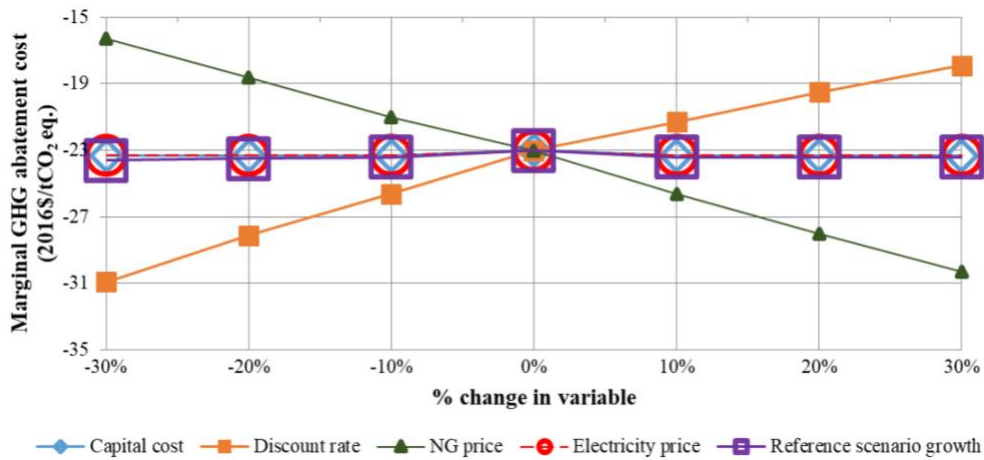


Figure 3-10: PO-SG&PD scenario sensitivity of abatement cost to capital cost, discount rate, natural gas price, electricity price, and reference scenario growth

3.4 Conclusion

In this study, a bottom-up integrated resource planning model was developed for the iron, gold, and potash mining sectors. The model was used to assess various technology and energy-efficiency improvement options in terms of their GHG mitigation potential and marginal GHG abatement

costs. We developed 8, 11, and 5 scenarios for Canada's iron, gold, and potash mining sectors, respectively. The market share of the technologies was modeled for scenarios with available cost data.

The cumulative GHG mitigation potential (for the years 2018-2050) of the 15 scenarios that can be implemented concurrently is 8, 10, and 3 Mt CO₂ eq. for Canada's iron, gold, and potash mining sectors, respectively. These correspond to 10%, 20%, and 2% of the total cumulative GHG emissions by 2050 in the iron, gold, and potash mining sectors, respectively. The total marginal GHG abatement costs for these sectors are -525, -1,176, and -258 \$/tonne of CO₂ eq., respectively. The scenarios IR-AHTs, GO-AHTs_P, and PO-SG&PD have the highest GHG mitigation potentials of 5.5 Mt, 3.6 Mt, and 1.5 Mt, respectively. The abatement cost of the scenarios ranged from -101 to -4120 \$/tonne in iron mining, 614 to -3096 \$/tonne in gold mining, and -23 to -701 \$/tonne in potash mining.

The marginal GHG abatement cost curves presented can be used by policy-makers and mining companies in Canada and elsewhere to prioritize strategies to reduce their environmental footprint in the most economical way. Additionally, the GHG mitigation cost curve can be used for decision-making and associated policy formulation. The framework developed in this study can be applied to mining sectors elsewhere by changing production data variables and adjusting the energy intensities to suit the mining processes, ore grades, strip ratios, and energy costs.

4 Chapter IV: Conclusion and future work

4.1 Conclusion

This study was conducted to disaggregate end-use energy and greenhouse gas (GHG) emissions at the regional and national levels and to quantify the potential of various GHG mitigation pathways and their associated costs in Canada's iron, gold, and potash mining sectors. These subsectors were responsible for more than half (about 65%) of the mineral extraction industry's energy use and GHG emissions in 2014. Energy use increased by 19%, 105%, and 8% between 2005 and 2014 in the iron, gold, and potash mining sectors, respectively. The data for 102 mine sites were analyzed to identify the currently used processes and technologies. Energy consumption demand trees were developed, and the energy intensities of the end-use processes were calculated. The production data of the mine sites showing various mining and extraction techniques was consolidated. It is assumed that the mine-specific characteristics such as the strip ratio and recovery factor will remain constant in future. A bottom-up energy and environmental model built in the Long-range Energy Alternatives Planning (LEAP) software was developed and validated for the years 2010 to 2015. Energy use and GHG emissions for the year 2015 for each subsector at the national and provincial levels were illustrated through Sankey diagrams. Then, 24 GHG mitigation options were identified and the cost of saved energy and total activity cost of the technologies were calculated through techno-economic assessment model. The penetration rate was modelled for these options. The scenarios were developed in the LEAP-CANMIN model and the results were used to compare energy savings, GHG mitigation potential, and marginal abatement costs.

The overall energy and GHG emissions intensities for iron, gold, and potash mining are 0.6, 164.8, and 1.8 GJ/tonne of product and 31, 5278, and 157 kg CO₂ eq./tonne of product, respectively. The

energy use and GHG emissions in these sectors are illustrated in Figures 4-1 to 4-3. The ore extraction and processing activities are different for the three subsectors. Iron ore is extracted using open pit techniques, gold ore using both open pit and underground techniques, and potash ore using underground and solution mining techniques. Iron production from direct shipping ores require less energy because of their high grade and coarser-grained structure compared to metataconite ores. Newfoundland & Labrador and Quebec shared 55% and 45% of iron mining energy demand (29 PJ) in 2015. The pelletization process has the highest energy use share (56%), while extraction, beneficiation, and other activities had 16%, 17%, and 11%. The total emissions were 1506 thousand tonnes of CO₂ eq. Firing in pelletization and haulage in ore extraction processes are GHG emission-intensive; 68% and 15% of the emissions were from heavy fuel oil use in pelletization and diesel use for haulage, respectively.

Gold production involves various gold extraction and recovery technologies. They were responsible for only about 9% of energy demand and 4% of GHG emissions in 2015. 54% and 28% of the energy demand were from Ontario and Quebec, respectively. The ore extraction processes (including mine air heating) accounted for 62% of the 23.8 PJ energy demand in 2015. The ventilation of underground mines and comminution processes were each responsible for 21% of the energy use. 57% of the energy demand was met by electricity. Total GHG emissions were 762 thousand tonnes, of which 76% were from ore extraction processes, 8% from comminution, 4% from gold extraction, recovery, and post-recovery processes, 11% from mill heating, and the rest from supporting activities. About 50% of the ore extraction emissions were from diesel use in ore haulage and handling.

For potash mining, the energy demand was 33.1 PJ in 2015, shared between Saskatchewan (98%) and New Brunswick (2%). Recovery and extraction processes shared 63% and 37% of the energy

use, respectively. Steam-generation end-use processes were responsible for about 66% of the energy demand. GHG emissions were 2974 thousand tonnes in 2015. 50%, 49%, and 1% of these were from natural gas, electricity, and diesel use, respectively. A significant amount of GHG emissions was from product drying and steam generation (34%) and crushing and grinding (25%) end-use processes.

Twenty-four GHG mitigation scenarios related to ore extraction activities, ventilation, comminution, pelletization, operator efficiency, and steam generation and product drying were identified. Figure 4-4 shows the GHG reduction potential and abatement costs of the options. The cumulative energy savings and GHG mitigation potentials are 98 PJ and 8 Mt CO₂ eq. for iron mining, 323 PJ and 10 Mt CO₂ eq. for gold mining, and 45 PJ and 3 Mt CO₂ eq. for the potash mining sector by 2050. These GHG mitigation potentials correspond to 10%, 20%, and 2% of the total cumulative GHG emissions between 2018 and 2050 in iron, gold, and potash mining, respectively. The average GHG abatement costs were -525, -1,176, and -258 \$/tonne of CO₂ eq. It should be noted that the developed GHG abatement cost curves are based on the resulting energy savings and associated costs for the aggregated activity of all the mines together. As the energy consumption varies widely for each mine depending on the extracted ore grades and processing routes, a mitigation option with high cost savings in the cost curve may not be cost effective for every mine.

The energy intensities calculated in this study can be used to benchmark the current performance and identify energy-intensive processes. The disaggregated Sankey diagrams provide an understanding of what is required in these sectors at the provincial level to meet national climate targets. The wedge curves and GHG abatement cost curves illustrate the long-term GHG mitigation potential of different technology options. These results will aid decision- and policy-

makers to identify strategies to reduce the environmental footprint in an economical way and to assess the potential of the iron, gold, and potash mining sectors to contribute to national and provincial GHG reduction targets.

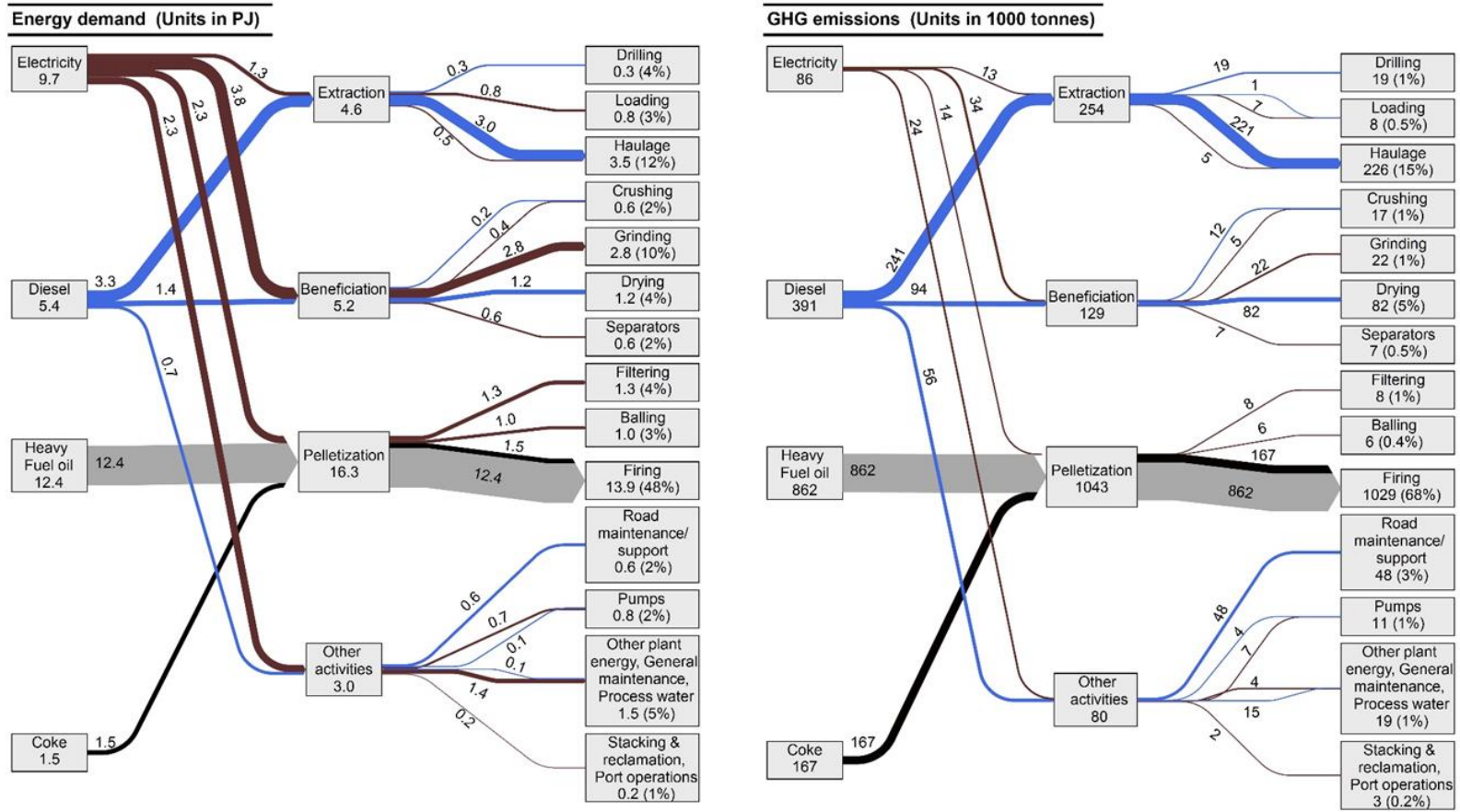


Figure 4-1: Sankey diagram for Canada's iron mining energy demand (left) and GHG emissions (right) in 2015

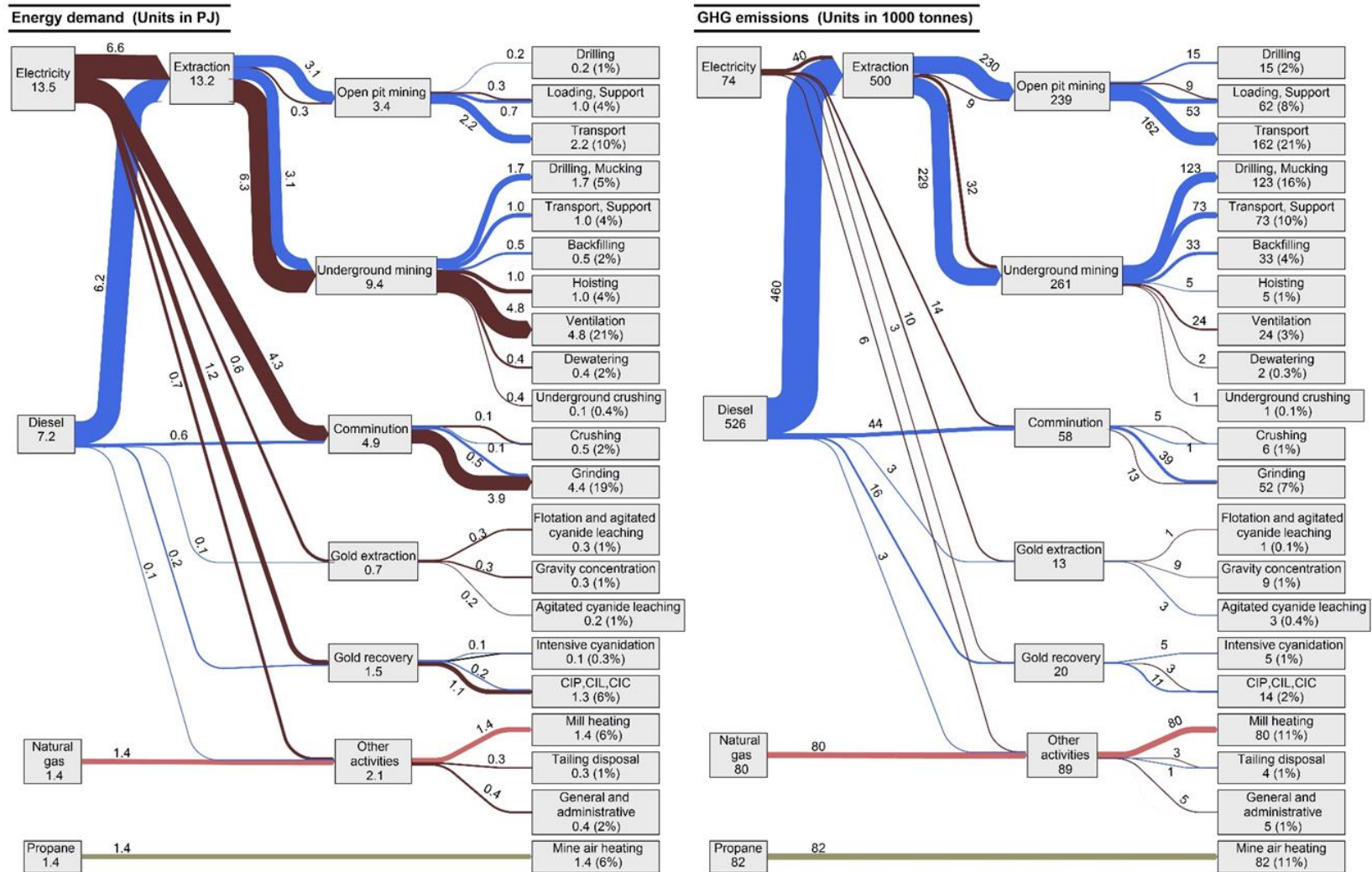


Figure 4-2: Sankey diagram for Canada's gold mining energy demand (left) and GHG emissions (right) in 2015

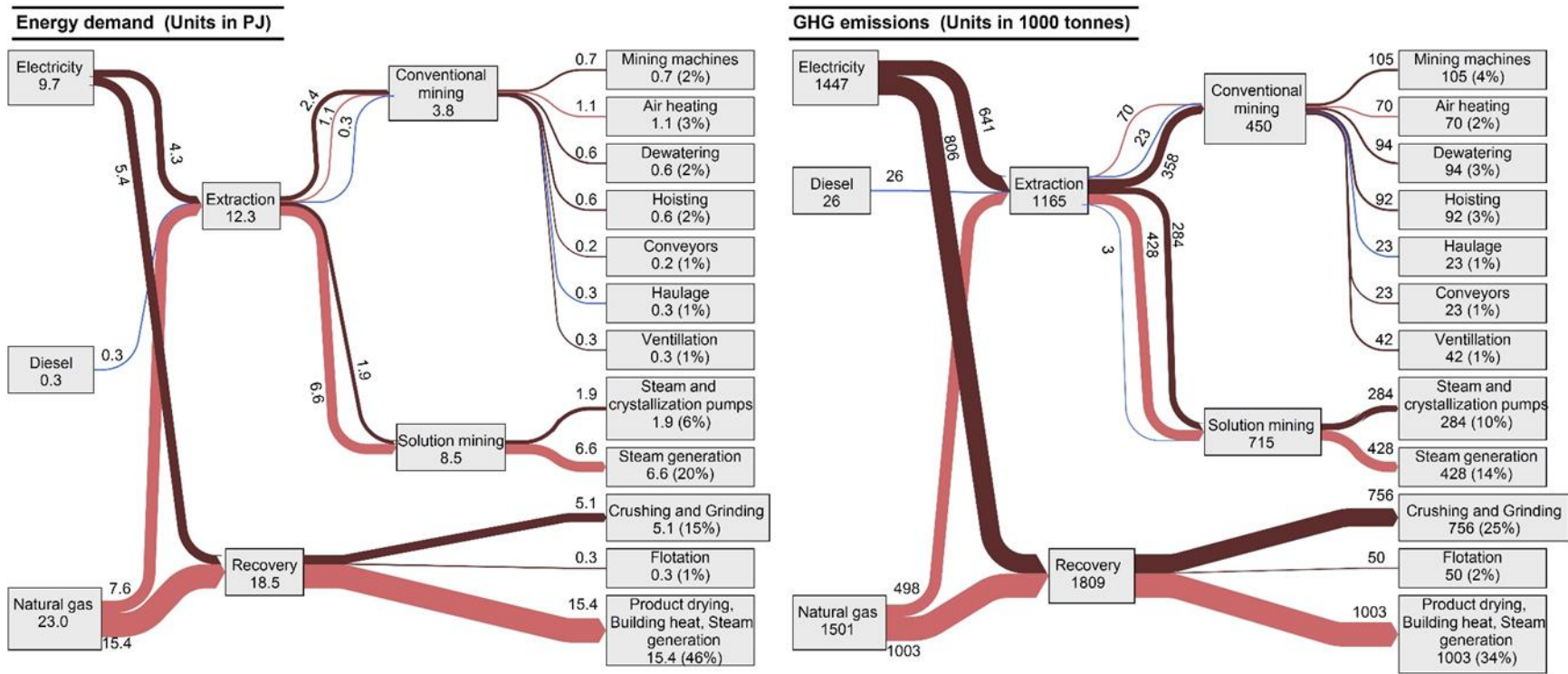
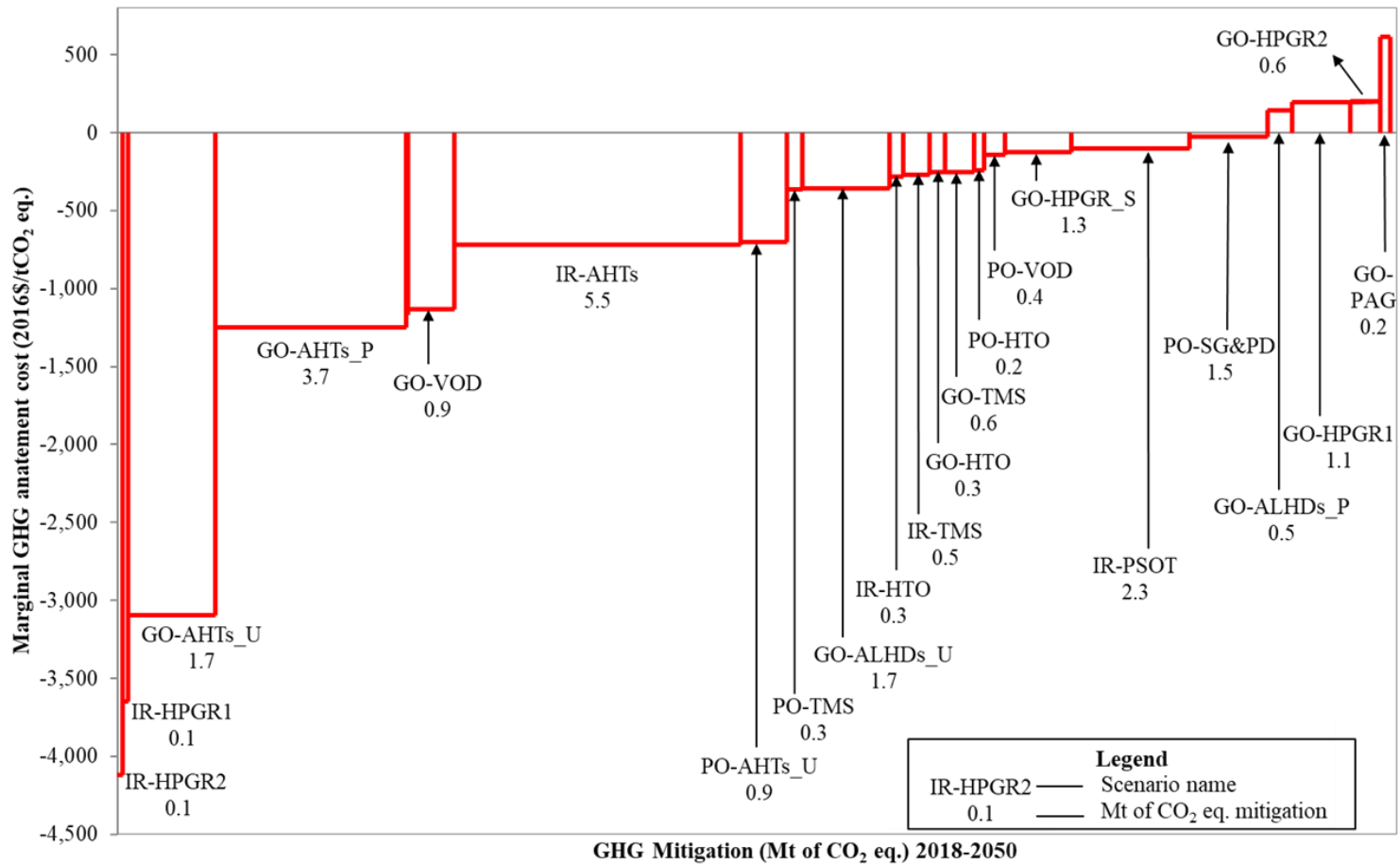


Figure 4-3: Sankey diagrams for Canada's potash mining energy demand and GHG emissions in 2015



* NPV of costs discounted to 2018

Figure 4-4: Canada’s iron, gold, and potash mining sectors combined marginal GHG emission abatement cost curve

* IR: iron mining, GO: gold mining, PO: potash mining, P: open pit mining, U: underground mining, HPGR2: high pressure grinding roll technology option 2, HPGR1: high pressure grinding roll technology option 1, AHTs: new alternative haul truck powertrain technologies, VOD: ventilation on demand, TMS: thermal management system, HTO: haul truck operating mode improvement, ALHDs: new alternative load, haul, dump machines powertrain technologies, HPGR_S: high pressure grinding roll and stirred mill technology, PSOT: pellet-size optimization technology, SG&PD: steam generation and product drying, PAG: pebble addition in grinding. Two scenarios are not included because their mitigation potential is low.

4.2 Recommendations for future work

The following are recommended to extend this work:

1. This study was done only for the iron, gold, and potash mining sectors as they are responsible for nearly 2/3 of Canada's mineral mining industry's energy demand and GHG emissions. The LEAP-CANMIN model can be extended to include all the other sectors of the mineral mining industry.
2. The framework developed in this research can be applied to mining sectors in other jurisdictions by changing production data variables and adjusting the energy intensities to suit the mining processes, ore grades, strip ratios, and energy costs.
3. Future production is estimated based on mining sector growth rates and GDP projections. A better estimate can be made when sub-sectorial growth data is available.
4. Other technology options exist (such as plasma-based iron ore pelletization) at a pilot scale but no cost data is available. New scenarios can be developed when these options reach higher technology readiness levels.
5. The mining industry consumes a significant amount of water. A Water Evaluation and Planning system (WEAP) model can be developed to integrate water and energy use and run combined scenarios.

References

Abouzeid, A.-Z.M. and Fuerstenau, D.W., 2009. Grinding of mineral mixtures in high-pressure grinding rolls. *International Journal of Mineral Processing* 93(1), 59-65.

Arcelor Mittal, 2017. Annual Reports 2010-2016. <https://corporate.arcelormittal.com/investors/financial-reports/annual-reports> (accessed August 2017).

Australian Government-Department of Resources, 2011. Energy efficiency opportunities case study: Analysis of diesel use for mine haul and transport operations. Australian Government-Department of Resources, Energy and Tourism. <https://www.eex.gov.au/sites/g/files/net1896/f/files/2014/06/Analyses-of-Diesel-Use-for-Mine-Haul-and-Transport-Operations.pdf> (accessed August 2017).

Awuah-Offei, K., 2016. Energy efficiency in mining: a review with emphasis on the role of operators in loading and hauling operations. *Journal of Cleaner Production* 117, 89-97.

Babiker, M.H.M., Reilly, J.M., Mayer, M., Eckaus, R.S., Sue Wing, I. and Hyman, R.C., 2001. The MIT Emissions Prediction and Policy Analysis (EPPA) model : revisions, sensitivities, and comparisons of results. MIT Joint Program on the Science and Policy of Global Change. <https://dspace.mit.edu/handle/1721.1/35574> (accessed August 2018).

Ballantyne, G.R., Hilden, M. and van der Meer, F.P., 2018. Improved characterisation of ball milling energy requirements for HPGR products. *Minerals Engineering* 116, 72-81.

Bank of Canada, 2017. Inflation calculator. <https://www.bankofcanada.ca/rates/related/inflation-calculator> (accessed December 2017).

Barnett, T.P., Pierce, D.W., AchutaRao, K.M., Gleckler, P.J., Santer, B.D., Gregory, J.M. and Washington, W.M., 2005. Penetration of human-induced warming into the world's oceans. *Science* 309(5732), 284-287.

Baumert, A.K., Herzog, T. and Pershing, J., 2005. Navigating the Numbers: Greenhouse Gas Data and International Climate Policy. World Resources Institute. http://pdf.wri.org/navigating_numbers.pdf (accessed January 2018).

Bleiwas, D.I., 2011. Estimates of Electricity Requirements for the Recovery of Mineral Commodities, with Examples Applied to Sub-Saharan Africa. US Geological Survey. <https://pubs.usgs.gov/of/2011/1253/report/OF11-1253.pdf> (accessed September 2017).

Bonyad, M., 2014. The Development of a Framework for the Assessment of Energy Demand-based Greenhouse Gas Mitigation Options for Alberta's Agriculture Sector, MSc thesis. University of Alberta, Edmonton, Alberta.

Boothe, P. and Boudreault, F.-A., 2016. By the Numbers: Canadian GHG Emissions. Lawrence National Centre for Policy and Management, Ivey Business School at Western University. <https://www.ivey.uwo.ca/cmsmedia/2111508/4462-ghg-emissions-report-v02.pdf> (accessed January 2019).

Borim, J.C., de Freitas, R.O., Guyot, O., Cisa, M.M. and Lecomte, C., 2018. Automatic control of iron ore pellets size distribution at a pelletizing plant. Vale. https://www.academia.edu/8009338/AUTOMATIC_CONTROL_OF_IRON_ORE_PELLETS_SIZE_DISTRIBUTION_AT_A_PELLETIZING_PLANT (accessed November 2017).

Bouchard, J., Desbiens, A. and Poulin, É., 2017. Reducing the energy footprint of grinding circuits: the process control paradigm. IFAC-PapersOnLine 50(1), 1163-1168.

Brown, M.A., 2001. Market failures and barriers as a basis for clean energy policies. Energy Policy 29(14), 1197-1207.

Brueske, S., Sabouni, R., Zach, C. and Andres, H., 2012. US Manufacturing Energy Use and Greenhouse Gas Emissions Analysis. Energetics Incorporated, Oak Ridge National Laboratory (ORNL), US department of energy. https://www.energy.gov/sites/prod/files/2013/11/f4/energy_use_and_loss_and_emissions.pdf (accessed November 2018).

Cho, Y., Daim, T.U. and Sklar, P., 2015. Forecasting OLED TV technology using bibliometrics and Fisher-Pry diffusion model. Proceedings of PICMET'15: Management of the Technology Age. <https://core.ac.uk/download/pdf/37775716.pdf>. (accessed September 2017).

Cleveland Cliffs Inc., 2017. Annual Reports 2010-2016. Cliffs Cleveland - Cliffs inc. <http://www.clevelandcliffs.com/English/investors/financial-information/annual-reports/default.aspx> (accessed March 2018).

Conliffe, J., Kerr, A. and Hanchar, D., 2012. Mineral Commodities of Newfoundland and Labrador: Iron Ore. Department of Natural Resources. <http://www.nr.gov.nl.ca/nr/mines/geoscience/> (accessed March 2018).

Cullen, J.M. and Allwood, J.M., 2010. The efficient use of energy: Tracing the global flow of energy from fuel to service. Energy Policy 38(1), 75-81.

Davis, M., 2017. The Development of a Technology-Explicit Bottom-Up Integrated Multi-Regional Energy Model of Canada, MSc thesis. University of Alberta, Edmonton, Alberta.

Davis, M., Ahiduzzaman, M. and Kumar, A., 2018a. How will Canada's greenhouse gas emissions change by 2050? A disaggregated analysis of past and future greenhouse gas emissions using bottom-up energy modelling and Sankey diagrams. *Applied Energy* 220, 754-786.

Davis, M., Ahiduzzaman, M. and Kumar, A., 2018b. Mapping Canadian energy flow from primary fuel to end use. *Energy Conversion and Management* 156, 178-191.

Davis, M., Ahiduzzaman, M. and Kumar, A., 2019. How to model a complex national energy system? Developing an integrated energy systems framework for long-term energy and emissions analysis. *International Journal of Global Warming* 17(1), 23-58.

Dean, J., Bish, C., Jean-Charles, B., Moulaye, M., Laurent, P., Rock, G., Andre, B. and Robert, d.l.E., 2010. A technical report on the feasibility study of the direct shipping iron ore (DSO) project. New Millennium Capital Copr. (NML). <http://www.nmliron.com/data/document/en-CA/DSO-FS-Amended-Technical-Report-22-02-2011.pdf> (accessed October 2017).

Eckelman, M.J., 2010. Facility-level energy and greenhouse gas life-cycle assessment of the global nickel industry. *Resources, Conservation and Recycling* 54(4), 256-266.

Edenhofer, O., 2015. Intergovernmental Panel on Climate Change 2014: Mitigation of Climate Change: Working Group III Contribution to the IPCC Fifth Assessment Report. Cambridge University Press, Cambridge.

Environment and Climate Change Canada, 2018. National Inventory Report 1990–2016: Greenhouse Gas Sources and Sinks in Canada. Environment and Climate Change Canada. http://publications.gc.ca/collections/collection_2018/eccc/En81-4-2016-3-eng.pdf (accessed March 2019).

Environment and Climate Change Canada, 2019a. Canadian Environmental Sustainability Indicators: Global Greenhouse Gas Emissions. Environment and Climate Change Canada. <https://www.canada.ca/content/dam/eccc/documents/pdf/cesindicators/global-ghg-emissions/2019/global-GHG-emissions-en.pdf> (accessed March 2019).

Environment and Climate Change Canada, 2019b. Canadian Environmental Sustainability Indicators: Progress towards Canada's Greenhouse Gas Emission Reduction Target. Environment and Climate Change Canada. <https://www.canada.ca/content/dam/eccc/documents/pdf/cesindicators/progress-towards-canada->

[greenhouse-gas-reduction-target/2019/progress-towards-ghg-emissions-target-en.pdf](#) (accessed March 2019).

Ericsson, M., 2010. Global mining towards 2030: Background material and food for thought for the Finnish mineral strategy process 2010. Luleå University of Technology. https://www.sintef.no/globalassets/project/minforsk/documents/referansedokumenter/global_mining_towards_20301.pdf (accessed August 2018).

Esfahanian, E. and Meech, J.A., 2013. Hybrid electric haulage trucks for open pit mining. IFAC Proceedings Volumes 46(16), 104-109.

Ferreira, H. and Leite, M.G.P., 2015. A Life Cycle Assessment study of iron ore mining. Journal of cleaner production 108, 1081-1091.

Fischedick, M., Roy, J., Abdel-Aziz, A., Allwood, J.M., Ceron, J.-P., Geng, Y., Kheshgi, H., Lanza, A., Perczyk, D., Price, L., Santalla, E., Sheinbaum, C. and Tanaka, K., 2014. Industry. In: Climate Change 2014: Mitigation of Climate Change. https://www.ipcc.ch/site/assets/uploads/2018/02/ipcc_wg3_ar5_chapter10.pdf (accessed October 2018).

Fishbone, L.G. and Abilock, H., 1981. Markal, a linear-programming model for energy systems analysis: Technical description of the bnl version. International Journal of Energy Research 5(4), 353-375.

Fisher, J.C. and Pry, R.H., 1971. A simple substitution model of technological change. Technological Forecasting and Social Change 3, 75-88.

Food and Agriculture Organization of the United Nations, 2017. World fertilizer trends and outlook to 2020 summary report. Food and Agriculture organization of the United Nations. <http://www.fao.org/3/a-i6895e.pdf> (accessed January 2019).

Fuerstenau, D.W. and Abouzeid, A.Z.M., 2002. The energy efficiency of ball milling in comminution. International Journal of Mineral Processing 67(1), 161-185.

Furedy, S., 2010. Metso-Iron ore pelletization: The right choice. Metso. <https://www.metalbulletin.com/events/download.ashx/document/speaker/6579/a0ID000000X0jeqMAB/Presentation> (accessed December 2018).

Garrett, D.E., 1996. Potash: deposits, processing, properties and uses. Springer Science & Business Media, Chapman & Hall, London, UK.

Gillett, N.P.,Zwiers, F.W.,Weaver, A.J.and Stott, P.A., 2003. Detection of human influence on sea-level pressure. *Nature* 422(6929), 292.

Global climate and energy program (GCEP), 2009. Global exergy and carbon flow charts. <https://gcep.stanford.edu/pdfs/GCEPExergyCarbonFlowCharts-April2009.pdf> (accessed January 2019).

Government of Canada, 2003. Energy Benchmarking: Canadian Potash Production Facilities. Natural Resources Canada. <http://publications.gc.ca/site/eng/293722/publication.html> (accessed September 2017).

Government of Canada, 2016. Pan-Canadian Framework on Clean Growth and Climate Change. http://publications.gc.ca/collections/collection_2017/eccc/En4-294-2016-eng.pdf (accessed March 2019).

Government of Canada, 2018a. Climatology of temperature and precipitation. https://weather.gc.ca/saisons/image_e.html?format=clim_stn&season=jfm&type=temp (accessed April 2018).

Government of Canada, 2018b. Code of practice - potash sector. <http://ec.gc.ca/lcpe-cepa/default.asp?lang=En&n=A92426AA-1&offset=2> (accessed March 2018).

Government of Newfoundland and Labrador, 2017. Iron in Labrador - Iron Flyer. Natural Resources - Government of Newfoundland and Labrador. https://www.nr.gov.nl.ca/nr/mines/investments/Commodity_Flyers/IRON_NL_Flyer.pdf (accessed March 2018).

Griffin, P.,Hammond, G.and Norman, J., 2013. Industrial Energy Use from a Bottom-up Perspective: Developing the Usable Energy Database (beta version). http://data.ukedc.rl.ac.uk/browse/edc/efficiency/industry/EnergyConsumption/UED_Documentation.pdf (accessed April 2018).

Griffin, P.W.,Hammond, G.P.and Norman, J.B., 2018. Industrial decarbonisation of the pulp and paper sector: a UK perspective. *Applied Thermal Engineering* 134, 152-162.

Griffing, E.and Overcash, M., 2010. Iron ore mining and pelletizing in US-Chemical Life Cycle Database. www.environmentalclarity.com (accessed September 2017).

Gros, D.and Alcidi, C., 2014. The global economy in 2030: Trends and strategies for Europe. Centre for European policy studies.

<https://espas.secure.europarl.europa.eu/orbis/sites/default/files/generated/document/en/The%20Global%20Economy%20in%202030.pdf> (accessed March 2018).

Gupta, S., Mathias, S. and Al Harbi, I., 2011. To know the hindrance or obstacles in hand hygiene practice among healthcare workers of Qassim province of Saudi Arabia. *Journal of Engineering and Technology* 1(1), 52-56.

Gurgel, A.C. and Paltsev, S., 2014. Costs of reducing GHG emissions in Brazil. *Climate Policy* 14(2), 209-223.

Hall, L.M. and Buckley, A.R., 2016. A review of energy systems models in the UK: Prevalent usage and categorisation. *Applied Energy* 169, 607-628.

Hamburg, i., 2019. e!Sankey 3.2. <https://www.ifu.com/e-sankey/> (accessed September 2018).

Haque, N. and Norgate, T., 2015. 20 - Life cycle assessment of iron ore mining and processing, in: Lu, L. (Ed.) *Iron Ore*. Woodhead Publishing, pp. 615-630.

Härkisaari, P., 2015. Wear and friction effects on energy consumption in the mining industry, MSc thesis. Tampere University of Technology, Tampere, Finland.

Heaps, C.G., 2016. Long-range Energy Alternatives Planning (LEAP) system. [Software version 2018.0.1.2] Stockholm Environment Institute Somerville, MA, USA. <https://www.energycommunity.org> (accessed January 2017).

Hill, N., Finnegan, S., Norris, J., Brannigan, C., Wynn, D., Baker, H. and Skinner, I., 2011. Reduction and testing of greenhouse gas (GHG) emissions from heavy duty vehicles—Lot 1: strategy. https://ec.europa.eu/clima/sites/clima/files/transport/vehicles/docs/ec_hdv_ghg_strategy_en.pdf (accessed November 2017).

Huang, Y., Bor, Y.J. and Peng, C.-Y., 2011. The long-term forecast of Taiwan's energy supply and demand: LEAP model application. *Energy Policy* 39(11), 6790-6803.

Hydrogen energy systems, 2016. Hydrogen fuel cost vs gasoline. Hydrogen energy systems. <http://heshydrogen.com/hydrogen-fuel-cost-vs-gasoline/> (accessed May 2018).

Intergovernmental Panel on Climate Change, 2018. Global warming of 1.5 C. Intergovernmental Panel for Climate Change. <https://www.ipcc.ch/sr15/chapter/summary-for-policy-makers/> (accessed March 2019).

Interlaboratory Working Group, 2000. Scenarios for a clean energy future. Oak Ridge, TN: Oak Ridge National Laboratory; Berkeley, CA: Lawrence Berkeley National Laboratory; and Golden, CO: National Renewable Energy Laboratory. <https://www.nrel.gov/docs/fy01osti/29379.pdf> (accessed November 2018).

International Energy Agency, 2019. World balance Sankey. international Energy Agency. <https://www.iea.org/sankey/> (accessed January 2019).

International mining, 2018. Future mining equipment demand and a move to electric power. <https://im-mining.com/2018/12/10/future-mining-equipment-demand-move-electric-power/> (accessed December 2018).

Jankovic, A., 2015. Developments in iron ore comminution and classification technologies, Iron Ore. Elsevier, pp. 251-282.

Jia, L.I.U.,Wenying, C.and Deshun, L.I.U., 2011. Scenario analysis of China's future energy demand based on TIMES model system. Energy Procedia 5, 1803-1808.

Kaarsberg, T.M.,HuangFu, E.and Roop, J.M., 2007. Extreme energy efficiency in the US: industrial, economic and environmental impacts, 2007 ACEEE Summer Study on Energy Efficiency in Industry, 4-24-4-35.

Katta, A.,Davis, M.,Ahiduzzaman, M.,Subramanyam, V.,Dar, A.F.,Mondal, M.A.H.and Kumar, A., 2019. Energy and greenhouse gas impacts of mining and mineral processing operations. Journal of Cleaner Production (under review).

Krause, F., 1996. The costs of mitigating carbon emissions : A review of methods and findings from European studies. Energy Policy(10-11), 899.

Kubach, C., 1994. Gold mining and processing in South Africa. <http://www.mine-engineer.com/mining/mineral/gold.htm> (accessed November 2017).

Lajunen, A., 2015. Energy efficiency of conventional, hybrid electric, and fuel cell hybrid powertrains in heavy machinery. <https://doi.org/10.4271/2015-01-2829>. (accessed November 2018).

Lawrence Livermore National Laboratory, 2018. Energy flow charts: Charting the complex relationships among energy, water, and carbon. <https://flowcharts.llnl.gov/> (accessed January 2019).

Leal-Ayala, D.R.,Allwood, J.M.,Petavratzi, E.,Brown, T.J.and Gunn, G., 2015. Mapping the global flow of tungsten to identify key material efficiency and supply security opportunities. *Resources, Conservation and Recycling* 103, 19-28.

Levesque, M.,Millar, D.and Paraszcak, J., 2014. Energy and mining—the home truths. *Journal of Cleaner Production* 84, 233-255.

Loulou, R.and Labriet, M., 2008. ETSAP-TIAM: the TIMES integrated assessment model Part I: Model structure. *Computational Management Science* 5(1), 7-40.

Maré, E.,Beven, B.and Crisafio, C., 2015. Developments in nonmagnetic physical separation technologies for hematitic/goethitic iron ore, *Iron Ore*. Elsevier, pp. 309-338.

Marsden, J., 2006. Overview of gold processing techniques around the world. *Minerals and Metallurgical Processing* 23(3), 121-125.

Marshall, B., 2017. Facts and figures of the Canadian mining industry: F&F 2017. Ottawa. <http://mining.ca/documents/facts-and-figures-2017> (accessed August 2018).

Mau, P.,Eyzaguirre, J.,Jaccard, M.,Collins-Dodd, C.and Tiedemann, K., 2008. The ‘neighbor effect’: Simulating dynamics in consumer preferences for new vehicle technologies. *Ecological Economics* 68(1-2), 504-516.

McCambridge, T.and Kuruppu, M., 2009. Ventilation on demand at Gwalia Gold Mine, *Mine Ventilation*. Oxford & IBH Publishing Co, pp. 83-91.

McKinney, J.,Bond, E.,Crowell, M.and Odufuwa, E., 2015. Joint agency staff report on assembly bill 8: assessment of time and cost needed to attain 100 hydrogen refueling stations in California. California Energy Commission. <https://www.energy.ca.gov/2015publications/CEC-600-2015-016/CEC-600-2015-016.pdf> (accessed October 2017).

McNab, B.,Jankovic, A.,David, D.and Payne, P., 2009. Processing of magnetite iron ores—comparing grinding options, *Proceedings of Iron Ore 2009 Conference*, Perth, Australia. pp. 27-29.

Mine Wiki, 2018. Mine Design - Ventilation air heating. http://minewiki.engineering.queensu.ca/mediawiki/index.php/Ventilation_air_heating (accessed April 2018).

Mining Association of Canada, 2016. Facts and Figures of the Canadian Mining Industry. The Mining Association of Canada. <http://mining.ca/resources/reports> (accessed March 2017).

Mudd, G.M., 2007a. An analysis of historic production trends in Australian base metal mining. *Ore Geology Reviews* 32(1-2), 227-261.

Mudd, G.M., 2007b. Global trends in gold mining: Towards quantifying environmental and resource sustainability. *Resources Policy* 32(1-2), 42-56.

National Energy Board, 2017. Canada's energy future 2016 update-Energy supply and demand projections to 2040. National Energy Board. <https://www.neb-one.gc.ca/nrg/ntgrtd/ft/2016updt/index-eng.html> (accessed November 2017).

National Energy Board, 2018. Canada's energy future 2018: Energy supply and demand projections to 2040. National Energy Board. <https://www.neb-one.gc.ca/nrg/ntgrtd/ft/2018/index-eng.html> (accessed January 2018).

Natural Resources Canada, 2005a. Benchmarking the Energy Consumption of Canadian Open-pit Mines. Natural Resources Canada. <http://www.publications.gc.ca/site/eng/287279/publication.html> (accessed August 2017).

Natural Resources Canada, 2005b. Benchmarking the Energy Consumption of Canadian Underground Bulk Mines. Natural Resources Canada. <http://publications.gc.ca/site/eng/287264/publication.html> (accessed October 2017).

Natural Resources Canada, 2016a. Energy efficiency in mining. <https://www.nrcan.gc.ca/mining-materials/green-mining/18312> (accessed November 2017).

Natural Resources Canada, 2016b. Energy Efficiency Trends in Canada 1990 to 2013. Natural Resources Canada. <https://www.nrcan.gc.ca/sites/www.nrcan.gc.ca/files/energy/pdf/trends2013.pdf> (accessed March 2019).

Natural Resources Canada, 2018a. Annual Statistics of Mineral Production. Natural Resources Canada. <https://www.nrcan.gc.ca/mining-materials/statistics/8850> (accessed June 2018).

Natural Resources Canada, 2018b. Comprehensive Energy Use Database. Natural Resources Canada. http://oee.nrcan.gc.ca/corporate/statistics/neud/dpa/menus/trends/comprehensive_tables/list.cfm (accessed April 2018).

Natural Resources Canada, 2018c. Energy efficiency trends analysis tables. Natural Resources Canada. <http://oee.nrcan.gc.ca/corporate/statistics/neud/dpa/menus/trends/analysis/tables.cfm> (accessed March 2019).

Natural Resources Canada, 2019a. The Atlas of Canada - Minerals and Mining. <http://atlas.gc.ca/mins/en/index.html> (accessed April 2019).

Natural Resources Canada, 2019b. Energy use in the industrial sector. Natural Resources Canada. <http://oee.nrcan.gc.ca/publications/statistics/trends/2015/industrial.cfm#L4> (accessed March 2019).

Nel, W.P., 2004. The diffusion of fuel cell vehicles and its impact on the demand for platinum group metals: research framework and initial results. International Platinum Conference 'Platinum Adding Value', The South African Institute of Mining and Metallurgy. <http://citeseerx.ist.psu.edu/viewdoc/download?doi=10.1.1.452.39&rep=rep1&type=pdf>. (accessed February 2018).

Nessim, W., Zhang, F.J., Zhao, C.L. and Zhu, Z.X., 2013. Optimizing operational performance of diesel mining truck using thermal management, *Advanced Materials Research*. Trans Tech Publications, pp. 273-277.

New Millennium Capital Corp., 2010. A Technical Report on the Feasibility Study of the Direct Shipping Iron Ore (DSO) project. New Millennium Capital Corp. www.sedar.com (accessed April 2018).

Nkwanyana, S. and Loveday, B., 2017. Addition of pebbles to a ball-mill to improve grinding efficiency. *Minerals Engineering* 103, 72-77.

Norgate, T. and Haque, N., 2010. Energy and greenhouse gas impacts of mining and mineral processing operations. *Journal of Cleaner Production* 18(3), 266-274.

Norgate, T. and Haque, N., 2012. Using life cycle assessment to evaluate some environmental impacts of gold production. *Journal of Cleaner Production* 29, 53-63.

Numbi, B.P., Zhang, J. and Xia, X., 2014. Optimal energy management for a jaw crushing process in deep mines. *Energy* 68, 337-348.

Nyboer, J., 1997. Simulating evolution of technology: an aid to energy policy analysis: a case study of strategies to control greenhouse gases in Canada, PhD thesis. Environment: School of Resource and Environmental Management, Simon Fraser University, Ottawa.

Oeters, F., Ottow, M., Senk, D., Beyzavi, A., Güntner, J., Lungen, H.B., Koltermann, M. and Buhr, A., 2011. Iron, 1. Fundamentals and Principles of Reduction Processes, Ullmann's Encyclopedia of Industrial Chemistry.

Perez-Lombard, L., Ortiz, J. and Maestre, I.R., 2011. The map of energy flow in HVAC systems. Applied energy 88(12), 5020-5031.

Rockwell Automation, 2017. BESTECH delivers new ventilation-on-demand system for underground mine. Rockwell Automation. https://www.rockwellautomation.com/global/news/case-studies/detail.page?pagetitle=BESTECH-Delivers-New-Ventilation-on-Demand-System-for-Underground-Mines%2C-Saves-Significant-Energy-Costs-%7C-Case-Study&content_type=casestudy&docid=3641757fdf67292dd6882278e9bab1f6 (accessed September 2017).

Schmidt, M., 2008. The Sankey diagram in energy and material flow management: Part I: History. Journal of industrial ecology 12(1), 82-94.

SEDAR, 2017. System for Electronic Document Analysis and Retrieval. https://www.sedar.com/homepage_en.htm (accessed August 2017).

Shafique, H.U., 2017. Assessment of energy-demand based GHG mitigation options for the pulp and paper sector, MSc thesis. University of Alberta.

Singh, G., Choudhary, R., Vardhan, H., Aruna, M. and Akolkar, A., 2015. Iron ore pelletization technology and its environmental impact assessment in eastern region of India—a case study. Procedia Earth and Planetary Science 11, 582-597.

Song, X., Hu, S., Chen, D. and Zhu, B., 2017. Estimation of waste battery generation and analysis of the waste battery recycling system in China. Journal of Industrial Ecology 21(1), 57-69.

Statistics Canada, 2018. North American Industry Classification System (NAICS) Canada. Statistics Canada. <https://www.statcan.gc.ca/eng/concepts/industry> (accessed April 2018).

Stockholm Environment Institute, 2018. LEAP: Applications. <https://www.energycommunity.org/default.asp?action=applications> (accessed November 2018).

Stott, P.A., 2003. Attribution of regional-scale temperature changes to anthropogenic and natural causes. Geophysical Research Letters 30(14).

Subramanyam, V., Ahiduzzaman, M. and Kumar, A., 2017a. Greenhouse gas emissions mitigation potential in the commercial and institutional sector. *Energy and Buildings* 140(Supplement C), 295-304.

Subramanyam, V., Kumar, A., Talaei, A. and Mondal, M.A.H., 2017b. Energy efficiency improvement opportunities and associated greenhouse gas abatement costs for the residential sector. *Energy* 118(Supplement C), 795-807.

Subramanyam, V., Paramshivan, D., Kumar, A. and Mondal, M.A.H., 2015. Using Sankey diagrams to map energy flow from primary fuel to end use. *Energy Conversion and Management* 91, 342-352.

Systematic Solutions Inc, 2017a. Energy 2020. Systematic Solution, inc. https://docs.wixstatic.com/ugd/af9ba3_f17daa4f43dc479c93cec596293081f1.pdf (accessed March 2019).

Systematic Solutions Inc, 2017b. Energy 2020 documentation : Volume 1 overview 2017. https://docs.wixstatic.com/ugd/af9ba3_f17daa4f43dc479c93cec596293081f1.pdf (accessed March 2019).

Talaei, A., 2019. Assessment of energy efficiency improvement opportunities and the long-term potential for greenhouse gas mitigation in industrial sector, PhD thesis. University of Alberta, Edmonton, Alberta.

Talaei, A., Ahiduzzaman, M. and Kumar, A., 2018. Assessment of long-term energy efficiency improvement and greenhouse gas emissions mitigation potentials in the chemical sector. *Energy* 153, 231-247.

Talaei, A., Pier, D., Iyer, A.V., Ahiduzzaman, M. and Kumar, A., 2019. Assessment of long-term energy efficiency improvement and greenhouse gas emissions mitigation options for the cement industry. *Energy* 170, 1051-1066.

Tao, Z., Zhao, L. and Changxin, Z., 2011. Research on the prospects of low-carbon economic development in China based on LEAP model. *Energy Procedia* 5, 695-699.

The Conference Board of Canada, 2017. Territorial outlook economic forecast: Summer 2017. The Conference Board of Canada. <https://www.conferenceboard.ca/e-library/abstract.aspx?did=8979> (accessed January 2018).

The Mining Association of Canada, 2017. Facts and figures of the Canadian mining industry: 2011-2016. The mining association of Canada. <http://mining.ca/resources/reports> (accessed August 2017).

Tost, M., Hitch, M., Chandurkar, V., Moser, P. and Feiel, S., 2018. The state of environmental sustainability considerations in mining. *Journal of Cleaner Production* 182, 969-977.

U.S. Department of Energy, 2007. Mining Industry Energy Bandwidth Study. https://www.energy.gov/sites/prod/files/2013/11/f4/mining_bandwidth.pdf (accessed April 2018).

United Nations Framework Convention on Climate Change, 2015. Adoption of the Paris Agreement. Report No. FCCC/CP/2015/L.9/Rev.1. United Nations Framework Convention on Climate Change. <http://unfccc.int/resource/docs/2015/cop21/eng/l09r01.pdf> (accessed March 2019).

United Nations Framework Convention on Climate Change, 2016. Synthesis Report on the Aggregate Effect of INDCs. United Nations Framework Convention on Climate Change. <https://unfccc.int/process/the-paris-agreement/nationally-determined-contributions/synthesis-report-on-the-aggregate-effect-of-intended-nationally-determined-contributions> (accessed April 2019).

United Nations Framework Convention on Climate Change, 2018. The Katowice Climate Package: Making the Paris Agreement Work for All. <https://unfccc.int/process-and-meetings/the-paris-agreement/katowice-climate-package#eq-2> (accessed March 2019).

US Department of Energy, 2002a. Energy and Environmental Profile of the US Mining Industry - Gold and silver. <https://www.energy.gov/sites/prod/files/2013/11/f4/gold-silver.pdf> (accessed October 2017).

US Department of Energy, 2002b. Energy and Environmental Profile of the US Mining Industry - Iron. <https://www.energy.gov/sites/prod/files/2013/11/f4/iron.pdf> (accessed October 2017).

US Department of Energy, 2002c. Energy and Environmental Profile of the US Mining Industry - Potash, soda ash, and borates. US Department of Energy Office of Energy Efficiency and Renewable Energy. Energiebilanz der Nuklearindustrie. https://www.energy.gov/sites/prod/files/2013/11/f4/potash_soda_borate.pdf (accessed October 2017).

US Department of Energy, 2007. Mining Industry Energy Bandwidth Study. https://www.energy.gov/sites/prod/files/2013/11/f4/mining_bandwidth.pdf (accessed April 2018).

US Geological Survey, 2016. Minerals information volume 1: Metals and minerals. US Department of the Interior | US Geological Survey. <https://minerals.usgs.gov/minerals/pubs/myb.html> (accessed November 2018).

US Securities and Exchange Commission, 2018. EDGAR-Company Filings Annual report FORM 10-K. <https://www.sec.gov/edgar/searchedgar/companysearch.html> (accessed May 2018).

Varaschin, J., 2016. The Economic Case for Electric Mining Equipment and Technical Considerations Relating to their Implementation, MASc thesis. Queen's University, Kingston, Ontario.

Varaschin, J. and De Souza, E., 2015. Economics of diesel fleet replacement by electric mining equipment. 15th North American Mine Ventilation Symposium. <http://www.airfinders.ca/wp-content/uploads/2015/06/Economics-of-Diesel-Fleet-Replacement-by-Electric-Mining-Equipment.pdf>. (accessed September 2017).

Wallace, K., 2001. General operational characteristics and industry practices of mine ventilation systems. Proceedings of the 7th International Mine Ventilation Congress (Ed: S. Wasilewski).

Wang, C., 2013. Comparison of HPGR-ball mill and HPGR-stirred mill circuits to the existing AG/SAG mill-ball mill circuits. University of British Columbia.

Wang, C., Nadolski, S., Mejia, O., Drozdiak, J. and Klein, B., 2013. Energy and cost comparisons of HPGR based circuits with the SABC circuit installed at the huckleberry mine. 45th Annual Canadian Mineral Processors Operators Conference, Ottawa, Ontario. <http://www.ceecthefuture.org/wp-content/uploads/2013/10/Energy-and-cost-comparisons-Wang-et-al.pdf>. (accessed September 2017).

Wen, Z., Meng, F. and Chen, M., 2014. Estimates of the potential for energy conservation and CO₂ emissions mitigation based on Asian-Pacific Integrated Model (AIM): the case of the iron and steel industry in China. Journal of Cleaner Production 65, 120-130.

World Gold Council, 2019. Gold 2048: The next 30 years for gold. <https://www.valuwalk.com/wp-content/uploads/2018/05/Gold-2048.pdf> (accessed November 2018).

Xu, G.Y.,Qin, W.F.,Ti, S.G.and Xu, Y.C., 2012. Energy and environmental scenario analysis for residential sector based on LEAP, Applied Mechanics and Materials. Trans Tech Publ, pp. 3133-3138.

Yamaguchi, S.,Fujii, T.,Yamamoto, N.and Nomura, T., 2010. Kobelco pelletizing process. Kobelco Technology Review 29, 58-59.

Yang, C.,Yeh, S.,Zakerinia, S.,Ramea, K.and McCollum, D., 2015. Achieving California's 80% greenhouse gas reduction target in 2050: Technology, policy and scenario analysis using CA-TIMES energy economic systems model. Energy Policy 77, 118-130.

Yellishetty, M.,Ranjith, P.and Tharumarajah, A., 2010. Iron ore and steel production trends and material flows in the world: Is this really sustainable? Resources, conservation and recycling 54(12), 1084-1094.

Zhang, X.,Zwiers, F.W.,Hegerl, G.C.,Lambert, F.H.,Gillett, N.P.,Solomon, S.,Stott, P.A.and Nozawa, T., 2007. Detection of human influence on twentieth-century precipitation trends. Nature 448(7152), 461.

Zhao, Z.,Wang, T.,Liu, P.and Li, Z., 2016. A Sankey diagram approach to quantifying industrial residual energy in China. Chemical Engineering Transactions 52, 37-42.

Appendix A

Table A1: Iron ore extracted and production of iron concentrate and pellets (million tonnes)

Year	NFL					QC			NU	
	Ore	Concentrate production	Pellet production	DSO share	Metacornite ore share	Ore	Concentrate production	Pellet production	Ore	Concentrate production
2010	56.6	21.5	15.8	0%	100%	44.7	15.8	9.5	0	0
2011	52.8	20.6	12.1	1%	99%	43.3	15.8	9.3	0	0
2012	62.6	23.4	12.8	3%	97%	46.9	15.7	9.0	0	0
2013	64.5	25.9	11.4	7%	93%	58.6	18.6	9.1	0	0
2014	53.8	21	8.7	0%	100%	66.8	24.0	10.0	0.3	0.3
2015	49.4	20	9.3	12%	89%	70.7	26.6	10.0	1.5	1.3

Table A2: Activity variables of gold mining (million tonnes)

Province	Year	Ore and waste extraction	Ore milled	Open-pit ore mined	Underground ore mined	Ore processed in gold extraction	Ore processed in gold recovery
Newfoundland & Labrador	2010	999505	114517	128993	0	114517	114517
	2011	1170989	184226	135669	97140	184226	184226
	2012	1671312	378721	272854	92295	378721	378721
	2013	2024371	373818	289743	85220	373818	373818
	2014	2010194	395194	296152	90498	395194	395194
	2015	2158550	417883	321532	74705	417883	417883
Nunavut	2010	14688000	2040000	2040000	0	3468000	2040000
	2011	21439605	2977723	2977723	0	5062129	2977723
	2012	34762000	3820000	3820000	0	6494000	3820000
	2013	36456992	4142840	4142840	0	7042828	4142840
	2014	36988400	4156000	4156000	0	7065200	4156000
	2015	27423386	4032851	4032851	0	6855846	4032851
Saskatchewan	2010	203958	203958	0	203958	203958	203958
	2011	1105220	349086	403010	387862	440991	349086
	2012	1179369	415376	447616	382612	555517	415376
	2013	461258	428883	41506	387377	577766	428883
	2014	350236	350236	29440	320796	420875	350236
	2015	277368	277368	0	277368	277368	277368
British Columbia	2010	28237903	27351596	27351758	606817	7894596	0
	2011	27367152	7730758	10756942	358156	7716856	0
	2012	30452900	10148205	8121878	2026327	12121878	0
	2013	31954066	12062221	7956738	4105483	16112738	0
	2014	20798594	9428139	4548182	4879957	14191203	0

Province	Year	Ore and waste extraction	Ore milled	Open-pit ore mined	Underground ore mined	Ore processed in gold extraction	Ore processed in gold recovery
	2015	11532233	6919735	1781799	5295936	12016735	0
Manitoba	2010	0	275860	0	0	551720	275860
	2011	486579	491150	0	486579	982300	491150
	2012	615344	629276	0	615344	1258552	629276
	2013	615344	629276	0	615344	1258552	629276
	2014	629311	641710	0	629311	1283420	641710
Yukon	2010	262883	262883	262883	0	262883	262883
	2011	234322	234322	234322	0	234322	234322
	2012	264301	264301	264301	0	264301	264301
	2013	298472	298472	298472	0	298472	298472
	2014	296157	296157	296157	0	296157	296157
	2015	298049	298049	298049	0	298049	298049
Ontario	2010	23960893	12021115	1084655	15629865	17559111	12021115
	2011	25379411	12544963	884609	16423224	18446155	12544963
	2012	31101337	14532035	2347235	17857302	20593494	14532035
	2013	95668344	28780988	17918368	17547077	35015652	28780988
	2014	98904506	34244604	18552723	18166526	39311952	32901521
	2015	108773157	33691104	24231245	17309638	40082633	33691104
Quebec	2010	4811279	7510084	0	4811279	11060384	7510084
	2011	30802817	15433665	8502323	4445616	18750112	15433665
	2012	47844793	18298240	14046526	4300562	18938546	18298240
	2013	61062485	23037850	18081104	4799784	24681925	23037850
	2014	66836330	25728778	19630945	7037867	28958462	25728778
	2015	67776005	26217760	19965496	7160564	29589222	26217760

Table A3: Gold production through various extraction and recovery technologies (kgs)

Province	Gold extraction/recovery technology	Year						
		2010	2011	2012	2013	2014	2015	
Newfoundland & Labrador	Gold extraction	Flotation and agitated cyanide leaching	387	320	712	652	673	713
	Gold recovery	Merill Crowe	387	171	383	476	466	506
		CIP, CIL	0	149	329	176	206	207
	Post recovery	Electrowinning	387	320	712	652	673	713
Nunavut	Gold extraction	Gravity concentration	2550	2600	3514	4134	4128	3665
		Agitated cyanide leaching	5951	6066	8199	9646	9632	8552
	Gold recovery	Intensive cyanidation	2550	2600	3514	4134	4128	3665
		CIP, CIL	5951	6066	8199	9646	9632	8552
Post recovery	Electrowinning	8501	8666	11713	13780	13760	12218	
Saskatchewan	Gold extraction	Gravity concentration	0	693	599	496	192	0
		Agitated cyanide leaching	1513	1779	1886	1651	2111	2424

Province	Gold extraction/recovery technology	Year							
		2010	2011	2012	2013	2014	2015		
British Columbia	Gold recovery	CIP, CIL	1513	1779	1886	1651	2111	2424	
	Post recovery	Direct smelting of gravity concentrate	0	693	599	496	192	0	
		Electrowinning	1513	1779	1886	1651	2111	2424	
	Gold extraction	Gravity concentration	74	190	714	2091	7439	8719	
		Agitated cyanide leaching	148	233	0	0	0	0	
		Flotation only	4811	1399	2340	2910	2584	3177	
		DMS and gravity concentration	0	0	0	0	465	350	
		Gold recovery	CIP, CIL	148	233	0	0	0	0
			Electrowinning	148	233	0	0	0	0
	Post recovery	Direct smelting of gravity concentrate	74	190	125	60	82	111	
Smelting of concentrate		4811	1399	2929	4941	10406	12135		
Manitoba	Gold extraction	Flotation and agitated cyanide leaching	877	1497	1744	1744	1516	0	
		Gravity concentration	515	879	1024	1024	891	0	
	Gold recovery	CIP, CIL	877	1497	1744	1744	1516	0	
		Electrowinning	877	1497	1744	1744	1516	0	
	Post recovery	Direct smelting of gravity concentrate	515	879	1024	1024	891	0	
Yukon	Gold extraction	Gravity concentration	31946	31199	27313	32121	35770	1520	
Ontario	Gold extraction	Flotation and agitated cyanide leaching	9452	8360	8620	11202	10586	10181	
		Gravity concentration	16566	15349	13401	16411	17933	17359	
		Agitated cyanide leaching	28703	28843	2084	37815	43778	41956	
		Cyanidation in grinding	1761	2310	975	3067	3546	3374	
	Gold recovery	Flotation concentrate autoclave	1350	1194	947	947	796	721	
		Merill Crowe	705	542	710	868	1013	969	
		Intensive cyanidation	0	0	0	2527	4968	5500	
	Post recovery	CIP, CIL	38801	37855	38089	49095	54147	51889	
		CIC	1761	2310	2084	3067	3546	3374	
		Electrowinning	41267	40707	40884	55557	63674	61732	
Quebec	Gold extraction	Direct smelting of gravity concentrate	16566	15349	13401	13883	12965	11858	
		Flotation and agitated cyanide leaching	7896	5747	5792	6750	8745	16889	
		Gravity concentration	31946	31199	6713	7079	9361	10541	
		Agitated Cyanide leaching	3066	8393	14263	20774	9257	12633	
		Gravity concentration and oxidation	2067	1884	1869	1773	1630	1601	
		Merill Crowe	2528	1944	2508	1594	2212	1596	

Province	Gold extraction/recovery technology	Year					
		2010	2011	2012	2013	2014	2015
Gold recovery	Intensive cyanidation	2258	2622	2520	1001	2169	3762
	CIP, CIL	61140	17415	23029	28703	19472	31572
	Electrowinning	65926	21981	28057	31298	23853	36931
Post recovery	Direct smelting of gravity concentrate	6384	5050	1673	5078	5140	4732

Table A4: Propane energy demand (GJ) in underground gold mining

Province	Average ambient air temperature (°C)	Propane energy consumption (GJ)					
		2010	2011	2012	2013	2014	2015
Newfoundland and Labrador	-10	0.00	0.01	0.01	0.00	0.00	0.00
Saskatchewan	-15	0.01	0.03	0.03	0.03	0.02	0.02
British Columbia	-5	0.02	0.01	0.01	0.03	0.04	0.04
Manitoba	-18	0.00	0.04	0.05	0.05	0.05	0.00
Yukon	-21	0.00	0.03	0.05	0.05	0.00	0.00
Quebec	-12	0.27	0.25	0.24	0.27	0.39	0.40
Ontario	-12	0.88	0.92	1.00	0.98	1.02	0.97

Table A5: Potash production through different mining methods

Extraction method	Province	2010	2011	2012	2013	2014	2015
Conventional (million tonnes)	Saskatchewan	12.2	14.2	13.2	13.6	13.5	15.8
	New Brunswick	0.6	0.7	0.7	0.6	0.6	0.7
Solution (million tonnes)	Saskatchewan	1.9	2.6	2.6	2.5	2.2	2.4
Total (million tonnes)	Saskatchewan	14.0	16.7	15.8	16.1	15.7	18.2
	New Brunswick	0.6	0.7	0.7	0.6	0.6	0.7
Conventional (%)	Saskatchewan	86.7	84.5	83.6	84.6	86.0	87.0
	New Brunswick	100.0	100.0	100.0	100.0	100.0	100.0
Solution (%)	Saskatchewan	13.3	15.5	16.4	15.4	14.0	13.0

Processing routes of iron, gold, and potash mining

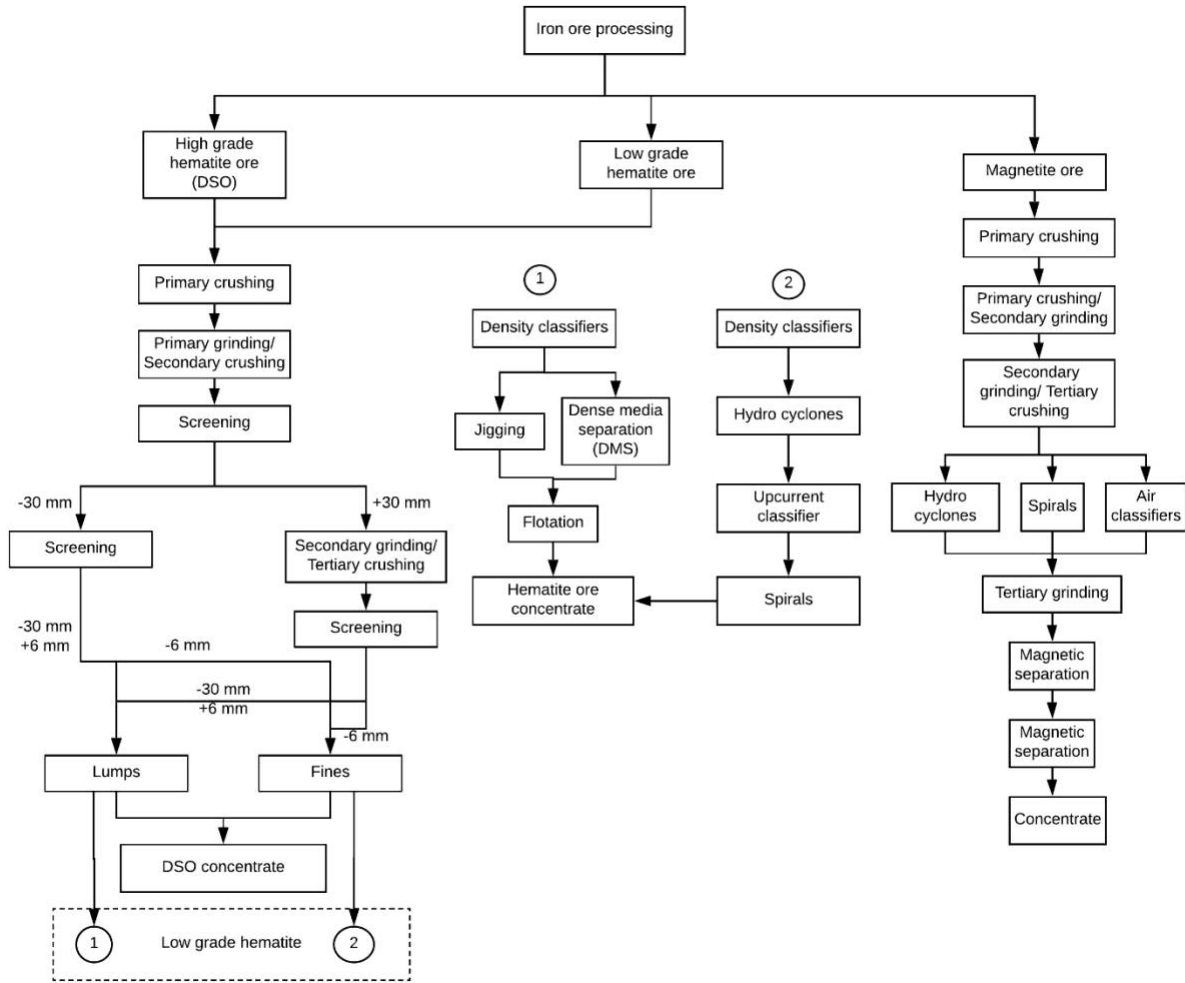


Figure A1: Iron ore processing flow diagram

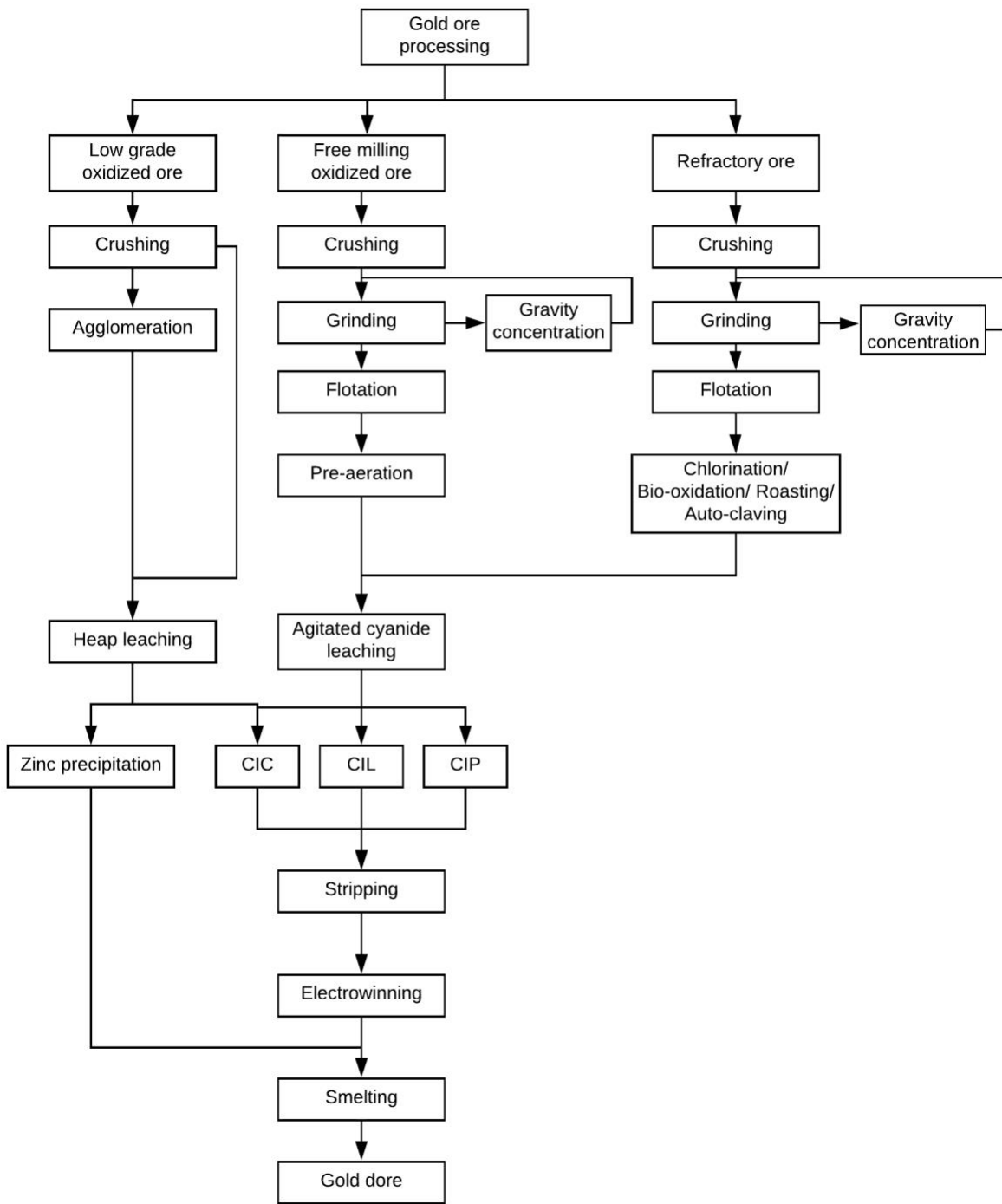


Figure A2: Gold ore processing flow diagram

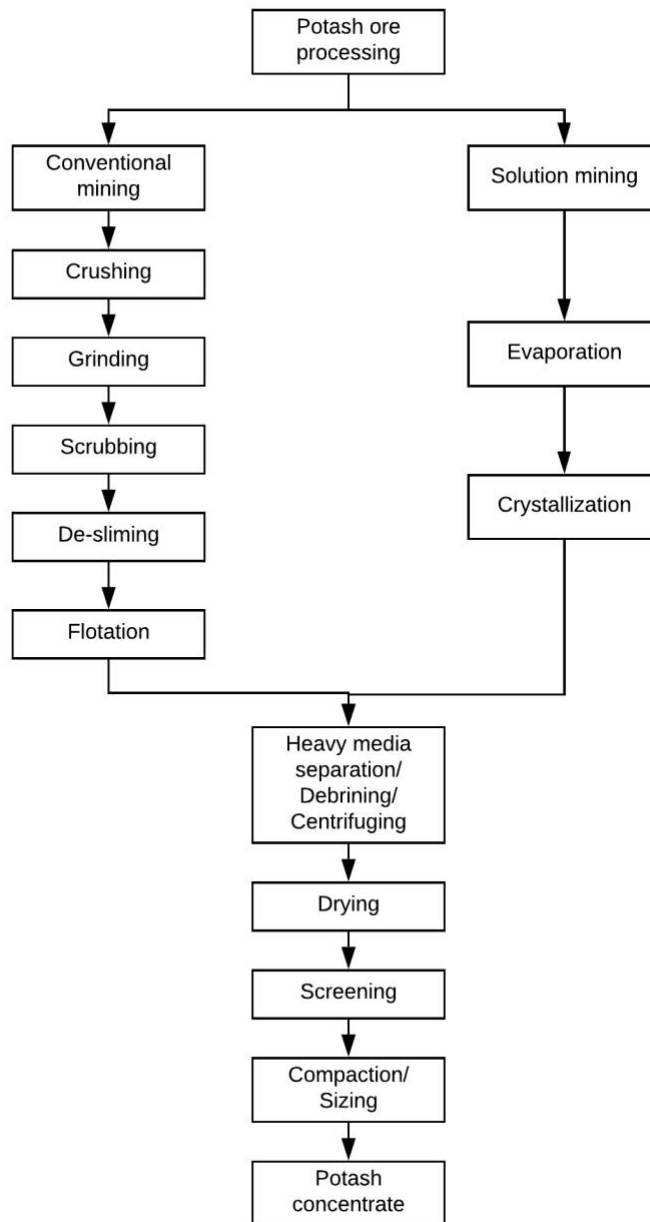


Figure A3: Potash ore processing flow diagram

Table A6: Electricity grid emission intensity factor (grams CO₂ eq./kilowatt-hour)

Province	2010	2015	2020	2025	2030	2035	2040	2045	2050
British Columbia (BC)	41.0	38.3	13.1	14.2	12.9	12.9	12.7	12.5	12.4
Saskatchewan (SK)	593.5	545.9	500.9	413.1	279.7	273.9	223.3	185.7	145.4
Manitoba (MB)	42.5	38.6	20.9	16.8	5.1	5.3	5.2	5.1	4.9
Ontario (ON)	121.3	8.3	32.2	70.4	49.6	37.6	41.1	44.0	46.6
Quebec (QC)	5.5	6.3	5.8	6.1	6.4	6.0	6.2	6.2	5.9
New Brunswick (NB)	344.5	214.9	213.0	211.4	205.7	205.3	199.4	198.9	198.3
Newfoundland and Labrador (NFL)	13.5	14.2	16.4	16.4	15.1	17.7	17.7	17.7	17.7
Yukon (YK)	36.7	1.4	122.3	8.6	1.3	1.3	1.3	1.3	1.3
Nunavut (NU)	639.2	638.8	441.0	450.3	449.8	457.9	457.1	458.5	460.0

Sectorial growth rates used in the BAU scenario

Table A7: Mining sector growth rate projections

Year	Province								
	British Columbia (metal)	Manitoba (metal)	Newfoundland & Labrador (metal)	Nunavut (metal)	Ontario (metal)	Quebec (metal)	Saskatchewan (metal)	Yukon (metal)	Saskatchewan (Non metal)
2016	-2%	-5%	-4%	18%	0%	1%	-1%	75%	3%
2017	-3%	0%	2%	15%	6%	2%	0%	-14%	3%
2018	14%	-11%	4%	-5%	5%	6%	8%	12%	6%
2019	1%	-38%	4%	20%	0%	9%	1%	23%	6%
2020	19%	-7%	1%	27%	1%	2%	1%	22%	0%
2021	6%	-21%	4%	9%	5%	3%	2%	1%	13%
2022	1%	1%	4%	6%	1%	1%	2%	7%	2%
2023	1%	1%	3%	6%	5%	1%	1%	5%	1%
2024	2%	1%	1%	-1%	2%	1%	2%	5%	2%
2025	2%	1%	0%	-2%	2%	1%	2%	-7%	2%
2026	1%	1%	-1%	5%	1%	1%	2%	73%	2%
2027	2%	1%	1%	9%	1%	1%	2%	54%	2%
2028	2%	1%	-2%	-15%	2%	2%	2%	1%	2%
2029	2%	1%	1%	-6%	2%	2%	2%	-12%	2%
2030	2%	1%	-3%	2%	2%	2%	2%	-8%	2%
2031	2%	1%	0%	2%	2%	2%	1%	1%	1%
2032	2%	1%	1%	2%	2%	2%	1%	1%	1%
2033	2%	1%	0%	2%	2%	2%	1%	-1%	1%
2034	2%	1%	1%	1%	2%	2%	1%	0%	1%
2035	2%	1%	1%	1%	2%	2%	1%	1%	1%
2036	2%	1%	0%	2%	2%	2%	1%	-1%	1%
2037	2%	1%	0%	1%	2%	2%	2%	-2%	2%
2038	2%	1%	0%	1%	2%	2%	2%	1%	2%
2039	1%	1%	1%	1%	2%	2%	2%	2%	2%

Year	Province								
	British Columbia (metal)	Manitoba (metal)	Newfoundland & Labrador (metal)	Nunavut (metal)	Ontario (metal)	Quebec (metal)	Saskatchewan (metal)	Yukon (metal)	Saskatchewan (Non metal)
2040	1%	1%	0%	1%	2%	2%	2%	-2%	2%
2041	2%	1%	1%	1%	2%	2%	1%	-1%	1%
2042	2%	1%	1%	1%	2%	2%	1%	-1%	1%
2043	2%	1%	1%	1%	2%	2%	1%	-1%	1%
2044	2%	1%	1%	1%	2%	2%	1%	-1%	1%
2045	2%	1%	1%	1%	2%	2%	1%	-1%	1%
2046	2%	1%	1%	1%	2%	2%	1%	-1%	1%
2047	2%	1%	1%	1%	2%	2%	1%	-1%	1%
2048	2%	1%	1%	1%	2%	2%	1%	-1%	1%
2049	2%	1%	1%	1%	2%	2%	1%	-2%	1%
2050	2%	1%	1%	1%	2%	2%	1%	-2%	1%

Input parameters for GHG mitigation scenario analysis

Table A8: Input parameters for energy savings calculation

Parameter	Diesel haul truck	Electric haul truck	Diesel hybrid
Total activity (A)	3000 tonnes/day	3000 tonnes/day	24500000 tonnes/year
Haul trucks kW used			3000 kW
Operating hours			3000 hours per year
Capacity			50 tonne
Horsepower			650 hp
Discount rate	10%		
Capital cost (million \$)	1.74	3.59	2.72 (Battery costs are expected to reduce by 45% by 2025)
Life span (years)	12	12	7
Salvage value (% of capital cost)	14	14	14
Labour cost (million \$)	0.4	0.36	0.4
Non-fuel operating expense (% of capital cost)	35	31.5	0.35
Overhaul expense (% of capital cost)	25	0	0
Effective utilization (%)	61	68	61
Number of trucks	10	9	10
Avg. load factor	0.55	0.8	-

Table A9: Input parameters for CSE calculation for the GO-ALHDs_P and GO-ALHDs_U scenarios

Parameter	Diesel LHD	Electric LHD	Fuel cell LHD
LHDs kW used		1350 kW	
Operating hours		3000 hours per year	
Capacity		256 kW	
Discount rate		10%	
Capital cost (million \$)	1.45	1.68	2.20
Salvage value (% of capital cost)	20	20	20
Labour cost (million \$)		Same	
Non-fuel operating expense (% of capital cost)	60	60	60
Fuel consumption	225 L/hour	-	1.7 kg/hour
Life span (years)	4	4	4
Effective utilization (%)	61	68	61
Number of LHDs	9	8	9
Avg. load factor	0.55	0.8	-

Table A10: Input parameters for CSE calculation for the IR-HPGR1 and IR-HPGR2 scenarios

Parameter	AG mill circuit	HPGR-ball mill circuit	HPGR-pebble mill circuit
Life span (years)		12	
Tonnes processed per year		8000000	
Discount rate (%)		10	
Capital cost (\$)	323,029,198	298,408,393	290,971,326
Operating cost (\$)	48,190,061	49,991,558	49,991,558

Table A11: Input parameters for CSE calculation for the IR-PAG scenario

Parameter	Value
Plant capacity (tonnes/year)	34600000
Energy savings (%)	13
Ball consumption (% less)	25
Ball cost (\$/t)	0.21

Table A12: Input parameters for CSE calculation for the GO-HPGR1, GO-HPGR2, and GO-HPGR_S scenarios

Parameter	SABC circuit	HPGR-ball mill circuit (GO-HPGR1, GO_HPGR2)	HPGR-stirred mill circuit (GO-HPGR_S)
Life span (years)	15	15	15
Tonnes processed per year	6173245	6173245	6173245
Discount rate (%)	10	10	10
Capital cost (\$)	167,586,650	191,982,175	229,105,800
Operating cost (\$)	24,030,450	18,202,902	19,970,810

Energy demand and GHG emissions projections to 2050 in the BAU scenario

Table A13: BAU scenario energy demand (PJ) for the iron, gold, and potash mining sectors

Sector/Province	2010	2015	2020	2025	2030	2035	2040	2045	2050
Iron mining									
Quebec	15.7	13.0	14.9	16.0	17.3	19.0	20.4	22.2	24.3
Newfoundland and Labrador	30.0	16.4	18.9	21.0	20.1	20.9	21.1	21.8	22.8
Nunavut	0.0	0.1	0.3	0.3	0.3	0.3	0.3	0.4	0.4
Total	45.7	29.4	34.1	37.4	37.7	40.2	41.8	44.3	47.4
Gold mining									
Quebec	3.8	6.7	7.9	8.5	9.2	10	10.7	11.7	12.7
Newfoundland and Labrador	0.0	0.1	0.1	0.1	0.1	0.1	0.1	0.1	0.1
Nunavut	0.8	1.5	2.9	3.5	3.2	3.4	3.6	3.9	4.1
British Columbia	3.2	2.5	3.2	3.6	3.9	4.3	4.7	5.1	5.5
Ontario	7.2	12.8	14.2	16	17.2	18.7	20.2	22	24.2
Saskatchewan	0.1	0.1	0.1	0.2	0.2	0.2	0.2	0.2	0.2
Yukon	0.0	0.1	0.2	0.2	0.5	0.5	0.5	0.5	0.4
Total	15.2	23.7	28.7	32.1	34.2	37.3	40	43.4	47.3
Potash mining									
Saskatchewan	27.5	32.2	38.9	47.4	51.8	55.2	59.8	64.1	68.2
New Brunswick	1.0	0.9	1.0	1.3	1.4	1.5	1.6	1.7	1.8
Total	28.5	33.1	39.9	48.6	53.2	56.7	61.5	65.8	70.1

Table A14: BAU scenario GHG emissions (Mt CO₂ eq.) (including electricity-related emissions) for the iron, gold, and potash mining sectors

Sector/Province	2010	2015	2020	2025	2030	2035	2040	2045	2050
Iron mining									
Quebec	1.3	0.9	0.8	0.9	0.9	1.0	1.1	1.2	1.3
Newfoundland and Labrador	1.5	1.0	0.9	1.0	0.9	1.0	1.0	1.0	1.0
Nunavut	0.0	0.0	0.0	0.0	0.0	0.0	0.0	0.0	0.0
Total	2.7	1.9	1.7	1.9	1.9	2.0	2.1	2.2	2.4
Gold mining									
Quebec	0.40	0.49	0.22	0.24	0.25	0.27	0.29	0.31	0.34
Newfoundland and Labrador	0.00	0.00	0.00	0.00	0.00	0.00	0.00	0.00	0.01
Nunavut	0.06	0.12	0.22	0.26	0.24	0.26	0.28	0.30	0.31
British Columbia	0.07	0.08	0.09	0.10	0.11	0.12	0.12	0.13	0.14
Ontario	0.30	0.47	0.46	0.62	0.60	0.61	0.66	0.73	0.80
Saskatchewan	0.00	0.02	0.02	0.02	0.01	0.01	0.01	0.01	0.01

Sector/Province	2010	2015	2020	2025	2030	2035	2040	2045	2050
Yukon	0.00	0.01	0.01	0.01	0.03	0.03	0.03	0.03	0.03
Total	0.83	1.19	1.02	1.25	1.24	1.30	1.40	1.51	1.63
Potash mining									
Saskatchewan	1.3	2.7	3.4	3.8	3.6	3.8	3.9	3.9	4.0
New Brunswick	0.0	0.1	0.1	0.1	0.1	0.1	0.1	0.1	0.1
Total	1.3	2.8	3.4	3.9	3.7	3.9	4.0	4.0	4.1

Fisher-Pry substitution model for market penetration

The market share for each technology can be fit into a growth curve using Fisher and Pry's substitution model wherever applicable. This model is used to project the penetration of superior technologies and new products that can substitute existing technologies. A transformed linear form of the Fisher-Pry model is given by Equation A1. The annual market share values for each technology are fitted to Equation A1 using MATLAB's Curve Fitting Toolbox.

$$\frac{Y}{L-Y} = 10^{A-Bt} \quad (\text{Equation A1})$$

where Y is the penetration %, L is the normalized upper growth limit (100), t is the year, and A and B are fitted parameters for each scenario. The Fisher-Pry model coefficients A and B for the penetration of electric vehicles are shown in Table A15. The $R^2 > 0.96$ indicates that the penetration rates of electric haul trucks and LHDs are closely fitted to an 'S' curve.

Table A15: Fisher-Pry model coefficients for electric vehicle penetration

Scenarios	Province	Fisher-Pry model coefficients		R ²
		A	B	
IR-AHTs, GO-AHTs_P, GO-AHTs_U, PO- AHTs_U	NFL	-0.8014	-0.1077	0.9648
	NB	-0.8131	-0.1137	0.9658
	QC	-0.8582	-0.1294	0.9685
	ON	-0.9772	-0.0944	0.9619
	MN	-0.8384	-0.1206	0.9678
	BC	-0.8085	-0.1125	0.9657

Scenarios	Province	Fisher-Pry model coefficients		R ²
		A	B	
GO-ALHDs_P, GO-ALHDs_U	SK	-0.7882	-0.1048	0.9637
	YK	-0.8118	-0.1115	0.9647
	NU	-0.7647	-0.8440	0.9641
	NFL	-1.4160	-0.1123	0.9888
	NB	-1.3970	-0.1115	0.9890
	QC	-1.3170	-0.1084	0.9886
	ON	-1.4780	-0.1141	0.9893
	MN	-1.3860	-0.1113	0.9889
	BC	-1.3970	-0.1115	0.9890
	SK	-1.4260	-0.1120	0.9894
	YK	-1.4040	-0.1119	0.9890
	NU	-1.5160	-0.1156	0.9892

Table A16: Summarized scenario results

Sector/Scenario	Cumulative energy reduction, PJ, compared to BAU scenario	Cumulative GHG mitigation, Mt, compared to BAU scenario	Incremental net present value (NPV) of costs (million 2016 CAD)	GHG mitigation cost (2016 CAD/tonne of CO ₂ eq.)
Iron mining				
IR-AHTs	35.4	5.5	-3,993	-720
IR-HTO	3.6	0.3	-74	-280
IR-TMS	6.9	0.5	-137	-271
IR-SOE	1.3	0.01	-14	-2,360
IR-HPGR1	25.9	0.1	-363	-3,651
IR-HPGR2	26.5	0.1	-418	-4,120
IR-PAG	9	0.02	-29	-1,166
IR-PSOT	31	2.3	-231	-101
Gold mining				
GO-AHTs_P	28.6	3.6	-4,552	-1,248
GO-AHTs_U	104.7	1.7	-5,162	-3,096
GO-ALHDs_P	5.1	0.5	69	141
GO-ALHDs_U	15.8	1.7	-601	-357
GO-HTO	3.4	0.2	-55	-254
GO-TMS	7.6	0.6	-142	-253
GO-PAG	5.7	0.2	94	614
GO-HPGR1	54.6	1.1	215	193
GO-HPGR2	28.3	0.6	116	201
GO-HPGR_S	62.7	1.3	-159	-124
GO-VOD	102.9	0.9	-967	-1,134

Sector/Scenario	Cumulative energy reduction, PJ, compared to BAU scenario	Cumulative GHG mitigation, Mt, compared to BAU scenario	Incremental net present value (NPV) of costs (million 2016 CAD)	GHG mitigation cost (2016 CAD/tonne of CO ₂ eq.)
Potash mining				
PO-AHTs_U	12.5	0.9	-632	-701
PO-VOD	6.5	0.4	-56	-141
PO-SG&PD	22.9	1.5	-35	-23
PO-HTO	3.0	0.2	-52	-239
PO-TMS	3.5	0.3	-94	-363

Sensitivity Analysis

Iron mining - Sensitivity of abatement cost to capital cost, discount rate, diesel price, electricity price, and reference scenario growth

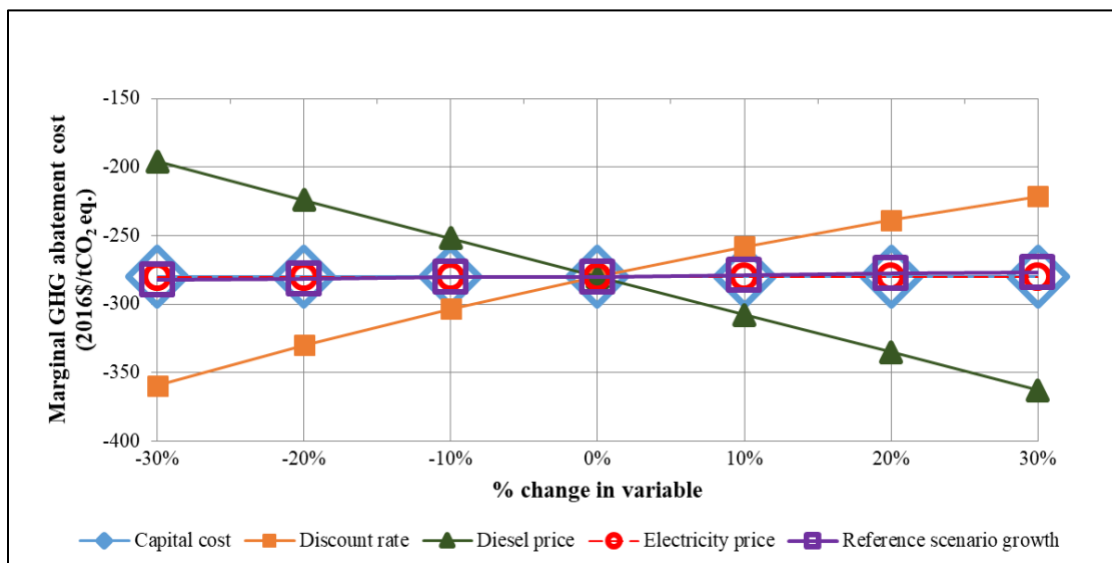


Figure A4: IR-HTO scenario sensitivity of abatement cost to capital cost, discount rate, diesel price, electricity price, and reference scenario growth



Figure A5: IR-TMS scenario sensitivity of abatement cost to capital cost, discount rate, diesel price, electricity price, and reference scenario growth

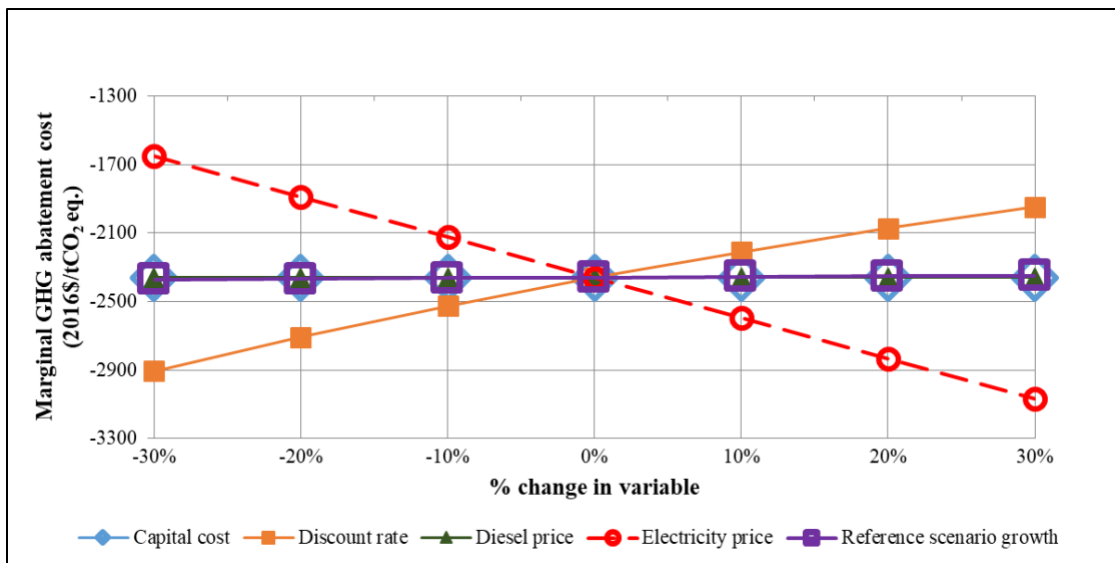


Figure A6: IR-SOE scenario sensitivity of abatement cost to capital cost, discount rate, diesel price, electricity price, and reference scenario growth

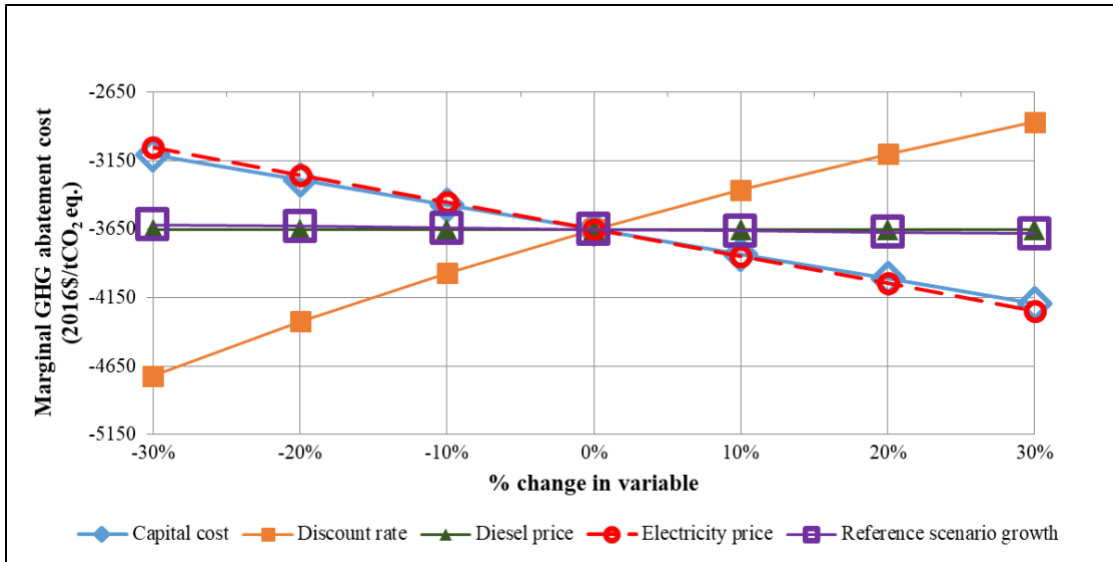


Figure A7: IR-HPGR1 scenario sensitivity of abatement cost to capital cost, discount rate, diesel price, electricity price, and reference scenario growth

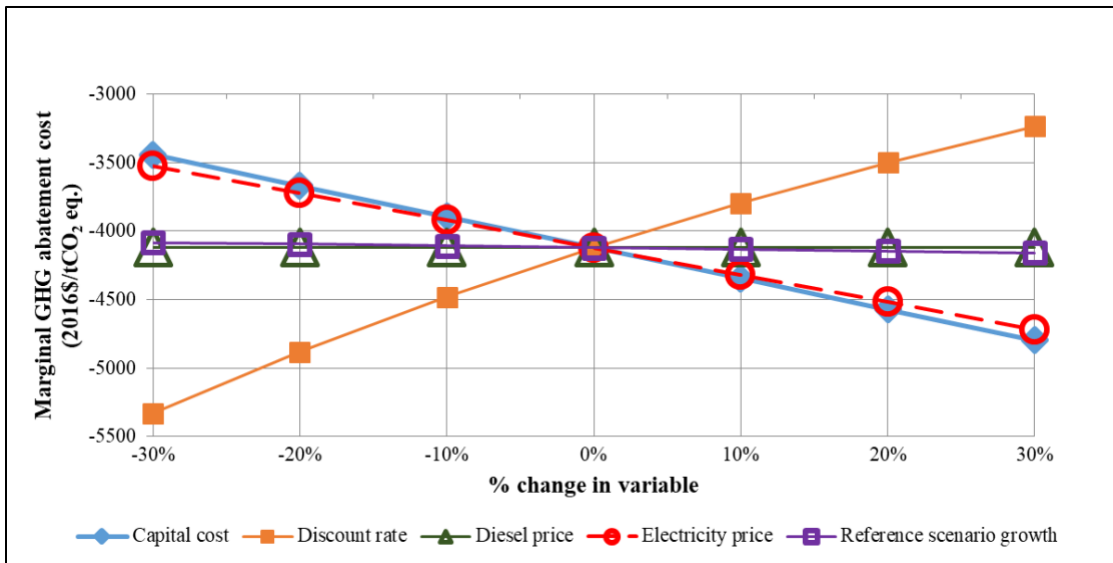


Figure A8: IR-HPGR2 scenario sensitivity of abatement cost to capital cost, discount rate, diesel price, electricity price, and reference scenario growth

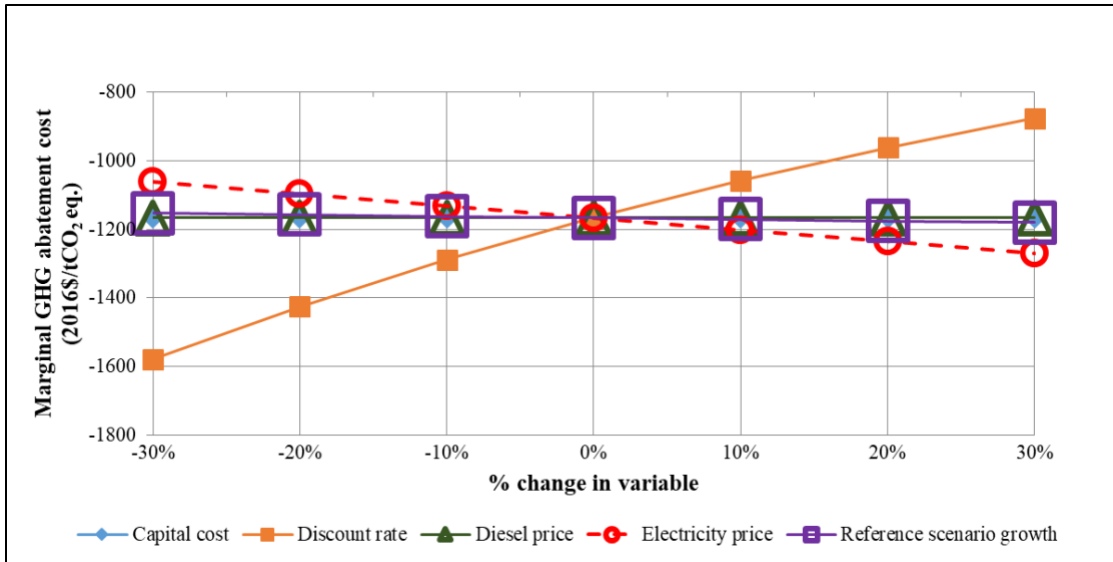


Figure A9: IR-PAG scenario sensitivity of abatement cost to capital cost, discount rate, diesel price, electricity price, and reference scenario growth

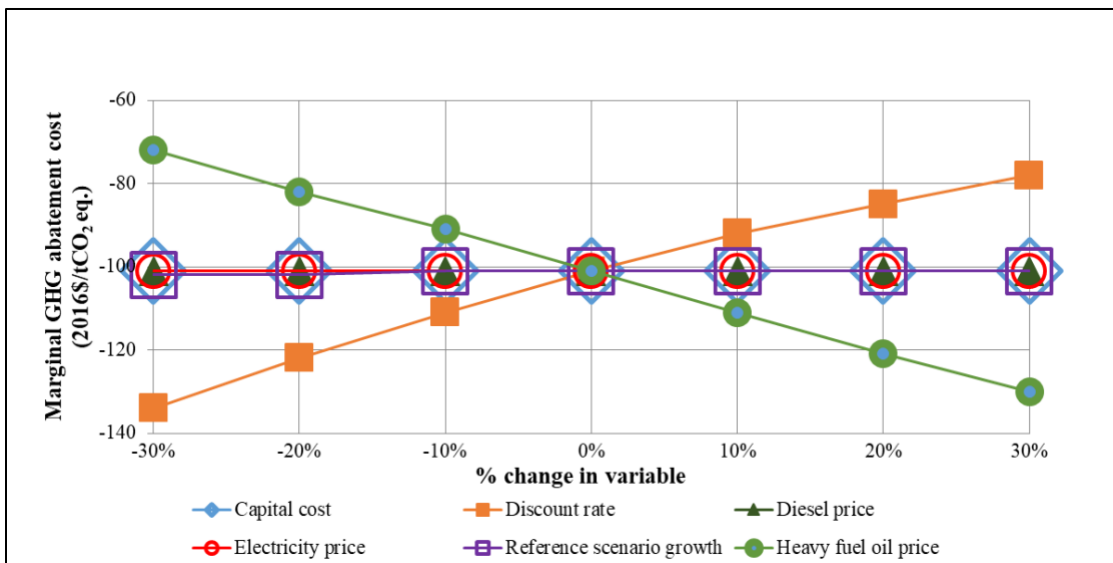


Figure A10: IR-PSOT scenario sensitivity of abatement cost to capital cost, discount rate, diesel price, electricity price, and reference scenario growth

Gold mining - Sensitivity of abatement cost to capital cost, discount rate, diesel price, electricity price, and reference scenario growth

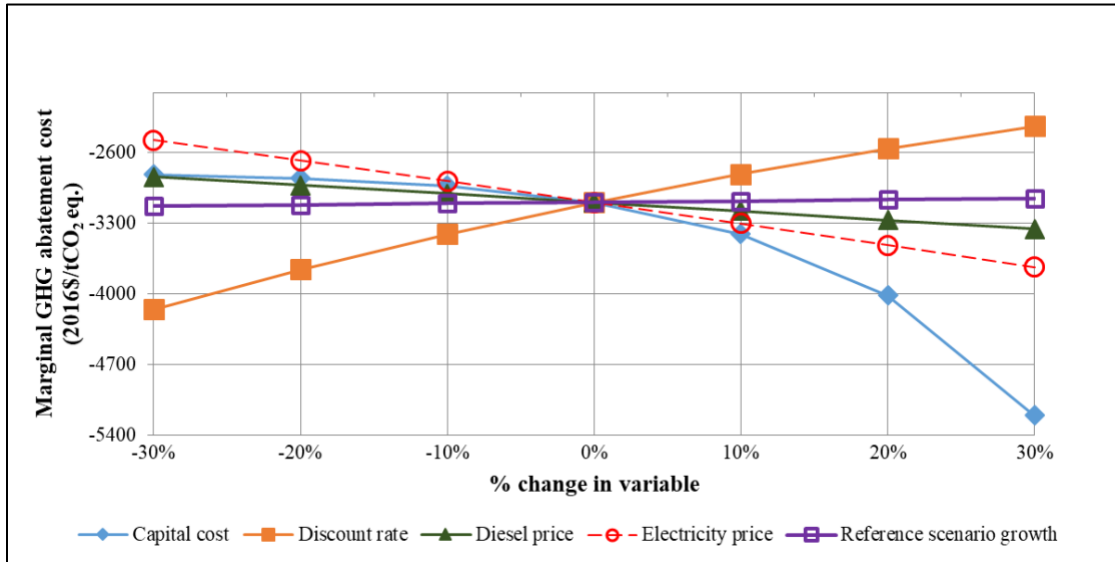


Figure A11: GO-AHTs_U scenario sensitivity of abatement cost to capital cost, discount rate, diesel price, electricity price, and reference scenario growth

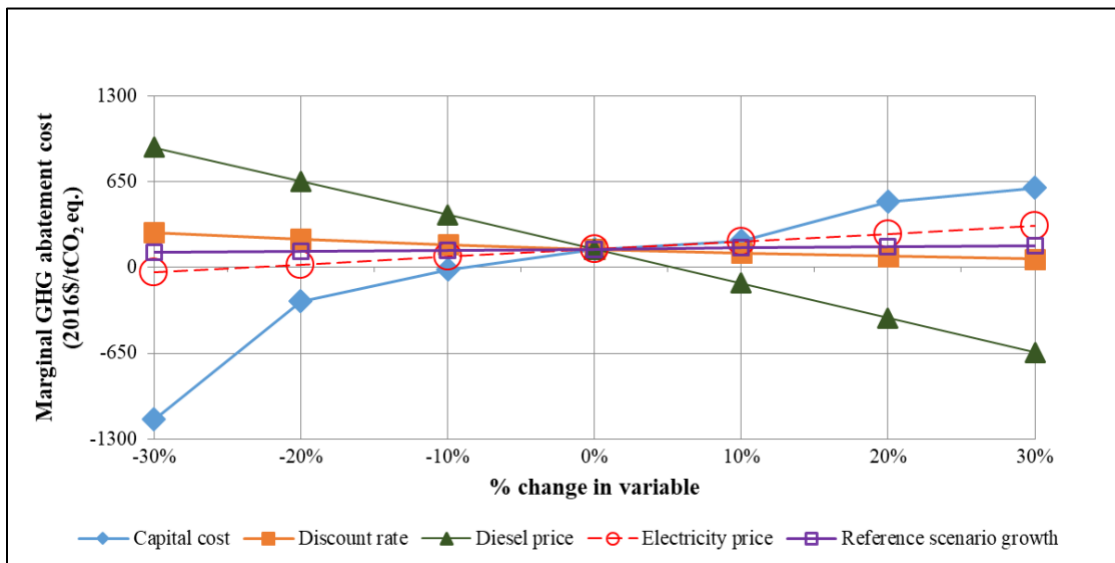


Figure A12: GO-ALHDs_P scenario sensitivity of abatement cost to capital cost, discount rate, diesel price, electricity price, and reference scenario growth

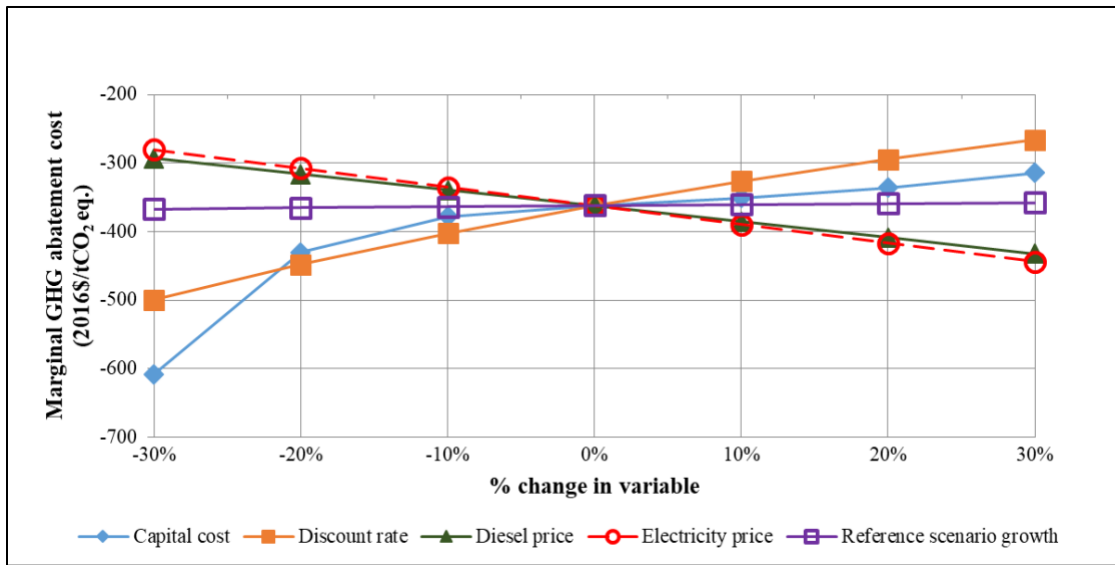


Figure A13: GO-ALHDs_U scenario sensitivity of abatement cost to capital cost, discount rate, diesel price, electricity price, and reference scenario growth

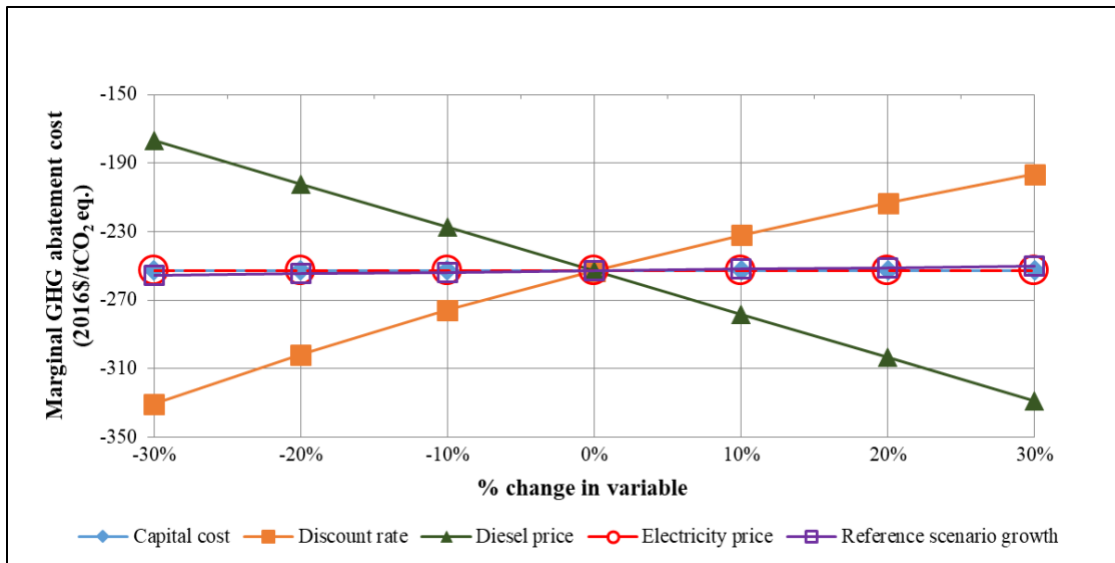


Figure A14: GO-HTO scenario sensitivity of abatement cost to capital cost, discount rate, diesel price, electricity price, and reference scenario growth

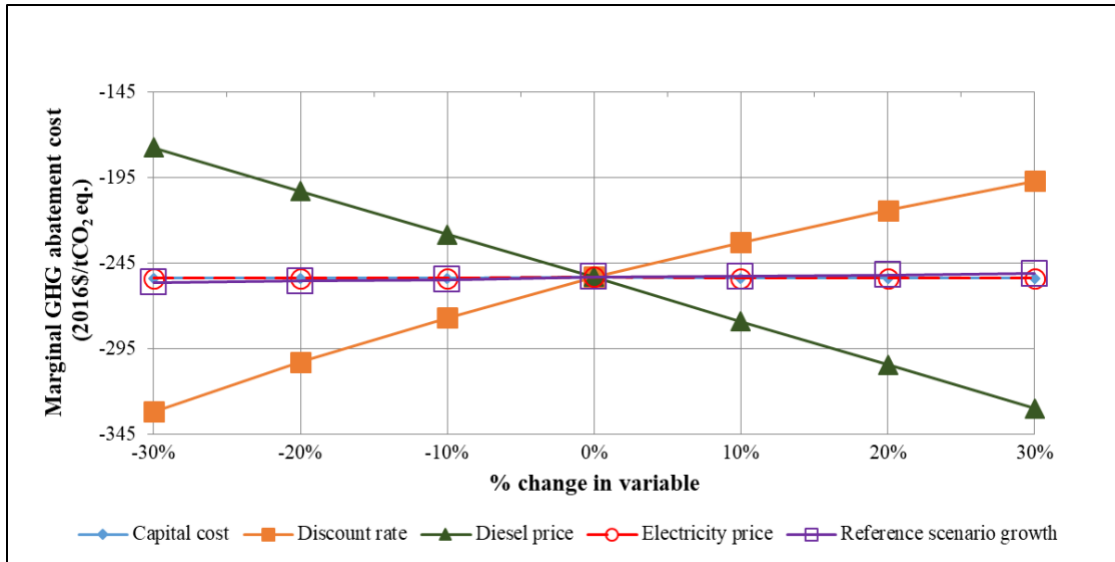


Figure A15: GO-TMS scenario sensitivity of abatement cost to capital cost, discount rate, diesel price, electricity price, and reference scenario growth

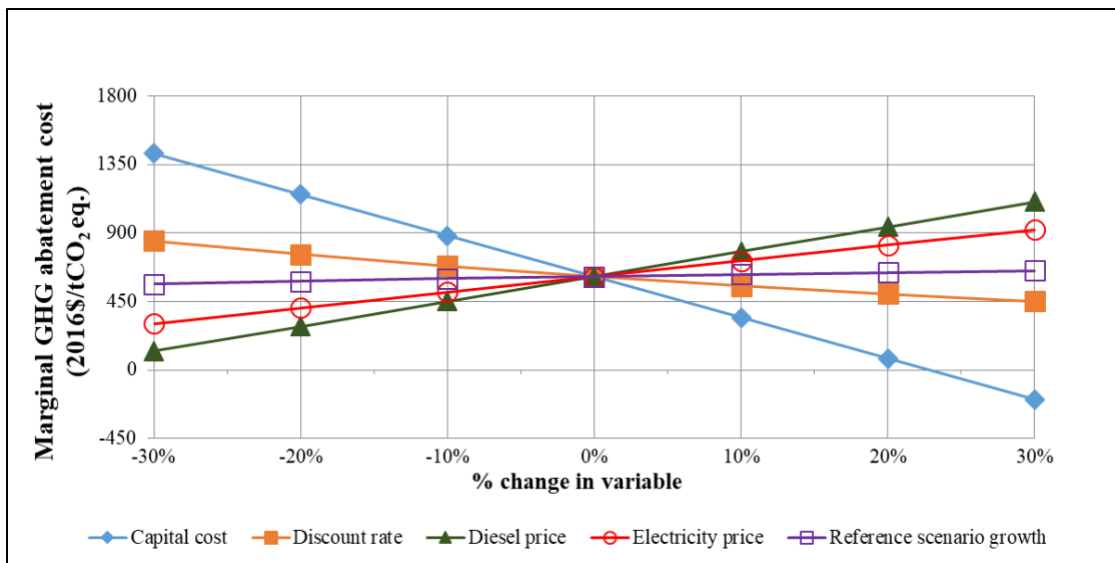


Figure A16: GO-PAG scenario sensitivity of abatement cost to capital cost, discount rate, diesel price, electricity price, and reference scenario growth

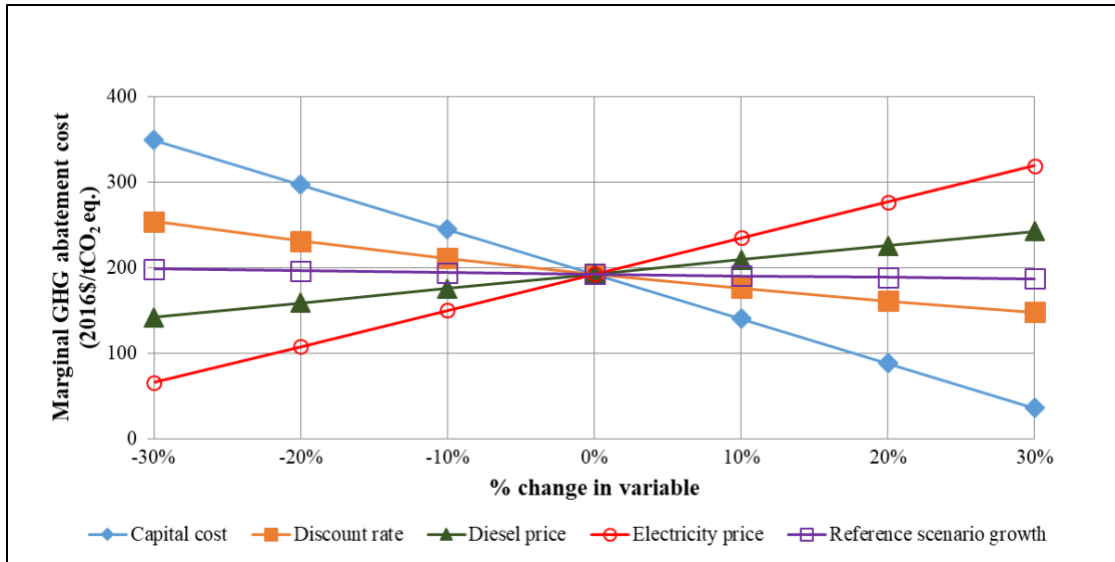


Figure A17: GO-HPGR1 scenario sensitivity of abatement cost to capital cost, discount rate, diesel price, electricity price, and reference scenario growth

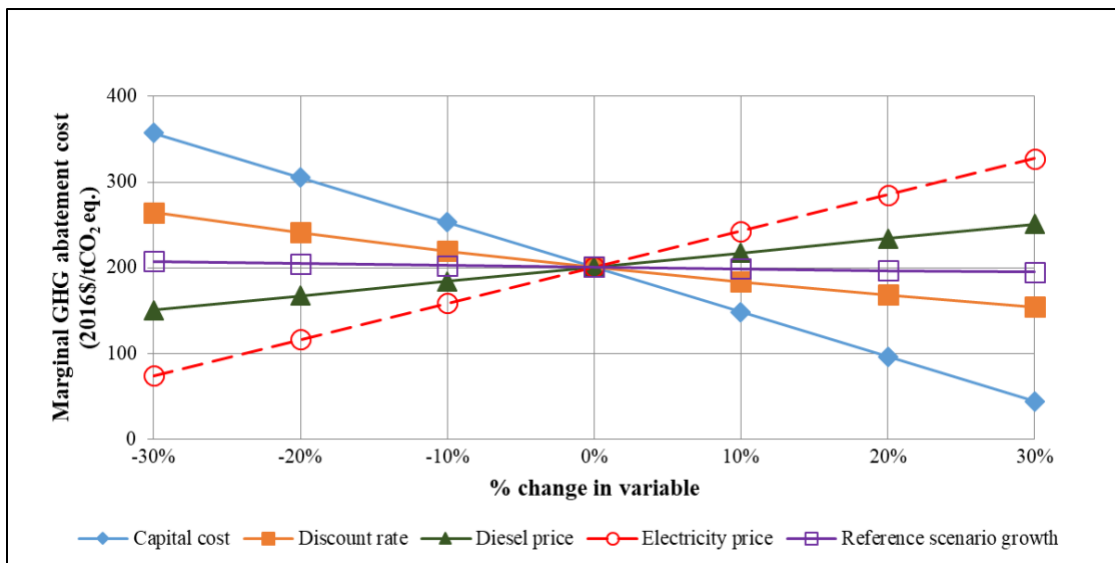


Figure A18: GO-HPGR2 scenario sensitivity of abatement cost to capital cost, discount rate, diesel price, electricity price, and reference scenario growth

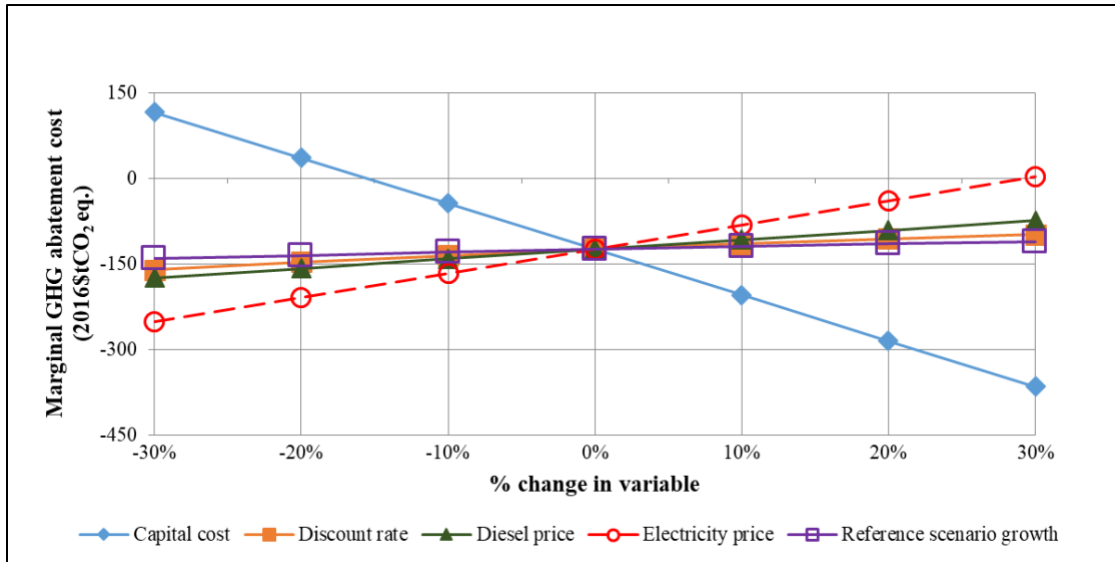


Figure A19: GO-HPGR_S scenario sensitivity of abatement cost to capital cost, discount rate, diesel price, electricity price, and reference scenario growth

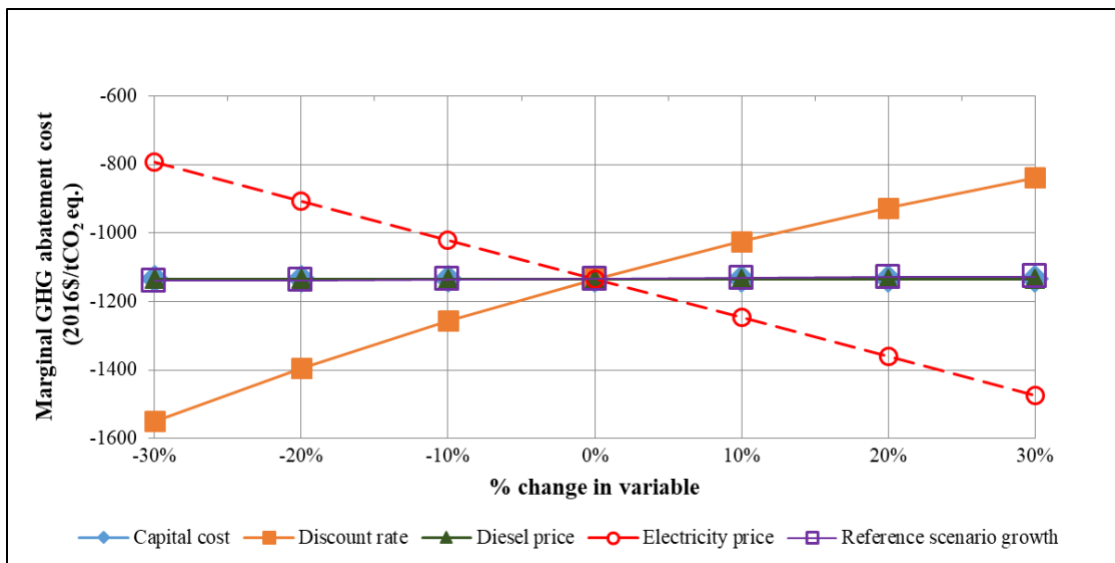


Figure A20: GO-VOD scenario sensitivity of abatement cost to capital cost, discount rate, diesel price, electricity price, and reference scenario growth

Potash mining - Sensitivity of abatement cost to capital cost, discount rate, diesel price, electricity price, and reference scenario growth

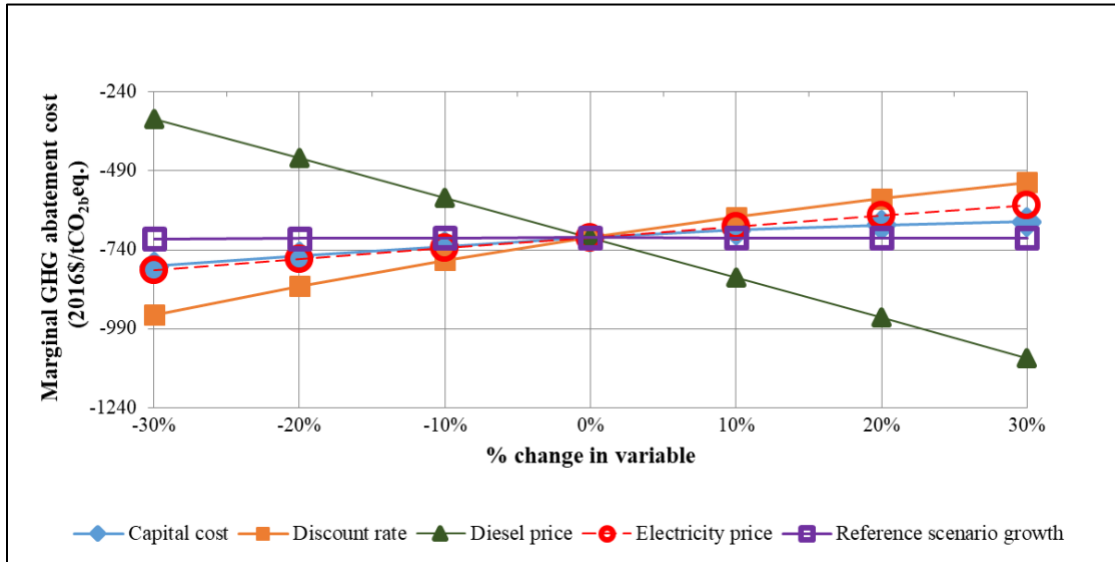


Figure A21: PO-AHTs_U scenario sensitivity of abatement cost to capital cost, discount rate, diesel price, electricity price, and reference scenario growth

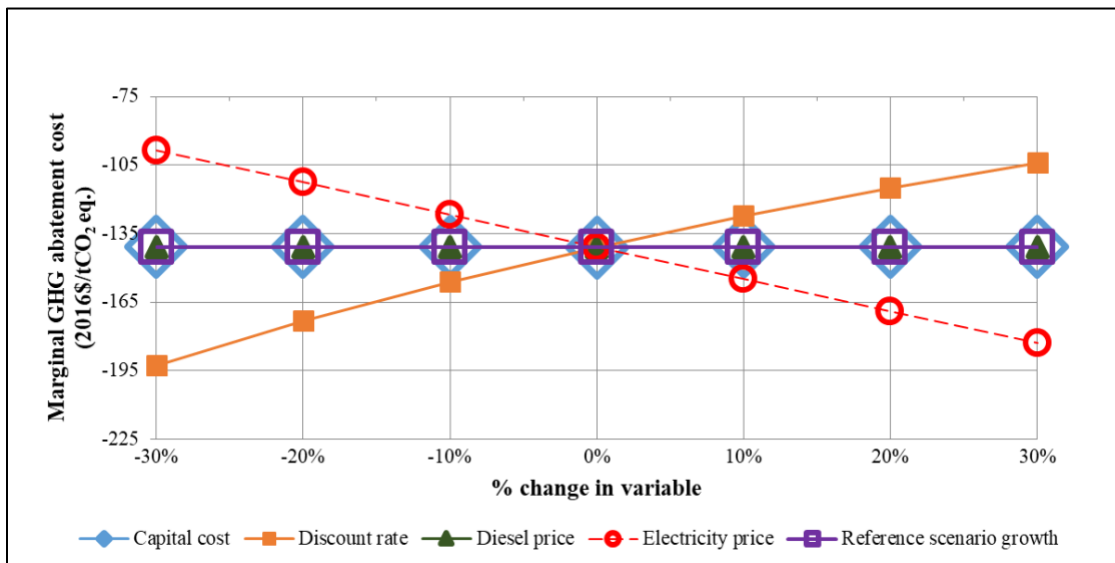


Figure A22: PO-VOD scenario sensitivity of abatement cost to capital cost, discount rate, diesel price, electricity price, and reference scenario growth

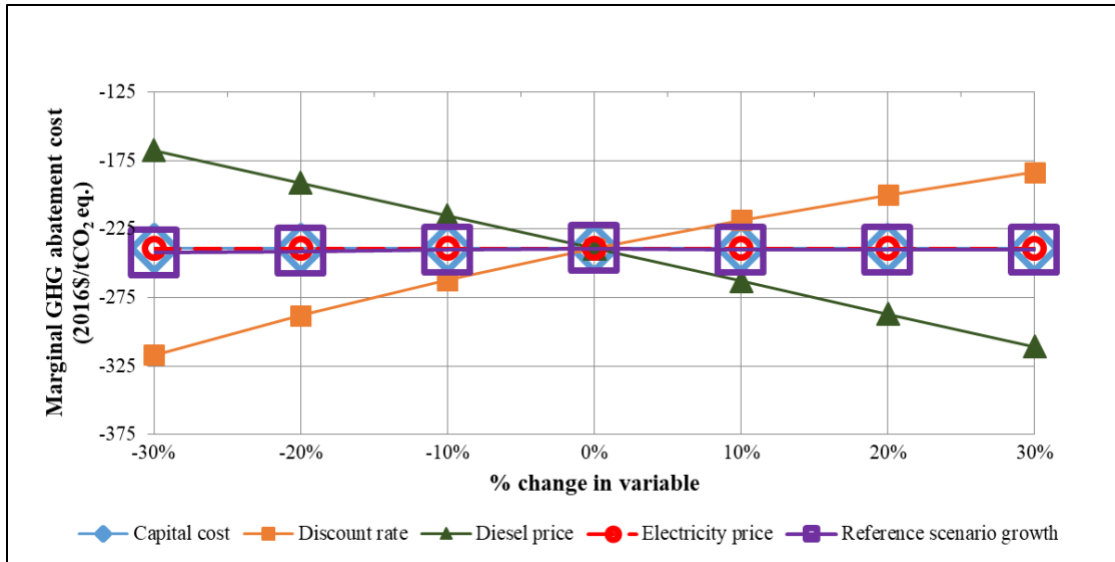


Figure A23: PO-HTO scenario sensitivity of abatement cost to capital cost, discount rate, diesel price, electricity price, and reference scenario growth